Wooden pegs in the retrofit of timber constructions

Alice Sartori

ADVANCED MASTERS IN STRUCTURAL ANALYSIS
OF MONUMENTS AND HISTORICAL CONSTRUCTIONS

Master's Thesis

Alice Sartori

Wooden pegs in the retrofit of timber constructions

University of Minho

Portugal | 2019

ARCCHIP
UPC

ADVANCED MASTERS IN STRUCTURAL ANALYSIS
OF MONUMENTS AND HISTORICAL CONSTRUCTIONS

Master's Thesis

Alice Sartori

Wooden pegs in the retrofit
of timber constructions

DECLARATION

Name: Alice Sartori

E-mail: alice.sartori@hotmail.it

Title of the thesis: Wooden pegs in the retrofit of timber constructions

Supervisors: Hélder Manuel da Silva e Sousa

                             Jorge Manuel Gonçalves Branco

Year of conclusion: 2019

I hereby declare that all information in this document has been obtained and presented in accordance with academic rules and ethical conduct. I also declare that, as required by these rules and conduct, I have fully cited and referenced all material and results that are not original to this work.

I hereby declare that the MSc Consortium responsible for the Advanced Masters in Structural Analysis of Monuments and Historical Constructions is allowed to store and make available electronically the present MSc Dissertation.

University of Minho, 17/07/ 2019

Signature:_____

This page is left blank on purpose

ACKNOWLEDGEMENTS

I would like to express my gratitude to all the people that helped me through everything and guided me to this point of my life.

First of all to my supervisors: Hélder Sousa for guiding and helping step by step with a lot of patience, availability and enthusiasm; Jorge Branco for always sharing his knowledge and experience.

I acknowledge the SAHC Consortium for granting me the opportunity to attend this Master and providing financial support.

To AOF Company (Augusto Oliveira Ferreira & Ca. Lda) team for being kindly available and for sharing their experience, advices and passion, a true thank you.

A sincere thankfulness to the technicians of LEST – Laboratory of Structures of the University of Minho which provided all the support necessary for the experimental campaign, you are special.

A special thank you to Claudio Tirabasso for simply everything.

Thanks to Leonardo Rodrigues for helping so much with the softwares and codes.

A huge acknowledgement to all the SAHC people I was so lucky to meet and I hope not just for a short period of my life, you literally saved my days, and to all the PhD students whose company made this journey brighter. You all are unforgettable.

To my friends but especially to my family for the support and encouragement and form gifted me with a healthy dose o madness.

A great warm thank you to Paulo for the patience and the encouragement which allowed me to go through these months. It would not have been the same without your presence.

This page is left blank on purpose

ABSTRACT

Observing the current panorama of historic buildings, the presence of a high number of timber structures is noteworthy, among those a consistent portion is in need of strengthening interventions due to different factors such as poor design or change of use. In the last decades the urgency of providing retrofitting technique suitable in matter of compatibility, durability and reversibility lead to a deep study of intervention strictly based on the use of timber.

With this intention, the work presented here focused on the analysis of a retrofit method, based on dry connections, through an experimental campaign. Derivation of a traditional technique which is applied on the extrados of timber floors, the object of study here differs from it by the use of reinforcing planks connected on the side of the existing beam by means of timber pegs. In order to replicate what results most in use in the historic buildings in Portugal, beams of Chestnut (*Castanea sativa Mill.*) originally part of a set of historic timber floors, were here reinforced with planks of Pine (*Pinus pinea*) with the use of Massaranduba (*Manilkara spp)* fasteners.

Mechanical properties of the adopted timber species were identified with local destructive tests and by reference to codes and existing literature. The main body of the experimental campaign was divided in a local scale, where the strength of the connection was tested through double shear tests, and global scale where the mechanical characteristic of bending strength and modulus of elasticity of two timber beams were identified and compared with the expected behaviour of an unreinforced element. The laboratory activity was then enriched by a statistic analysis aimed to find a correlation between the structural response of the results with the visual grading of the tested specimens.

Although this work represents a first approach to the topic and further and deeper studies are required, the final results showed a positive performance as the test on the real scale elements confirmed what was found on the small scale. In the meantime, no direct relation was found between the visual grading carried out and the structural behaviour of the specimens analysed, meaning that the success of the strengthening technique is not influenced by the conditions of the existing structure, unless of very significant defects that even in that case can be mitigated by the presence of the strengthening planks.

This page is left blank on purpose

RESUMO

Observando o panorama atual de edifícios históricos, destaca-se a presença de um elevado número de estruturas de madeira, dentro as quais uma quantidade significativa necessita de intervenções de reforço, devido a diferentes fatores, como a concepção deficiente ou a mudança de uso. Nas últimas décadas, a urgência de fornecer uma técnica de reabilitação adequada em termos de compatibilidade, durabilidade e reversibilidade leva a um estudo profundo de uma intervenção estritamente baseada no uso da madeira.

Com esse intuito, o trabalho aqui apresentado teve como foco a análise de um método de reabilitação, baseado em conexões secas, através de uma campanha experimental. Derivação de uma técnica tradicional que é aplicada nos extrados de telhados de madeira, o objeto deste estudo difere no uso de tábuas de reforço liagadas no lado da viga existente por meio de cavilhas de madeira. De modo a replicar os resultados mais utilizados nos edifícios históricos de Portugal, as vigas de castanho (*Castanea sativa Mill.*) que faziam originalmente parte de um conjunto de pisos históricos de madeira, foram aqui reforçadas com tábuas de pinheiro (*Pinus pinea*) e com o uso de cavilhas de Massaranduba (*Manilkara spp*).

As propriedades mecânicas das madeiras adotadas foram identificadas com testes locais destrutivos e por referência a normas e literatura existente. O corpo principal da campanha experimental foi dividido numa escala local, onde a força da ligação foi testada através de testes de corte duplo, e numa escala global onde as características mecânicas de resistência à flexão e módulo de elasticidade de duas vigas de madeira foram identificadas e comparadas com o comportamento esperado de um elemento não reforçado. A actividade laboratorial foi então enriquecida por uma análise estatística destinada a encontrar uma correlação entre a resposta estrutural dos resultados com a classificação visual dos espécimes testados.

Embora este trabalho represente uma primeira abordagem ao tema e sejam necessários estudos adicionais e mais aprofundados, os resultados finais mostraram um desempenho positivo, já que o teste nos elementos da escala estrutural confirmou o que foi encontrado em pequena escala. Entretanto, não foi encontrada relação direta entre a inspeção visual realizada e o comportamento estrutural dos espécimes analisados, significando que o sucesso da técnica de reforçonão é influenciado pelas condições da estrutura existente, a menos que defeitos muito significativos sejam presentes, mas mesmo nesse caso, pode ser mitigado pela presença das tábuas de reforço.

This page is left blank on purpose

SINTESI

Uno sguardo allo stato di fatto attuale mostra come gran parte degli edifici storici sia caratterizzato dalla presenza di strutture lignee, consistente percentuale di essa bisognosa di interventi di rinforzo strutturale a causa di differenti problematiche quali errori di progettazione o cambio d'uso. Negli ultimi decenni ha iniziato a manifestarsi l'urgenza di ricercare e studiare in maniera più approfondita nuove tecniche di consolidamento basate sulla compatibilità, durabilità e reversibilità dell'intervento e quindi legate all'uso del legno.

Il lavoro qui presentato ha come soggetto l'analisi, per mezzo di una campagna sperimentale, di un nuovo metodo di rinforzo contraddistinto dall'uso di sole connessioni a secco per mezzo di perni lignei. Evoluzione di una tecnica tradizionale già ampiamente studiata che va ad interessare l'estradosso di solai lignei, la tecnica qui oggetto di studio si contraddistingue per il fatto che le assi di rinforzo vengono applicate ai lati delle travi strutturali attraverso perni lignei. La scelta di replicare in maniera più possibile veritiera la realtà presente oggi giorno nell'ambito degli edifici storici in Portogallo, ha spinto a scegliere elementi in Castagno (*Castanea sativa Mill.*) per le travi facenti parte originariamente di solai lignei storici, da rinforzare con assi in Pino (*Pinus pinea*) attraverso connettori in Massaranduba (*Manilkara spp).*

Le caratteristiche meccaniche del materiale impiegato sono state identificate attraverso test distruttivi, consultazione dei codici e letteratura disponibile. Il corpo principale della campagna sperimentale si è concentrato dapprima su piccola scala, dove la capacità dei pioli è stata testata a doppio taglio. In seguito è stato eseguito un test in scala reale in cui sono state identificate le caratteristiche meccaniche di resistenza a flessione e modulo di elasticità di due travi rinforzate, allo scopo di compararle con il comportamento strutturale stimato per una trave non rinforzata. L'attività di laboratorio è stata arricchita da un'analisi statistica volta a trovare, se esistente, una correlazione tra la risposta strutturale registrata e la diagnosi visiva dello stato di conservazione dei test.

Sebbene questo lavoro rappresenti un primo approccio alla tematica e siano auspicabili ulteriori approfondimenti futuri, i risultati finali hanno dato un riscontro positivi, in quanto i test su scala reale hanno confermato i dati rilevati a scala locale. Allo stesso tempo nessuna diretta correlazione tra diagnosi visiva e comportamento strutturale è stato individuato, andando così a suggerire come la tecnica di rinforzo possa non essere influenzata dalle originarie condizioni della struttura, a meno che non vi sia una consistente presenza di degrado, il quale può venire ad ogni modo mitigato dalla presenza delle assi di rinforzo.

This page is left blank on purpose

TABLE OF CONTENTS

LIST OF TABLES

LIST OF FIGURES

NOMENCLATURE

a_1 – Minimum distance parallel to grain

a_2 – Minimum distance perpendicular to grain

$a_{3,t}$ - Minimum distance loaded end

$a_{3,c}$ – Minimum distance unloaded end

$a_{4,c}$ - Minimum distance unloaded edge

b - base of the sample

CoV – coefficient of variation

h - height of the sample

$E_{m,0}$ - Modulus of Elasticity

F - vertical load

$F_{max,est}$ - Maximum estimated vertical loaf

F_v - Shear strength

$f_{c,0,k}$ - Compressive strength

$f_{c,0,k}$ - Bending strength

K - coefficient of volumetric shrinkage

L - span between two supports

m_w - mass

V_w - volume

W - moisture content

δF - range of vertical load

δu - range of vertical displacement considered

ρ_w - density

This page is left blank on purpose

1. INTRODUCTION

An overview on the state of the art concerning cultural heritage buildings shows how timber structures have been widely used since ancient times. Their application is manifold, such as in floors, roofs and timber frameworks. Nevertheless, due to their complexity of installation, these type of structures require a high level of knowledge of the material, its behaviour and performance, which are challenging aspects when is necessary to approach an existing structure [1]. Among those, one important issue in timber structures construction is the connection between elements.

Focusing strictly on timber roofs, the current overall panorama highlights how existing structure are often in need of repair or strengthening interventions. This is mostly due to the lack of bending capacity and in-plane stiffness [2] which leads to important bending deformations often aggravated by different situations, such as: unsatisfying material properties, lack of maintenance and presence of decay, change of use of the structure, the lack of a diaphragm behaviour, fundamental in case of seismic events as this can transfer the horizontal forces to the bearing structure of the building [3].

Past studies show that the highest percentage (80%) of failure in timber beams and floors is due to bending followed by compression (8%), tension and shear [4]. These percentages explain why the majority of experimental studies are mainly focused on bending strengthening.

As previously mentioned, the presence of decay like fungi and insects attack along with cracks due to internal defects or high stresses, reduce the mechanical properties of timber and can cause a premature failure of the member itself. From here the importance of retrofitting and reinforcement, along with monitoring and repair in order to allow an extension of the structure's life.

The increasing interest in conservation and compatibility of materials in intervention actions led to a higher concern about strengthening methods which could consider only timber as fastener. However, what the present literature and more precisely the EN-1995-1-1 (2004) [5] provides are design rules focused only on metal fasteners. For this reason when it comes to timber dowels and strengthening interventions, the design formula applied are the one formulated for steel fasteners [6] or a derivation of what was developed for steel-to-timber and steel-to-concrete approaches. This deficiency is strongly related with a long and slow process occurred in the last century which saw a tendency of abandon materials considered too traditional, such as timber, to promote more new and advanced ones like concrete and steel. As a result of this process we witnessed in the recent past the loss of centuries of knowledge regarding timber which led to unsatisfying or poor quality interventions.

The lack of proper design formula codes exclusively for timber fasteners encouraged several experimental campaigns carried out by different experts in the last decades in order to remedy this lack of knowledge [2][3][7][8]. Such a consistent research is needed due to the anisotropic nature of

timber and a wide variety of existing applications, such as different species have different characteristics which brings to different behaviours once subjected to loads, meaning that is mandatory to study different species subjected to different load configurations. The scope of all these campaigns is to identify design formulas able to lead to a proper design of new timber structures and strengthening interventions of existing ones characterized by the use of only timber connections.

This work aims to adopt the same approach and study a new retrofitting technique through an experimental campaign and is the result of the cooperation with the company Augusto de Oliveira Ferreira & Ca. Lda (AOF) especially during the elaboration of this new technique, the guidelines ruling its applications and the supplying of the samples itself. More precisely, the work will focus on the study of a strengthening technique derived by a traditional method which applies timber planks on the sides of the timber beams, needing intervention, by mean of dry connection with timber pegs. The case study presented considers Chestnut (*Castanea sativa Mill.*) timber beams strengthened with planks of Pine (*Pinus pinea L.*) connected by means of Massaranduba (*Manilkara spp*) fasteners.

The analysis and experimental campaign carried out will focus on both local and global scales. This will be carried out with the main purpose of verifying the safety of the retrofitting technique itself and compare the results obtained with what is provided by the existing design codes.

A precise description of the methodology is explained in chapter 3. As previously mentioned, material, samples and advising were kindly provided by AOF. Figure 1 shows the framework of this dissertation which is organised into four main sections starting with the Introduction in chapter 1 where the purpose and the organization of this work is illustrated. Following, the second segment with the presentation of the retrofitting technique composed by chapters 2 and 3, respectively formed by the state of the art and the guidelines of the proposed strengthening method. Here is provided an overview of the current spectrum in matter of interventions on timber floors collected through the available literature. The work proceeds with the presentation of the guidelines aiming to outline the steps necessary to install the reinforcement on existing timber structure. The third section is the main body of the dissertation as it concerns the data collection constituted by the material characterization (chapter 4) and the experimental activity (chapter 5) where all the data was collected, processed and modelled in order to verify the effective contribution of the studied retrofitting technique. Conclusions along with recommendations and future proposed work are processed in the final section (chapter 6).
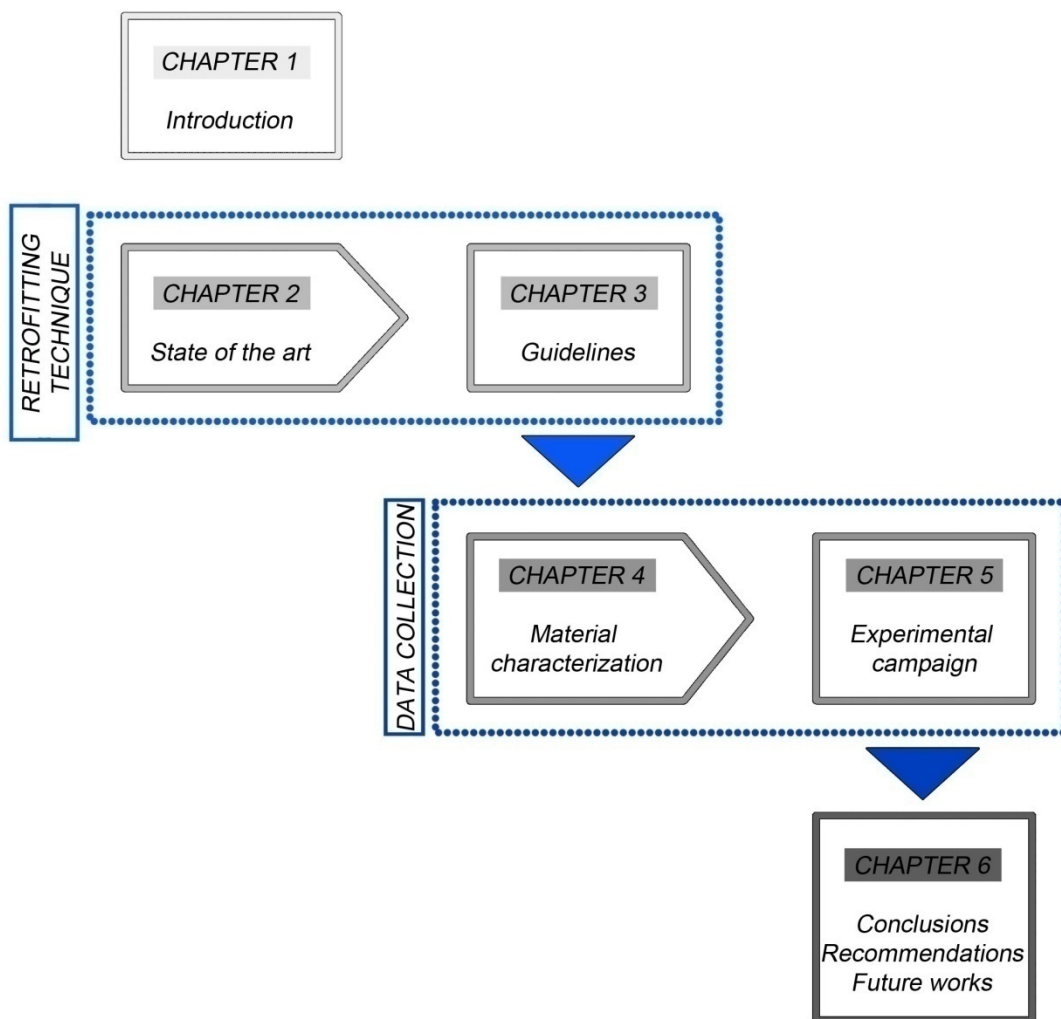
Figure 1 – Framework of the dissertation and interaction between chapters.

2.   STATE OF THE ART

When a strengthening intervention of a timber structure is required, different factors influence the choice of reinforcement approaches, for this reason several methods were investigated and the existence of a wide literature is the proof of the amount of research and studies already carried out. Each intervention method has its advantages and disadvantages and it relies upon the expert decision to choose which is more adequate. For example, because of timber's tendency for having a brittle failure in tension, the location of a reinforcement element in the tensioned face is often a very effective approach, nevertheless the possible presence of paintings or decorative elements leads to a different approach. One can say that the best approach depends on both ability of the method to meet the expected results in reinforcement and peculiar factors related with the structure itself, as aesthetic, reversibility and access or even others such as material availability, costs and social aspects. These aspects grew of importance with the elaboration of the Venice Charter [9] which highlighted the necessity of guaranteeing as much as possible the structural authenticity of a building along with its integrity of material and function, possible only with the employment of compatible and reversible techniques [3]. The respect for the existing structure and the adoption of a low invasive and highly reversible intervention is even more insistent in case of a building of historical value [4][10]. Even now, a growing concern about the use of compatible materials is visible especially in combination with the awareness for the use of sustainable materials and techniques.

Different retrofitting techniques are available in the modern panorama, some influence the floor itself, while others intervene on the structural elements composed by the beams. In the following chapter a brief description of the range of available technique is provided.

2.1   STRENGTHENING TECHNIQUES – TIMBER FLOORS

Every technique is basically based on three components: i) the existing element (structure); ii) the strengthening element; iii) the connection between i) and ii). Both the strengthening element and the connectors may be composed by different materials like concrete, fibre reinforced polymers or new timber members. In some cases, the strengthening element does not need an additional connector, such as the installation of steel elements such as metal screws, pins or dowels as reinforcement, which are also widely used techniques.

2.1.1   CONCRETE TO TIMBER

The most common method used to reinforce an existing timber floor, in the recent past, was the introduction of a concrete slab connected over the existing timber structure through metal fasteners (Figure 2) [10]. This method has lost some use in historic constructions, due to the lack of reversibility, load increase and the poor results that have been registered recently, especially in seismic zones. More precisely, this technique is now considered not satisfying in historic buildings because brings a

consistently higher stiffness in the floors which the bearing structure in masonry was not designed to support. The result is an inability of the structure to transmit and absorb the horizontal forces which the structure is subjected, which can lead to damages of part of the masonry wall (Figure 3).
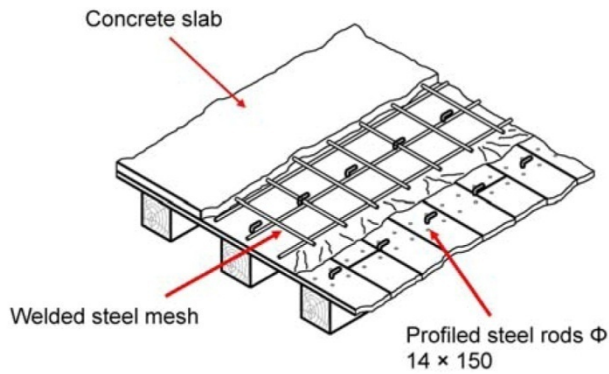
Figure 2 – Strengthening technique with concrete slab [11].

Figure 3 – Example of strengthening with concrete slab after seismic event.[12]

2.1.2 FRPS TO TIMBER

Another technique which is often not used when it comes to historic timber floors, especially in case of a painted intrados, is the application of FRPs in form of strips or bars which can be installed on both floor's boards or in the lower face of the timber beam element. If strips are used, the application of a thin adhesive layer is necessary for both configurations(Figure 4 and Figure 5). The use of this technique is often not used due to its costs. As for the previous considered technique, this method is not reversible and thus incompatible with the principles of conservation.
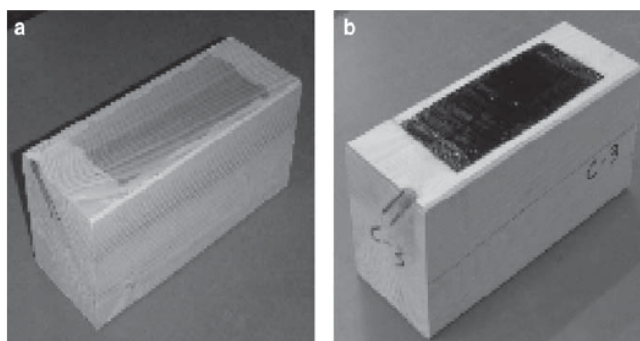
Figure 4 – Application of layer (a) and FRP strip (b) [2].
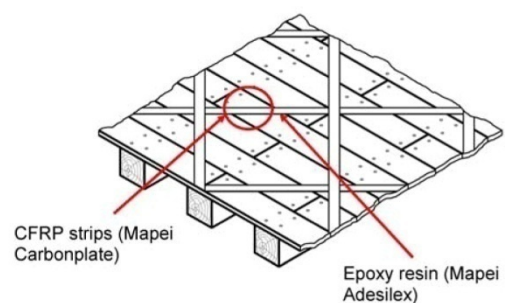
Figure 5 – Strengthening technique with CFRP and epoxy resin [11].

Experimental campaigns showed however that thanks to its high strength and stiffness, this innovative technique, can improve up to 100% both strength and stiffness of the structure. This increase mainly depends on the percentage of reinforcement used and the original properties of the timber beam [4].

2.1.3 STEEL TO TIMBER

Steel connections in form of metal plates can be used to connect the planks of an existing timber floor to avoid slip between the elements due to shear (Figure 6)[3]. However, due to the different thermal behaviour of the materials, this technique could lead to the presence of condensation in the interface between the two elements, and to an alteration in the moisture content of the timber elements.
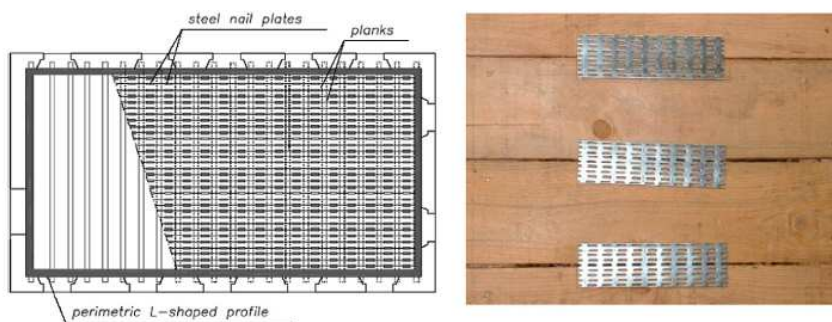
Figure 6 – Use of steel plates to connect timber floor's plank [3].

2.1.4 TIMBER TO TIMBER

A strengthening method used in the past especially in seismic zones considered the application of a new floorboard, laid orthogonally or at 45° on the existing one, to increase both stiffness and strength (Figure 7).
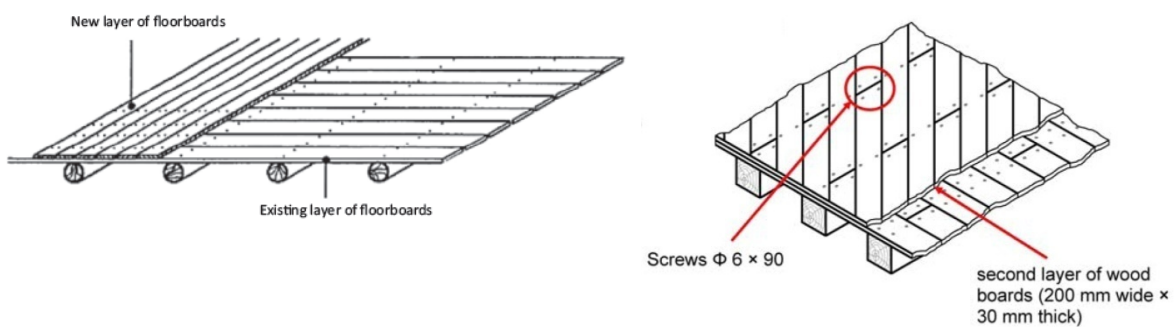
Figure 7 – Orthogonal layer of floorboards over an existing structure [3][11].

Another approach considers the application of plywood panels on more layers and connected with steel rods (Figure 8) to increase both strength and stiffness. All those methodologies which consider the use of timber are preferred due to their adherence to the principles of the Venice Charter, even though the presence of steel elements could imply issues related with the coexistence of non-compatible materials.
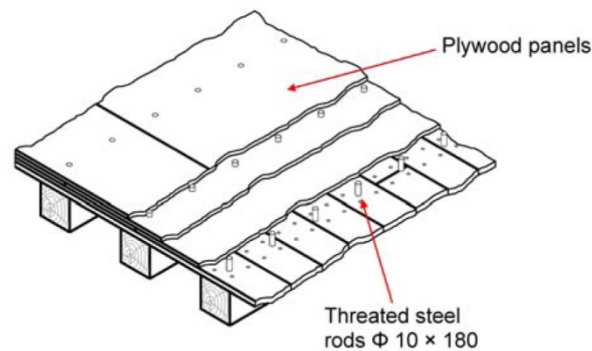
Figure 8 – Strengthening technique with plywood and steel rods [11].

2.2   STRENGTHENING TECHNIQUES – TIMBER BEAMS

All the strengthening techniques which are focused strictly on the structural elements of the timber floors, aim to reach an increased cross-section of the beams itself in order to increase the stiffness of the elements, mainly through the increase of inertia. This kind of methods are equally applied when strengthening or repair is needed. One can say that these approaches are valid only if the timber floor does not present a painted or decorated intrados.

Several approaches can be adopted to provide a higher stiffness of the timber beams: different material such as steel or timber can be used as well as different type of fasteners, also the location of the retrofitting can change considering the peculiar configuration of the considered timber structure. Figure 9 shows two examples of application on timber beams which consider the application of timber and steel elements. This method can also be applied on structural element of both timber roofs and floors [13]. Figure 10 shows a truss repaired by means of this procedure.
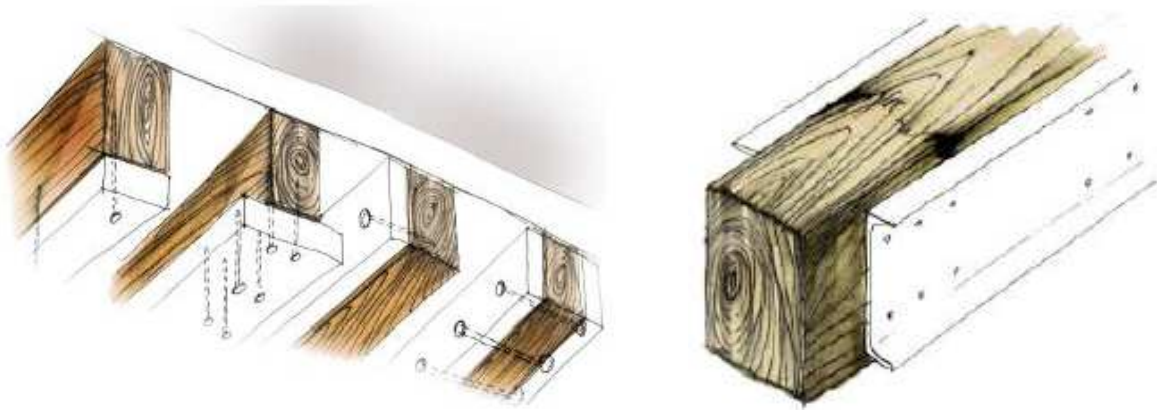
Figure 9 – Example of increased cross-section with timber planks (left) and steel elements (right) [14].

Figure 10 – Example of repairing on a timber truss.

Due to the problems related with material compatibility when two different elements like timber and steel or concrete coexist, another approach is more studied nowadays, namely the use of new timber elements in form of glulam (glued laminated timber) or plywood applied on the extrados of the beams in order to form a T-beam section, where the existing structure acts as a web while the new member behave as a flange. The connection can be made through steel elements, epoxy resin adhesives or timber pegs. As pointed out previously, connection methods which consider the coexistence of different materials (timber-steel and timber-epoxy resin), can cause issues related with moisture condensing in the interface. Issues related with aesthetic for both of the jointing methods and absence of reversibility, in case of resin adhesive, are additional disadvantages [15]. Because of the increased concern toward the conservation of cultural heritage, the urgency of maintaining as much as possible the authenticity and integrity of the original building directed researches to consider and study dry assembly methods with traditional material such as timber pegs. It is important to underline that for all type of composite sections, regardless of the kind of connection used, its mechanical characteristics are the main factor which influences the structural response [3].

As previously mentioned, timber floors are present in old existing buildings and also in historic ones, thus subjected to conservation principles based on the assurance of compatibility, reversibility, preservation of the authenticity and integrity of both structure and original material. These premises make the assumption of using traditional joints based on dry connection with timber pegs as one of the most suitable for strengthening intervention on historic timber floors. For these reasons this work will focus on the study of timber pegs as retrofitting technique.

The procedure studied and used in the experimental campaign carried out by the University of Padua [2] [3] considers the application of new timber planks on the existing structure beams by means of timber pegs. For compatibility reasons the dowels are made of hardwood placed as connection with a dry technique. No additional material is used in order to improve the adhesion in the interface. A T-beam is thus composed and normally the flange is separated by the net through the existing boarding. Figure 11 shows plans, axonometric view and cross-sections denoting the application of this technique.
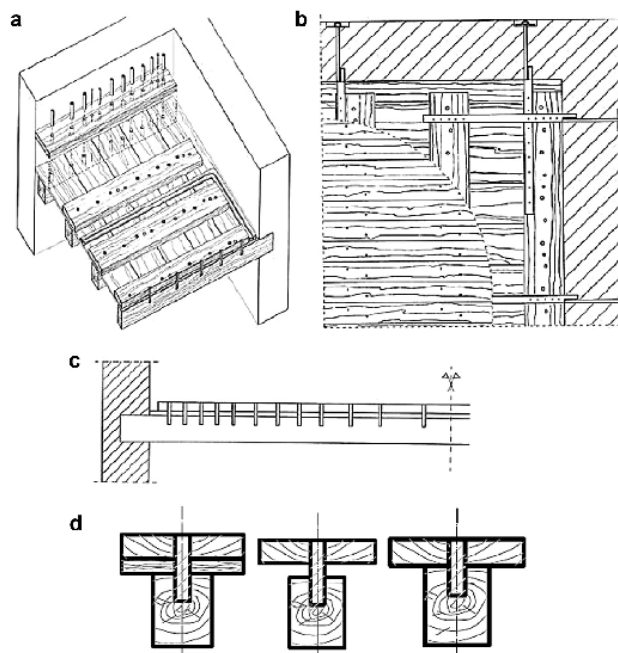
Figure 11 – Strengthening intervention timber-to-timber connected with timber pegs: (a) axonometry, (b) plan, (c) section, (d) different type of cross section, with and without existing boarding [2][3].

This kind of connection is subjected to shear, which is transferred by the dowels between the timber layers creating a composite beam with semi-rigid connections [16]. For this reason a higher number of timber pegs is placed along the beam where shear is prevalent, such as near the end of the beams (Figure 11c).

The application of timber pegs as connectors requires a previous inspection of the structure and, in case of decayed elements is mandatory a local repair or replacement (i.e. use of a timber prosthesis).

Once the existing structure is proved to be sound, the procedure starts with the installation of boards which have to be previously sawn and their underside surface prepared in order to guarantee a perfect adhesion with the existing structure. Screws can be used and placed every six dowels [17]in order to keep the plank in position guaranteeing a constant adhesion in the interface during the following phases of the installation. This may facilitate the intervention, especially when the beams are not propped, even if adequate propping is always recommended. In order to increase resistance to splitting, timber pegs are located in pre-bored holes staggered by half of the diameter of the dowel itself from the longitudinal axis. The used timber dowels are usually 1mm thicker than the pre-drilled hole and are forced in the connection by hammering. In order to increase the strength to slip in the longitudinal direction and avoid a high loss of material along the central axis of the beam, dowels are located in staggered position of at least half diameter from the centre. In case of planks shorter than the span itself, a carving of the bearing walls is averted and the possibility of technical installation in the thickness of the floor itself is promoted [2][17].

Experimental campaigns carried out on floors strengthened with this technique show how the existing floor board influence the collapse mechanism of the dowels, individuating as best performances of timber pegs when floor boards are present [3]. It is important to highlight that a proper connection wall-beams and an additional layer of planks in the extrados gives a satisfying strengthening technique valid even for seismic zones.

An important aspect to consider for this approach is the final increased thickness of the existing structure, for this reason attention has to be paid in order to guarantee a non-significant variation of the floor's level to preserve the threshold with elements such as doors and stairs.

In the last decades a high number of experimental studies both in laboratory and on the field [18]were carried out considering only beam elements [7] or complete timber floors [2][8]. Results of these campaigns showed how timber pegs can provide a satisfying performance when used as shear connections, and so represent suitable and environmentally friendly systems for retrofitting [7]. In the case of the experimental campaign carried out by the University of Padua, for more than a decade, dry timber pegs connections showed a better response then those with steel dowels for the reinforcement of timber floors [2].

To sum up and considering the positive feedback of the past studies, the existing literature underlines the necessity of further and deeper experimental investigations in order to verify the accuracy between analytical and numerical models. Moreover, specific design rules are needed for timber-to-timber dry connection because what exists so far is based on what is used for concrete-to-steel and concrete-to-timber composite sections[3].

3.   PROPOSED TECHNIQUE - GUIDELINES

This work will analyse a retrofitting method derived from a traditional technique, described in the previous chapter, based on the use of dry connections by mean of timber pegs, which focus only on the extrados of the structural elements of a floor. Several issues could, however, prevent the application of this method, such as the lack of space needed to increase the floor's thickness due to the presence of doors or uneven floor's level between divisions. Another case considers the presence of a sound floor's board which, because of its healthy state or its historical importance should be maintained. The sum of all these reasons led to the decision to propose a retrofitting technique with strengthening elements located along the sides of the beams. This factor can avoid the previously highlighted problematic but can only be applied in case of a structure without any decorated or painted intrados.

3.1   PROCEDURE

The procedure to follow in order to apply retrofitting planks on the side of the timber beams is extremely similar to the one needed for the implementation of the structure by the application of the planks on the extrados of the beam. Nevertheless, some peculiar arrangements are needed due to the location of the technique itself. First of all, it is mandatory to proceed with a mirrored and symmetric installation on both sided of the beam in order to avoid an irregular distribution of the stresses, as any non-symmetric application of this retrofitting technique can negatively affect the global behaviour of the timber structure. This and other steps are presented in the following guidelines for the proper installation of the procedure, considering a timber floor composed by irregular beams and simple timber boards connected by means of nails (Figure 12), which is a current situation found in existing timber structures on North Portugal.
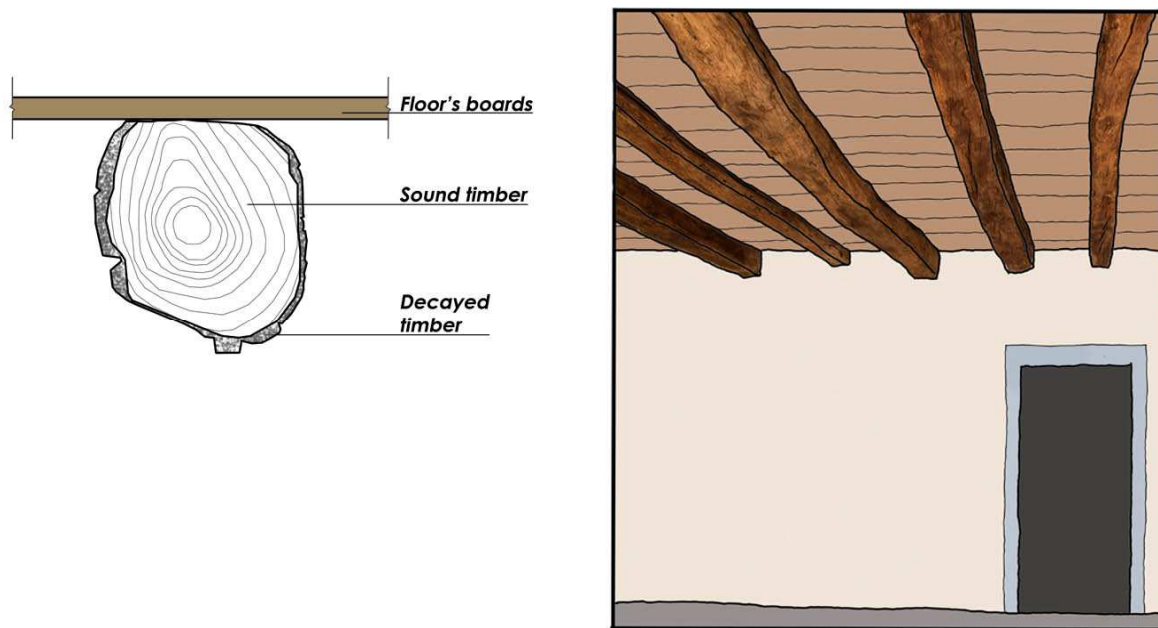
Figure 12 – Example of a timber floor.

STEP 1– Propping and inspection:

When in presence of an element needing reinforcement, before any intervention is carried out, a propping system has to be installed in order to avoid any further damages or collapse during the procedure (Figure 13), as well as to guarantee the safety of all workers. After this, it is possible to proceed with a visual inspection to identify the presence of decay or other relevant damages. Non-destructive tests (NDTs) such as drilling resistance and pin penetration tests are strongly recommended in this phase in order to evaluate an approximation of the depth of decay that has to be to removed and the quantification of the residual cross-section. This evaluation allows to evaluate if the structural element presents deeply decayed sections which are to be replaced or if the grading and the extension of the decay requires to intervene on either the entire length of the timber beam or simply in correspondence of the critical cross-sections. The absence of an active insect or fungi attack has to be also verified and, if present, appropriate countermeasures are mandatory. The propping system is maintained in position for the entire duration of the work.

Floor's boards

Sound timber

Decayed timber

Propping system
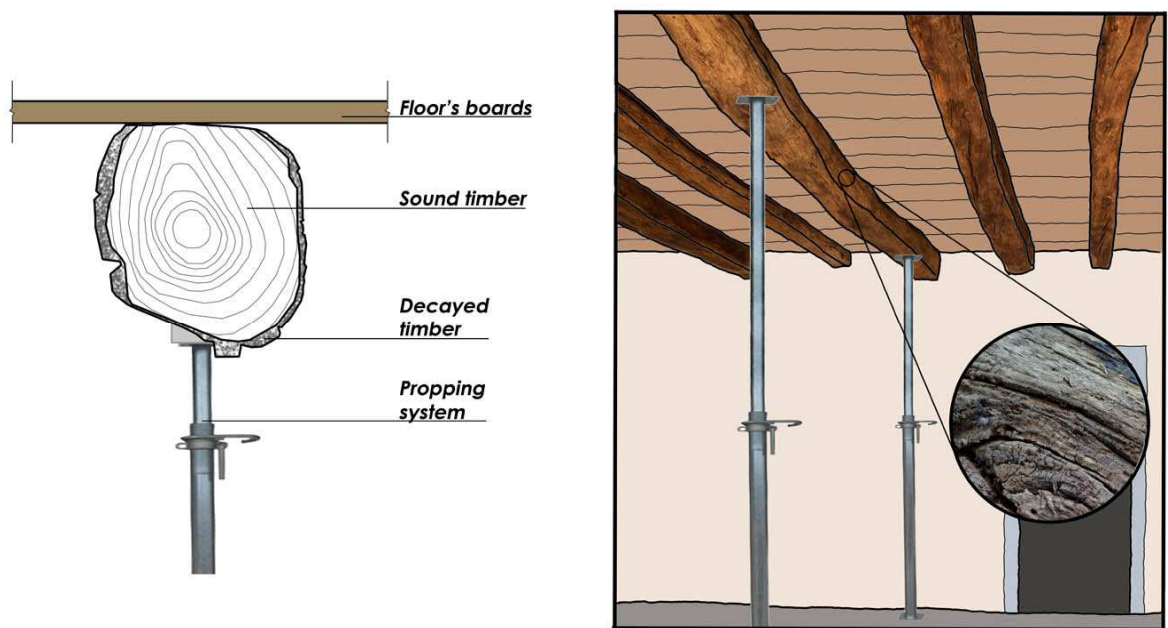
Figure 13 –Step 1: propping, visual inspection, location and estimation of the decayed cross-section.

STEP 2 - Cleaning:

The second step focus on the treatment of the existing structure through the elimination of the decayed part (Figure 14), This can be done manually or with the help of an proper machine. It is important to underline that no sound timber should be removed in order to reach a straight and smooth surface, every natural irregularity is maintained as long as proved not decayed. If old metal elements such as nails are present, it is advised to remove them as much as possible, without bringing more damage to the structure. Secondly, repair techniques are applied in case their need was pointed out in the previous step. During this step, the propping system may have to be locally removed or changed from its location. This must be made always ensuring that the element is being supported in safe conditions.
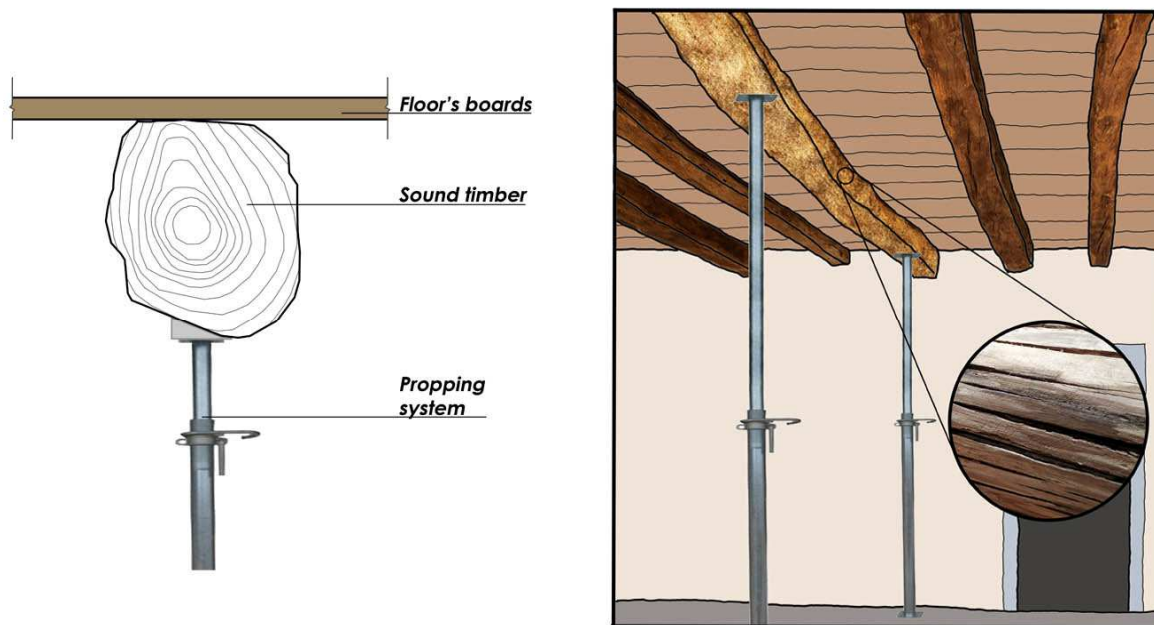
Figure 14 – Step 2: removal of the decayed section.

STEP 3 - Planks:

Once a sound base is guaranteed, in the third step of the procedure the planks are applied and maintained in their location by means of clamps (Figure 15). If the strengthening technique is applied for the entire length of the beam, the planks are recommended to have exactly the same length of the beam itself (Figure 16). The planks are to be inserted in the bearing wall previously opened, at least for a depth equal to the length of the beam itself. This gap is located on both sides of the beam's end to respect the necessity of symmetry. No fasteners are needed in the cross-section of the bearing wall in order to avoid huge openings in the masonry and because the planks are maintained in position by the wall itself. It is important to underline how this strengthening technique also participates actively giving a contribution to the bearing capacity of the existing structure and, unlike the traditional technique that is applied on the extrados, avoiding additional dead load maintained directly by the element in need of strengthening.
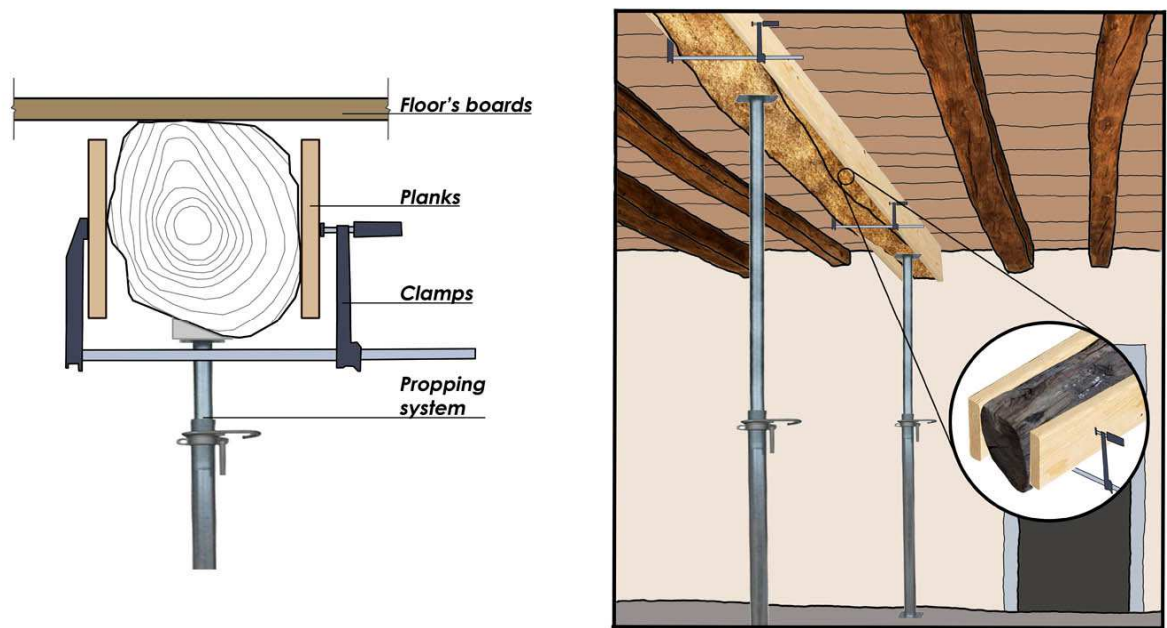
Figure 15 –Step 3: installation of the planks.
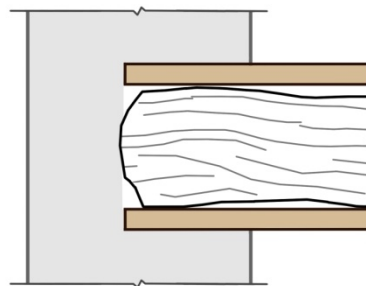
Figure 16 – Detail of the planks in the bearing wall.

STEP 4 - Wedges:

Existing timber elements may display irregularities both in length and in thickness. This aspect is related with the fact that in the past the structural elements were often composed by trunks of small trees or branches of considerable size which were subjected to a superficial treatment in order to get rid of the bark. The shape of the cross-section which is possible to find in situ may differ from a near circle shape to that of a perfectly shaped rectangular cross-section, passing through a wide range of barely sketched rectangular cross-section displaying different percentages of wane. However, providing a smooth and regular surface for the installation of fasteners is extremely important to guarantee an adequate connection between the elements. This is provided by the application of

wedges, preferably of the same timber species of the planks, which are custom-made in situ depending on the presented irregularities. These wedges are hammered in the gap between the beam and the plank and, at the discretion of the carpenter (or onsite worker), may be connected to the structural system by means of glue (e.g. white wood glue) (Figure 17). Dimension and shape of the wedge are parameters that may influence the choice to use of white glue. It is firmly recommended to avoid the use of very rigid glues as the intention is only to maintain the wedge in position prior to the placement of the wooden pegs.
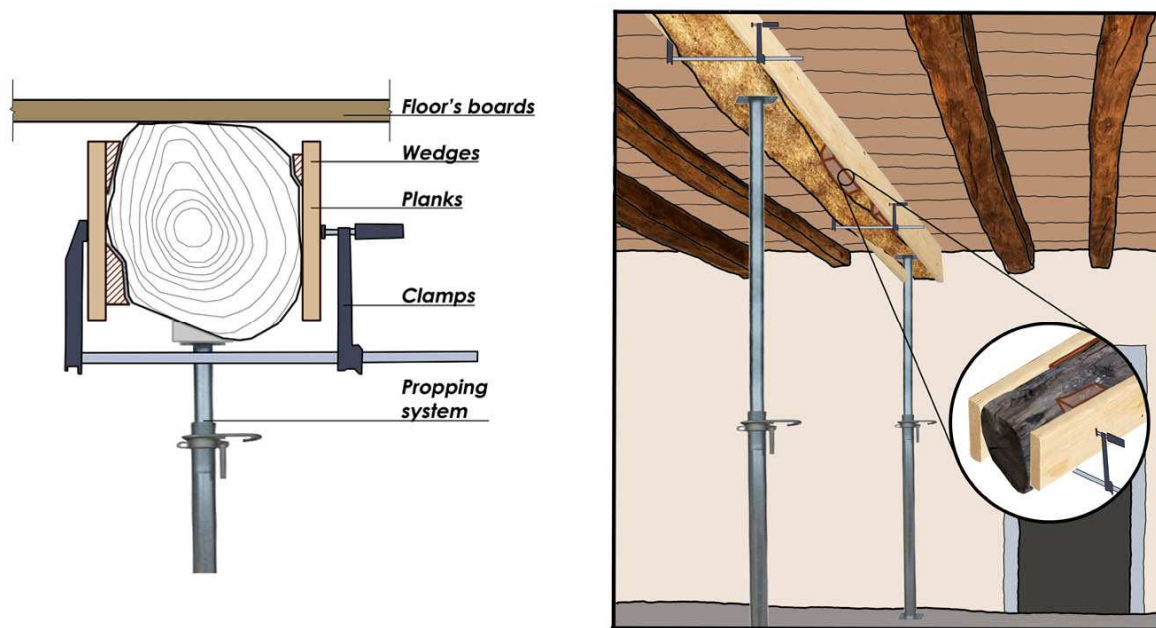
Figure 17 –Step 4: wedges positioning.

STEP 5 – Coring and location of timber pegs:

In this step, the holes of the timber fasteners are cored and the peg is inserted right after (Figure 18). It is recommended to proceed always symmetrically and progressively from one end of the beam to the other, and to intervene on both the sides at the same time alternating the sides of application. For this specific strengthening method, the penetration length is not defined by the code rules as it depends on the cross-section of the beam itself, more precisely the hole has to be at least 2 cm longer than half of the base of the beam, in this way an overlap of the area of interest of the pegs is guarantee. This aspect is extremely important due to the symmetry of the approach: if pegs shorter than half of the beam base were used, a failure line is induced during the procedure. This could lead to the formation of internal cracks along the grain direction. In the worst scenario this can cause the division of the cross- section creating two independent beams. This is especially critical for small width sections and when using large diameter pegs. The use of longer pegs allows an uniform distribution of

the stresses along the cross-section (Figure 19). As the rule code in [5] highlights, it is recommended to drill a hole with a diameter 1 mm thinner that the diameter of the used peg.

Because of the irregular nature of an existing timber element, the penetration length could be variable, thus it is strongly recommended to pre-cut the pegs and avoid to cut the fastener after its insertion because the hammering may cause the formation of cracks parallel to the grain due to the consistent length of the element. As for the wedges, white glue can be used to keep in position the pegs for the time necessary at the installation.

In the case of light irregularities on the surface due by too long fasteners, it is recommended to clean the surface until it reaches a level smooth again.
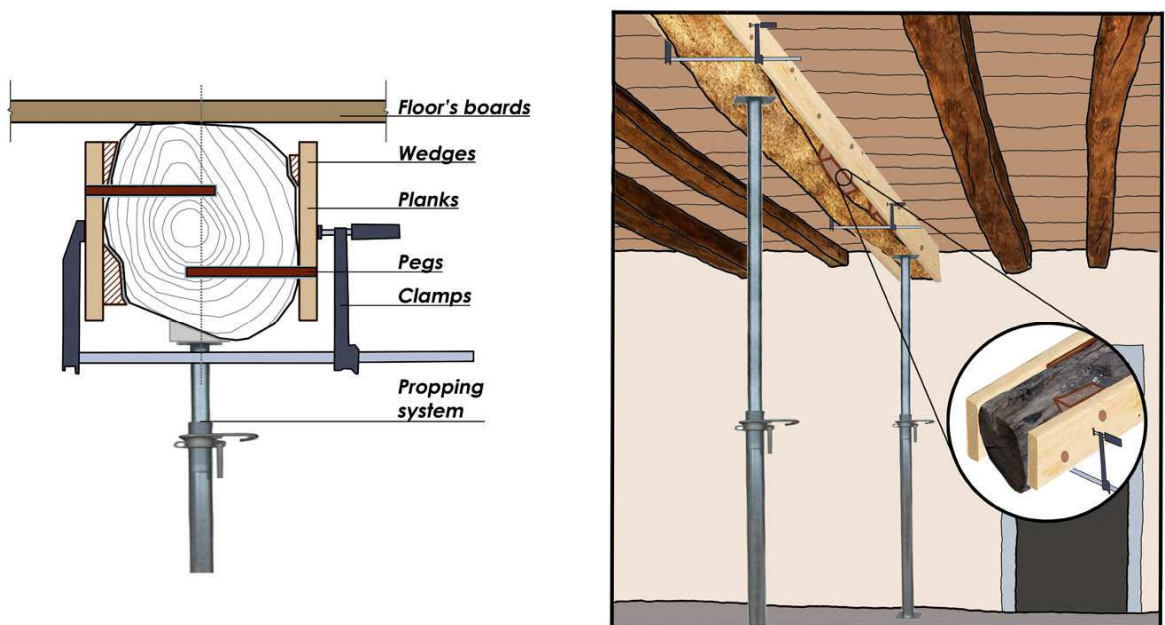
Figure 18 – Step 5: coring of the pegs' holes.
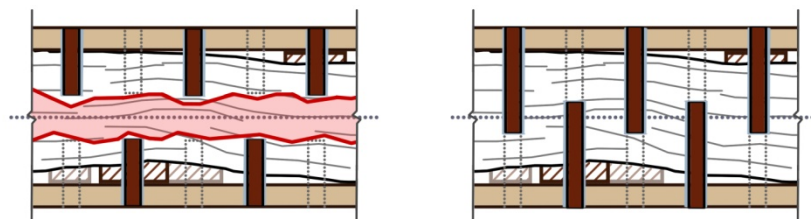
Figure 19 – Plan with cored holes shorter than half of the beam's thickness (left) and overlapped (right).

STEP 6 – Removal of the propping system:

Once the installation of the pegs is finished and the holes in the wall are filled, the propping system can be removed (Figure 20). Because of its dry nature, this technique does not require an additional time to set and to influence the structure.
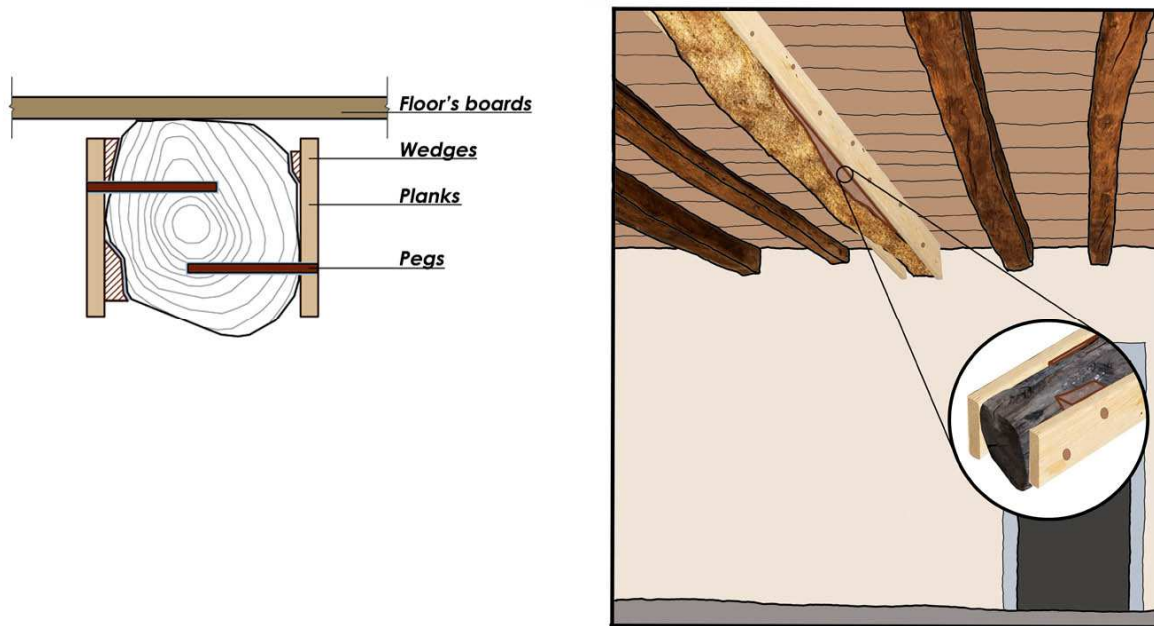
Figure 20 – Step 6: Removal of the propping system.

3.2   FRAMEWORK

The overall procedure of the technique, described in the previous topic, can be grouped in three main phases. The first one regards all the actions aimed to the preparation of the structure and to the intervention, being composed by steps 1 and 2 (installation of the propping system, inspection and cleaning). This section corresponds to the preliminary works do be done before the retrofitting technique itself. The following phase corresponds to the intervention itself structured on the steps 3, 4 and 5 which focus respectively on the installation of planks, wedges and pegs. The final section sees the dismantle of the propping system. Figure 21 shows the structure of the method.
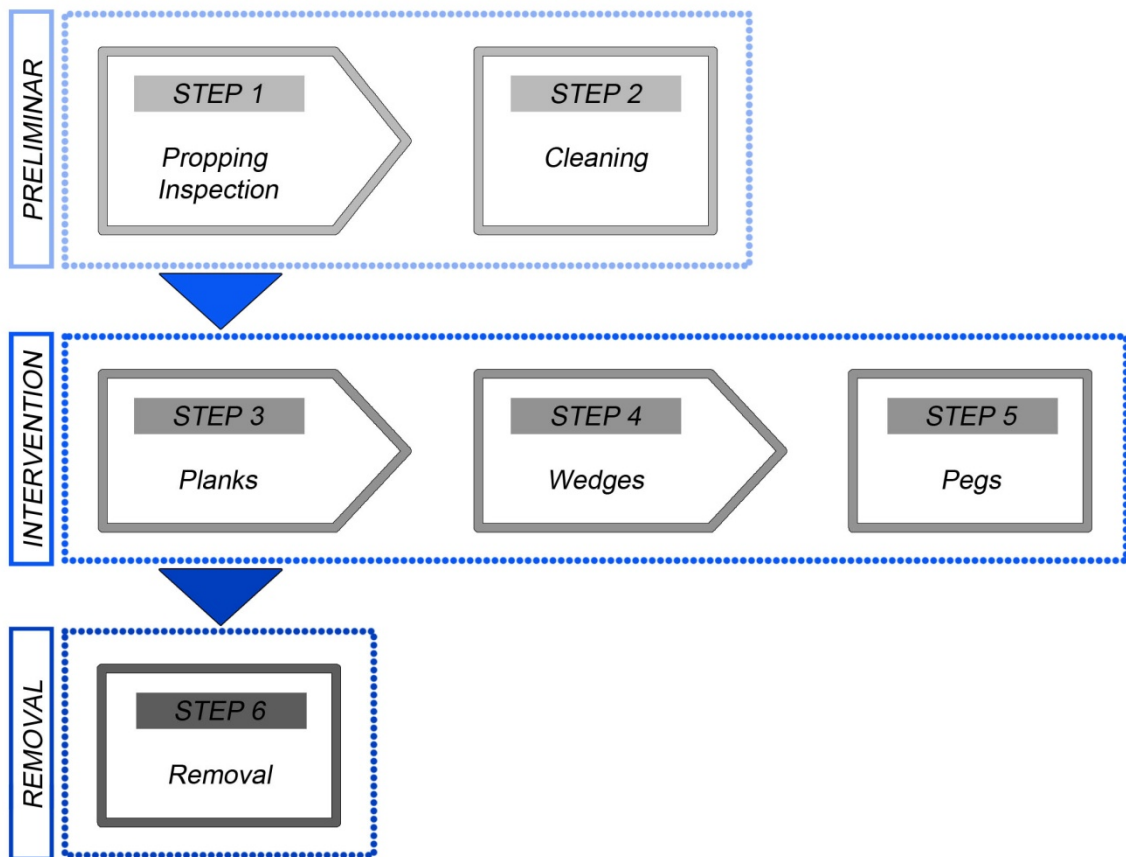
Figure 21 – Summary of the step of the strengthening technique.
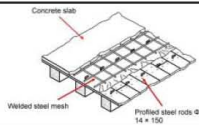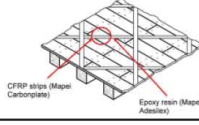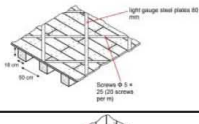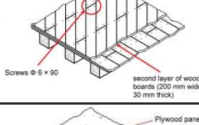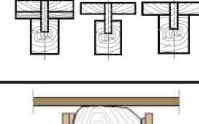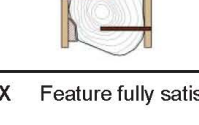
3.3 TECHNIQUE COMPARISON

The final result is a timber beam which cross-section was increased along with its stiffness and bending strength which result in a higher capacity of the structure when subjected to vertical load. Because of the type of application, this technology cannot be applied on timber floors with decorated or painted intrados, but can be used on historic timber structure guaranteeing the minimum loss of ancient material along with the lesser use of new material. Because of its dry connection its application is fast and does not require a significant time for application.

Table 1 summarizes the differences and the similarities of all the retrofitting methods considered and described in chapter 2 and compares it with the proposed technique. Considering what is highlighted in that table, one can say that the technique analysed in this work appears as one of the most suitable for historic structure in matter of compatibility for both structure and material and reversibility. These are points which aim at the preservation of the existing elements and structure. An important aspect as the lack of susceptibility to the environment at the moment of application, speed and easiness of

installation, highlights this technique as extremely interesting in the panorama of structural strengthening of existing timber elements.

Table 1 – Comparison of the strengthening techniques.

		Compatible w/ structure	Compatible w/ material	Reversible	Not susceptible during application	Fast to apply	Easy to apply	Increase thickness	Applied on extrados	Applied on intrados	Suitable for historic structures	Suitable for historic structures with artistic value
Concrete slabs		-	-	-	-	-	X	X	X	-	-	-
FRPs		X	-	-	-	X	-	-	X	-	-	-
Steel plates		X	-	/	X	X	X	-	X	-	/	X
Timber floor-boards		X	X	X	X	/	X	X	X	-	X	X
Plywood and steel rods		X	/	/	X	/	X	X	X	-	/	/
Timber planks in the extra-dos		X	X	X	X	/	/	X	X	-	X	X
Timber planks in the intra-dos		X	X	X	X	X	X	-	-	X	X	-

X   Feature fully satisfied   **/**   Feature partially satisfied   **-**   Feature not satisfied

4. MATERIAL CHARACTERIZATION

With the intention of replicate what the current panorama of historic buildings in Portugal offers, two timber species were chosen to be analysed, chestnut and pine. The chestnut (*Castanea sativa*) elements were retrieved from different buildings from the North of Portugal and were used as elements to be reinforced. The beams came from buildings with more than 70 years old and were previously used as timber floor beams. Planks of pine (*Pinus pinea*) were used as retrofitting elements as it corresponds to a material easily accessible. For the fasteners, hardwood timber pegs of Massaranduba (*Manilkara spp*) were used due to its hardness, durability and high mechanical properties suitable for the use has timber pegs [19].

In order to prepare the experimental campaign, the mechanical characteristic of the three timber species were identified with different approaches. Destructive tests for density and bending strength were carried out on samples of old Chestnut retrieved from parts of the elements to be used in the experimental campaign. The mechanical properties of pine planks were identifies following the information provided by the manufacturer and provided by reference codes [20],while the values for Massaranduba were determined through previous experimental campaigns available on literature[19].

4.1 CHESTNUT

Destructive tests were carried out in order to evaluate the properties of density and bending strength of the Chestnut beams. Both procedure and dimensions of the samples were extrapolated from the American standards (ASTM D 143) [21]. The results were then used to estimate the behaviour of the samples on the global scale (Chapter 4.4).

4.1.1 DENSITY

Destructive tests in order to compute the density were carried out on 10 samples (Figure 22) cut with dimensions of 25x20x20 mm^3 as defined by the code.

Figure 22 – Density samples.

Secondly, every element was accurately measured and weighted, their mass calculated and then placed in an oven set at 100.5 °C. Every 6 hours, with a total amount of 3 repetitions, the procedure of

measurement was repeated until an error lower than 0.5% in the mass was found. This allowed to evaluate the density (1) and moisture content (2) using the following equations from the codes (ISO 3130 and ISO 3131) [22] [23]:

$$\rho_w = \frac{m_w}{V_w} \tag{1}$$

$$W = \frac{m_1 - m_w}{m_1} \times 100 \tag{2}$$

where:

- m_w is the mass of the last measurement in kg;
- m_1 is the mass of the first measurement in kg;
- V_w is the volume of the first measurement in m^3.

The mean density was found equal to 571 kg/m^{3}and the mean moisture content corresponding to 12.16%. The value of density was eventually adjusted to 12% with the equation valid for a moisture content within the range of 7-17% [23] and was found equal to 570 kg/m^3, similar values were found in [24] and [25] also for the analysis of old chestnut elements. A value of Coefficient of Variation (CoV) equal to 4.4% was found, meaning that specimens had a fairly low variability.

$$\rho_{12} = \rho_w \left[1 - \frac{(1 - K)(W - 12)}{100} \right] \tag{3}$$

where:

- K is the coefficient of volumetric shrinkage equal to $0.85 \times 10^{-3} \rho_w$;
- ρ_w is the density previously calculated;
- W is the moisture content previously evaluated.

4.1.2 BENDING

A total amount of 7 samples with dimensions 300x20x20 mm^3 were tested with an actuator of 100kN at a displacement rate of 0.035 mm/sec (Figure 23). The specimens were retrieved from the end parts of the samples used in the double shear tests. Because all the samples were taken from old Chestnut beams which displayed a consistent pattern of damage and defects composed mainly by thin cracks and small knots, the specimens were cut with extreme attention in order to obtain elements composed by clear wood. In the cases where these conditions were not possible, the specimen was orientated in order to have the defect in the compressed face so that the failure mode (Figure 24) would not be influenced by it.

a) Specimens before the tests.   b) Bending test setup.

Figure 23 – Procedure of the bending tests.

Figure 24 – Failure modes of specimens tested for bending strength.

The vertical load which brought the specimen to failure was recorded for each sample and secondly both bending strength (see eq.(4)) and modulus of elasticity(see eq. (5)) were evaluated. The following equations were used:

$$\sigma_f = \frac{3FL}{2bh^2} \tag{4}$$

$$E_{m,0} = \frac{L^3}{4bh^3} \times \frac{\delta F}{\delta u} \tag{5}$$

Where:

- F is the vertical load in kN;
- L is the spacing between the two supports in mm;
- δF is the range of vertical load considered in kN;
- δu is the range of vertical displacement considered in mm;
- b is the base of the specimen in mm;
- h is the height of the specimen in mm.

Mean values were then determined and a mean value of 65 N/mm^2 (with a Coefficient of Variation of 17.1%) or the bending strength and 8448 N/mm^2 (CoV=19.8%) regarding the bending modulus of elasticity. As these values correspond to small clear wood specimens, it is needed to reduce them in order to have an indication of the value on an element scale. These values were thus decreased through by rate equal to 16.03% for stiffness and 46.18% for strength according to the scale (Table 2). These percentages were extrapolated from an experimental campaign based on the relation between mechanical properties on different scales of the same species previously carried out in [24].

Table 2 – Calculated and reduced values from the destructive tests.

	Bending strength (N/mm^2)	Density (kg/m^3)	MOE (N/mm^2)
Calculated	65	570	8443.5
Reduced	35	479	7092.5

4.2   PINE

The planks used to strengthen the existing beams were composed by pine (*Pinus pinea*) identified by the manufacturer as C24. Its mechanical characteristics were found following the indicative values present in EN 338[20], therefore the values in Table 3 were considered:

<div align="center">Table 3 – Mechanical properties of Pine (Pinus pinea) (C24).</div>

Bending strength	$f_{m,k}$	24 N/mm^2
Compression strength	$f_{c,0,k}$	2.5 N/mm^2
Modulus of Elasticity parallel to the grain	$E_{o,mean}$	11 kN/mm^2
Density	P_{mean}	420 kg/m^3

4.3   MASSARANDUBA

Mechanical properties regarding the Massaranduba pegs were extrapolated from existing literature, more precisely from the results of an experimental campaign carried out in the University of Minho focused on the study of double shear connections in Chestnut (*Castaneasativa*) and Spruce (*Piceaabies*). Massaranduba pegs with a diameter of 12mm and a length equal to 240 mm, moisture content of 17% and a density of 1100 kg/m^3 were used and tested as fastener for a dry timber connection. This study was able to estimate the maximum estimated force F_{est} of the connection for the Chestnut estimated equal to 14.5 kN per single peg [19].

4.4   RESULTS

The performed material characterization allowed an estimation of the local properties of each component of the retroffiting technique in order to have a first set of values for the prediction of the structural assemblage. The processed values were used in the experimental campaign carried out in the following step of the work and is presented in chapter 5. More in detail, the shear strength of the massaranduba pegstaken from [19] was utilised in the protocol of the double shear tests. Values for bending strength modulus of elasticity and density were used to estimate the overall performanceof the reinforced beams tested on the real scale. Reduced values calculated for chestnut were in addition used as comparison to verify the increased capacity provided by the strengthening technique.

Table 4 – Material characterization.

		Chestnut		Pine	Massaranduba
		Calculated	Reduced		
Bending strength	$f_{m,k}$ (N/mm^2)	65	35	24	-
Compression strength	$f_{c,0,k}$ (N/mm^2)	-	-	2.5	-
Modulus of Elasticity parallel to the grain	$E_{o,mean}$ (kN/mm^2)	8443.5	7092.5	11	-
Density	P_{mean} (kg/m^3)	570	479	420	1100
Shear strength	f_v (kN)	-	-	-	14.5

5. EXPERIMENTAL CAMPAIGN

The following described experimental campaign uses the strengthening technique explained in chapter 3 and is focused on two different scales: firstly on the local scale with a total amount of 30 double shear tests and eventually on a global scale through a 4-point bending test configuration carried out on two structural size beams.

Even though this technique is based on the concept of dry connection, as previously detailed, if considered necessary it is possible to use even a weak glue during the application in order to maintain the fasteners in position during the whole process. Because the possible structural influence of the glue is a variable to be considered, both scenarios were taken into account and a sample with white glue was compared with unglued specimens in order to verify if and how the presence of an adhesive (even though weak) could influence the structural response of the tests.

All the samples used in the experimental campaign were kindly provided by AOF.

5.1 DOUBLE SHEAR TEST

Double shear tests for each sample were carried out in order to evaluate the behaviour of the timber pegs once subjected to shear. The aim was to verify through the elaboration of the data collected if the technique adopted was able to provide a satisfying result in matter of shear strength and stiffness. To verify if the retrofitting technique could be considered satisfying and functional, particular attention was paid during the tests regarding the formation under solicitation of an active composite cross-section as long as the type of failures recorded on all the three used materials.

A total amount of 30 sample of various cross-sections in terms of shape were built in order to consider as much as possible the various range of cross-sections and geometric irregularities along the length of an existing beam. To provide the presence of a considerable irregularity consistent with the beam itself, a total length of the specimens equal to 70 cm was considered. The dimensions of the cross-section varied from a minimum of 17×8 cm^2 to a maximum of 20×16^2 cm and the geometry of cross-section itself considered several scenarios. Reinforcing timber planks in pine were then added by means of 6 Massaranduba pegs (3 per each side) with a diameter equal to 25 mm and a variable penetration length depending on the cross-section of the sample.

A peculiarity of this technique is the objective impediment of having a constant spacing between the fasteners. This feature is ruled by different reasons. First of all, the heavy difference in the geometry of the cross-sections along with the presence of defects (cracks and knots) which influence the location of the pegs. The third factor is the subjectivity of the technician himself who applies the retrofitting technique. His judgement will be conditioned by the visual inspection previously carried out and his

past personal experience. For all these reasons, it is recommended that the work is carried out by the same person, in order to have consistency along the same element.

Considering a variation in the geometry caused by the intrinsic irregularity of the studied elements, Figure 25 shows the design followed in the construction of the double shear samples.
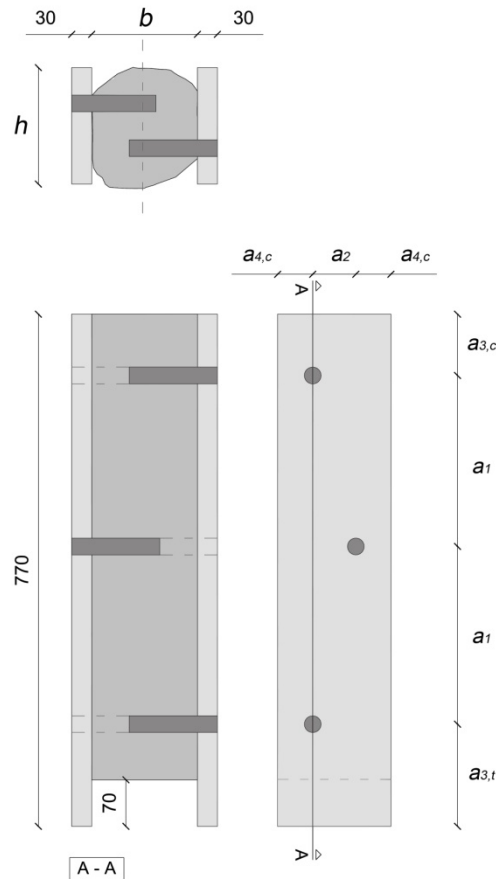
Figure 25 – Design for the double shear tests.

5.1.1 PREPARATION OF THE SAMPLES

Old chestnut beams of an average length equal to 2.80 m originally from different timber floors of private houses which were removed as a consequence of structural renovation, were used as base for the samples.

Figure 26 – Chestnut beams used for the samples.

Following the guidelines exposed previously, the specimens were built as Figure 27 shows. It is important to highlight that in this case the holes were all cored before the introduction of the pegs due to the reduced dimension of the specimen itself. On the real scale is recommended to insert one peg at a time has to promote a better fit of the planks with the element to be retrofitted.

a) Cleaning of the surface.

b) Positioning of the planks.

c) Introduction of the wedges.

d) Coring of the holes for the pegs.

e) Introduction of the pegs.

f) Filing of the surface.

Figure 27 – Procedure to the construction of the tests.

A geometrical survey followed by a visual grading inspection was made for all the samples in order to separate them into different possible samples as to estimate their structural behaviour. A preliminary division in groups of the elements was thus necessary and to reach this purpose factors like shape of the cross section and the presence of glue was considered. Eventually the panorama provided 18 glued samples divided in 4 groups and 12 unglued sample divided in 3 groups. Figure 28 shows their grouping along with the cross-section of both the end of the specimen. The labelling of the specimens is based on three groups of letters, where the first refers to if the cross-section is regular (R) of irregular (I), the second letter refers to the geometry of the cross-section: circular (C), squared (S), semi-circular (SC) or with parallel edges (P). The last letter explains if the sample is glued (G) or unglued (NG).
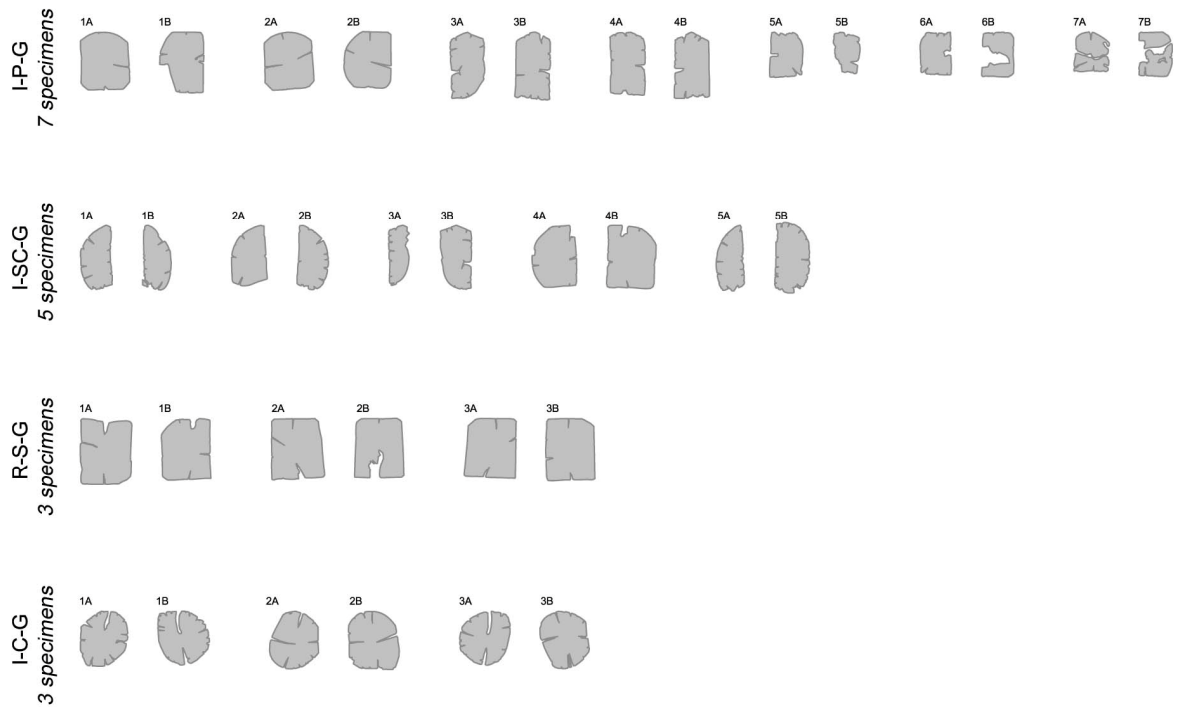
a) Glued elements
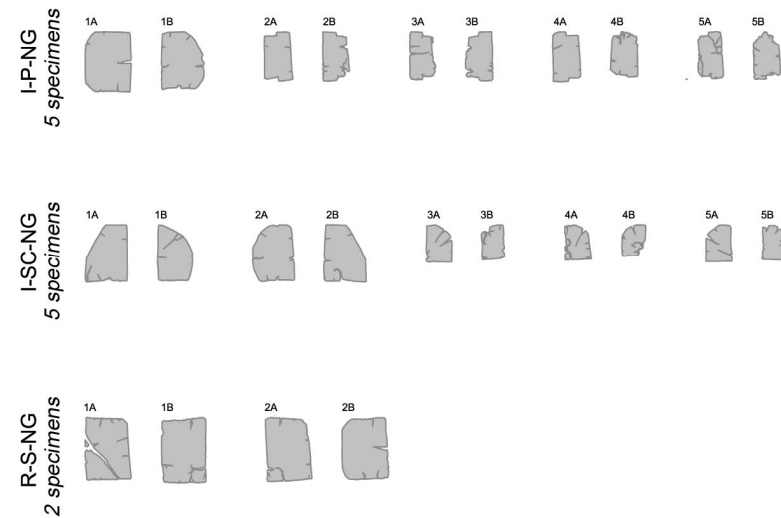
b) Unglued elements.

Figure 28 – Grouping and labelling of the samples.

The geometrical survey aimed to identify the precise dimension, mean area and inertia considering both the sides of the chestnut elements. The pine planks were also measured, as well as location and spacing of the pegs were recorded for each sample.

A visual grading of the samples was made following the procedure provided by the codes (UNI11119_2004) [26] which aims to verify if the indicative values, given by visual inspection, can be used as benchmark for the element's performance. The procedure is based on the identification of the critical zones for each type of defects (knots, wanes and cracks) to which is given a value based on the ratio between the dimension of the defect itself and the cross-section where it is located. The grading is ruled by the most conditioning parameter (Table 5).
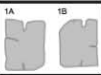
Not considered in [26], the influence of the wedges was however evaluated due o its importance through a ratio between the total length of all the wedges present and the length of the sample itself. The grading was given equal to I in case of wedges ≤ 1/8, if wedges in the range 1/8 ≤ x ≤ 1/5 were present the grading given was II, for wedges ≥ 1/3 the lowest grading (III) was attributed.

 Table 6 shows an example of the survey done.

Table 5 – Grades of timber members [26].

Feature	On site grade		
	I	II	III
Wanes	1/8	1/5	1/3
Various damages frost cracks ring shakes	absent	absent	admissible only if limited
Single knots	≤1/5 ≤50mm	≤1/3 ≤70mm	≤1/2
Group of knots	≤2/5	≤2/3	≤3/4
Slope of grain in radial section	≤1/14 (-7%)	≤1/8 (-12%)	≤1/5 (20%)
inclination% in tangential section	≤1/10 (10%)	≤1/5 (20%)	≤1/3 (-33%)
shrinkage checks	admissible if not passing through the pith		

Table 6 – Geometrical survey and visual grading of the double shear samples.

	Cross sections	Area (cm²)	Length (cm)	Inertia (cm⁴)	Wedges	Wane	Knots	Groups of knots	Cracks
R-S-G-1		320.8	69.5	10843.5	I	I	-	I	III
R-S-G-2		325.2	66.8	9758.9	I	I	-	II	III
R-S-G-3		316.8	66.1	10360.2	I	I	III	-	III
R-S-NG-1		278.2	72.3	8110.2	I	I	-	I	III
R-S-NG-2		282.4	73.2	9229.8	I	I	-	I	III

5.1.2 SET UP

The procedure from EN 26891 – 1991 [27]was adopted for all the samples and the set up was prepared as Figure **29** shows. An actuator of 200kN was used.
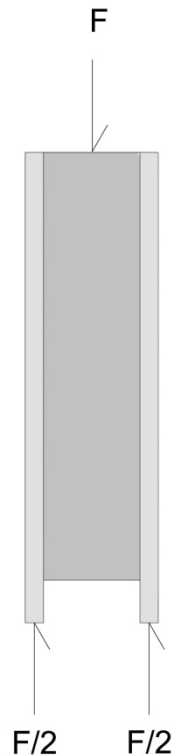
Figure 29 – Double shears tests' set up.

5.1.3 TESTS

The protocol to carry out the tests was planned extrapolating the expected maximum force $F_{max,est}$ from the literature available [19] which identified the estimated load of a timber connection of Chestnut elements by mean of a Massaranduba timber peg with a diameter equal to 12 mm. Because of the bigger diameter of the peg and the presence of a higher number of fasteners and the use of old timber with irregular cross-section, the protocol for the experimental campaign was planned considering an estimated maximum force $F_{max,est}$ equal to 40 kN.

The procedure adopted was composed by the following steps: with a force-control approach a load of 16kNequal to $0.2F_{max,est}$was applied monotonically and then maintained for 30 seconds. Secondly the force was reduced at 4 kN equal to $0.1 F_{max,est}$ and maintained again for 30 seconds. Eventually the load was increased until the sample reached failure with a constant velocity of 0.16 mm/sec, after the failure the test stopped once the force reached 0.5 of the maximum vertical load recorded during each

test. Displacement rate was calculated as to promote reaching failure at 300 ± 120 s after the beginning of the final cycle. In this way the failure occurred averagely in 210 sec.

Figure 30 shows graphs of the loading procedure and the expected load-deformation curve.
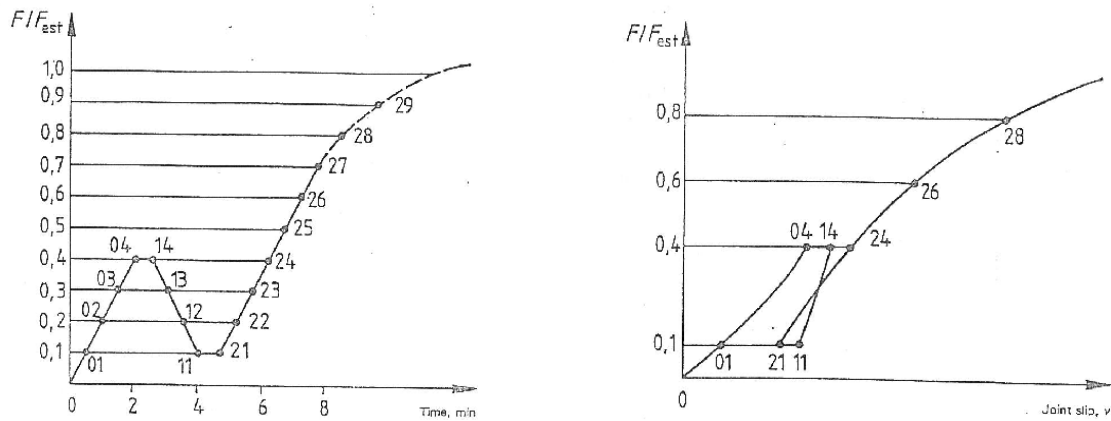
Figure 30 – Loading procedure (left) and idealized load-deformation curve and measurements[27]**.**

For each test the sample was confined laterally in order to avoid horizontal displacements and was maintained in position with the use of clamps, two LVDTs were then applied on the front and on the back of the test specimen in order to record the relative vertical displacement between both the reinforcement planks and the middle element (Figure 31).

Figure 31 – Sample R-S-NG-1 front (right) and beck (left).

First the glued sample and then the unglued one were tested and the data collected. For each case, the mean value of the displacement recorded by the two LVDTs was considered and graphs of their structural response were plotted. Figure 32 and Figure 33 show an example of respectively one glued and one unglued sample with the pictures taken at the beginning, maximum vertical load and end of the test.
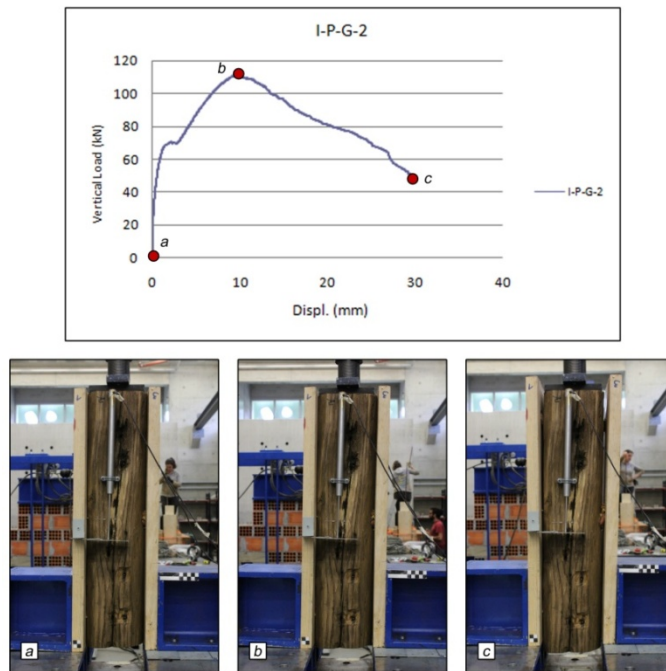
Figure 32 – Sample I-P-G-2 double shear test.
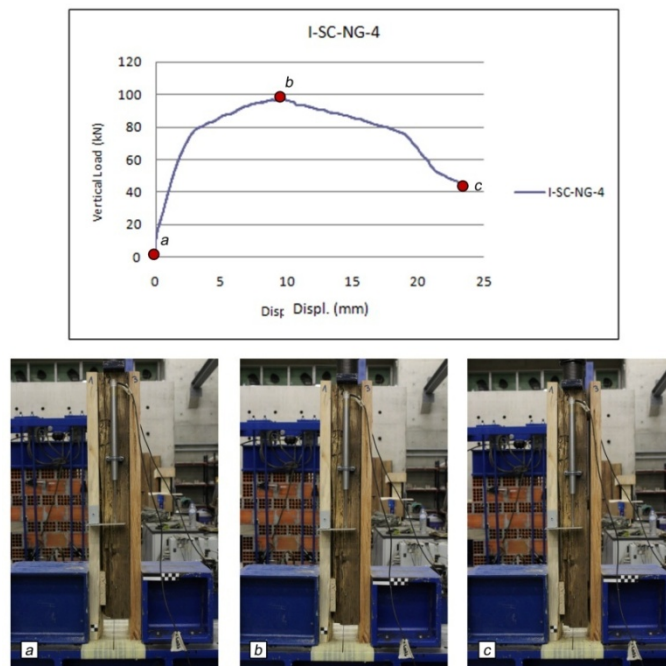
Figure 33 – Sample I-SC-NG-2 double shear test.

5.1.4 RESULTS

Data from all the 30 specimen were collected and analysed, values of maximum, minimum and mean vertical load and slip were recorded. Table 7 shows these values while Figure 35 shows the overlap of the areas of influence of the two types of tested sample. It is possible to notice how the glued samples reached a higher maximum load than that of the unglued specimens (111.49 kN against 97 kN) but at the same time provided a less uniform response when compared with the unglued specimens. In fact, the obtained standard deviation was equal to 29.18 kN for the unglued sample and 14.24 kN for the glued elements which allowed to evaluate the coefficient of variation (CoV). For glued elements avalue of CoV=15.73%was found, while unglued elements the value was CoV=8.96% proving how the unglued samples provided a more unified behaviour.

Table 7 – Data collected from double shear tests.

Type	Parameter	Min	Max	Mean	CoV (%)
Glued	Vertical load (kN)	60.5	111.49	90.5	15.7
	Slip (mm)	12.18	25.63	15.67	21.8
Unglued	Vertical load (kN)	67.8	97	81.4	8.9
	Slip (mm)	12.46	18.39	13.95	8.9

Figure 34 shows the plot of the load-displacement relation evaluated through the double shear test for both glued (Figure 34a) and unglued (Figure 34b) specimens. These were used in order to plot the envelopes of load-displacement curves (Figure 35).

a)

b)
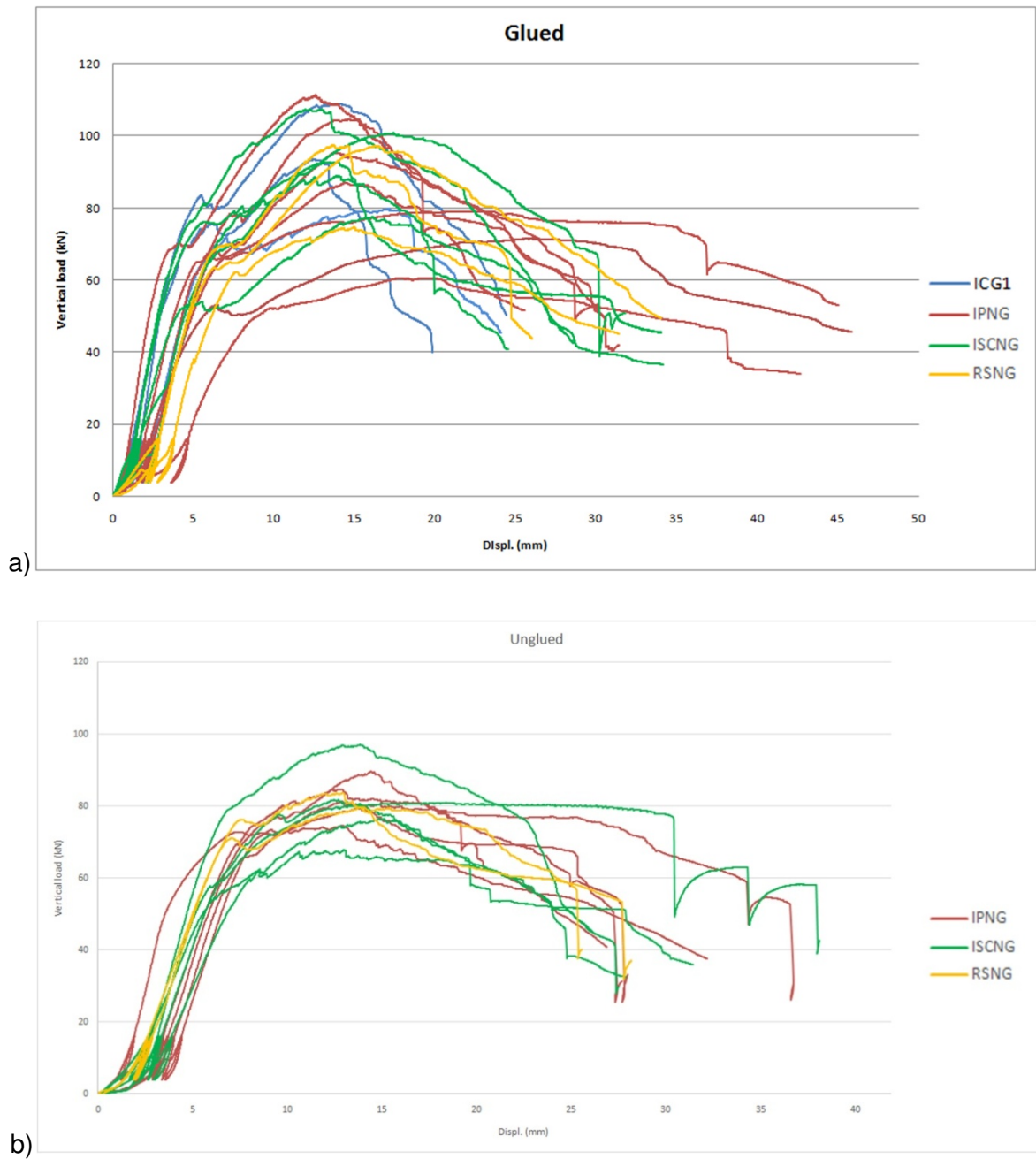
Figure 34 – Load – displacement curve of the double shear tests, glued (a) and unglued sample (b).
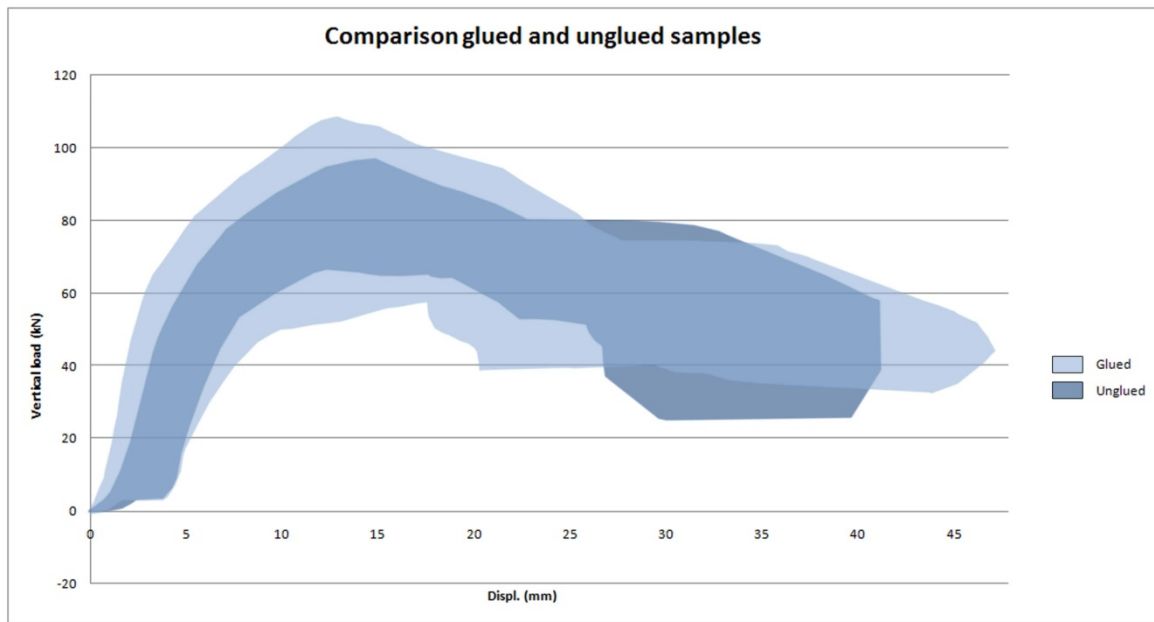
Figure 35 – Envelope of load displacement curve.

The ductility was then evaluated for each sample(example in Figure 36) through the computation of the Equivalent Energy Elastic-Plastic Curve (EEEP) [28] based on the bilinear curve representative of the balance of the energy dissipation as the area below the curve is equal to the area over it. The bilinear curve is evaluated through the initial stiffness K which lays between 0% and 40% of the peak load and is represented by the first line, while the deformation at failure is equal to 80% of the peak load. The yield load is evaluated with equation (6).

$$P_y = \left[\Delta_{failure} - \sqrt{\Delta^2{}_{failure} \; \frac{2w_{failure}}{K}} \right] \times K$$

(6)

where:

- P_y is the yield load;
- $\Delta_{failure}$ is the deformation at failure;
- $w_{failure}$ is the energy dissipater until failure;
- K is the initial stiffness.

Values of stiffness for both glued and unglued samples were calculated with the help of the software MATLAB. Figure 37a and b shows the envelopes respectively for glued and unglued samples, where the chromatic differentiation is ruled by the criterion based on the cross-section's shape used to originally subdivide the samples.
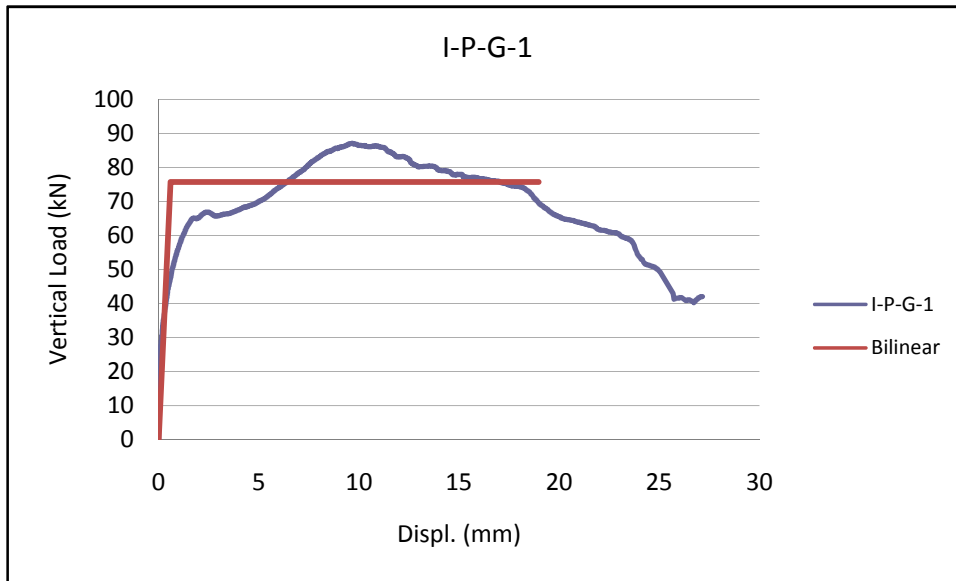
Figure 36 – Sample I-P-NG-1estimation of stiffness.

a)
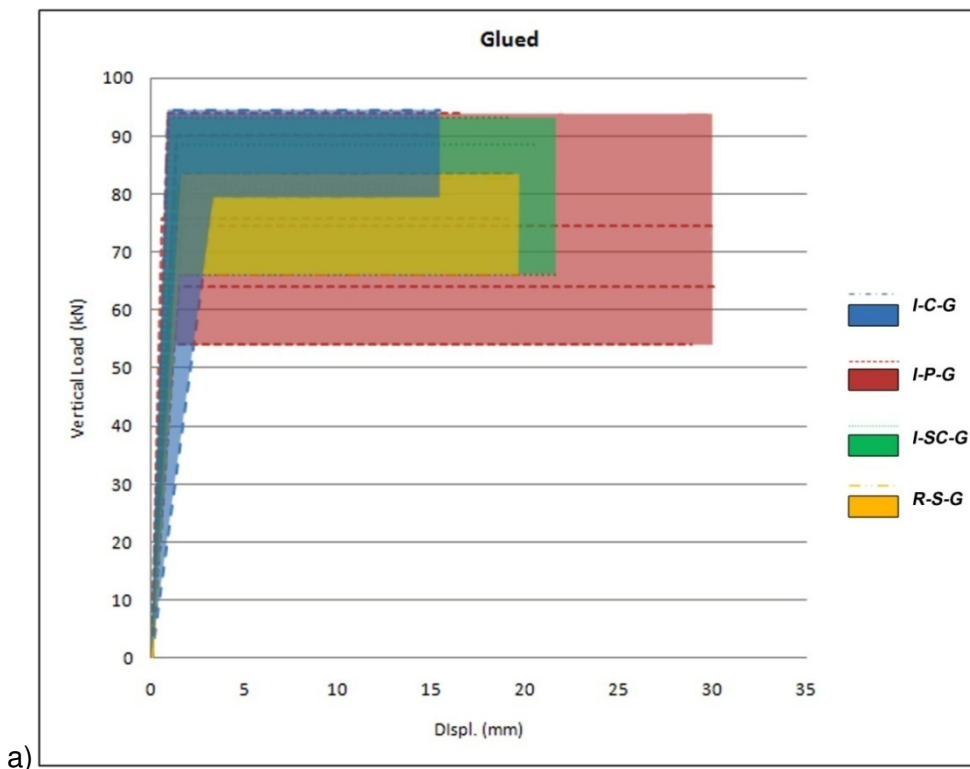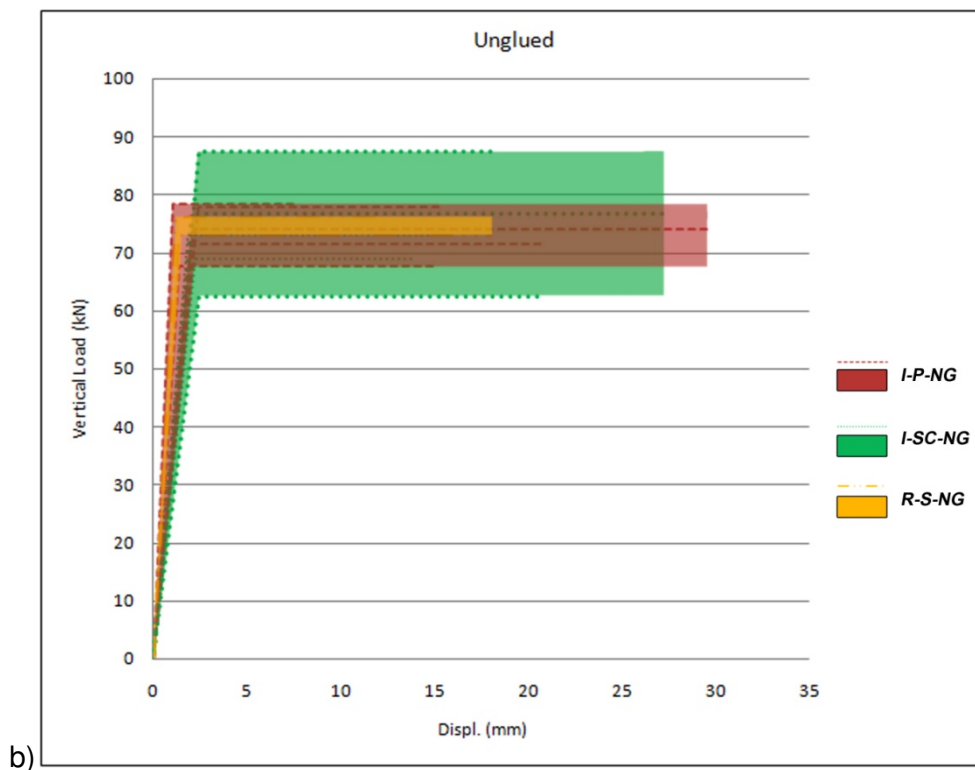
Figure 37 – Bilinear envelope curves for glued (a) and unglued samples (b).

After, from the mean values for glued and unglues specimens the coefficients of variation were calculated and compared (Table 8) with the scope of verifying a possible pattern in the structural behaviour. As already outlined, the unglued samples showed a more homogeneous response, this is clearly graphically visible in the envelopes' representation as in the values evaluated through the coefficient of variation.

Table 8 – Stiffness double shear tests.

	GLUED (18 samples)	UNGLUED (12 samples)
Maximum (kN)	27.67	14
Minimum (kN)	4.5	6.22
Mean (kN)	16.34	9.34
CoV (%)	45.2	28.1

With the purpose to identify a possible link between the structural behaviour and the visual grading conducted initially on the samples, a parametric analysis was carried out. More precisely, considering the grading given to the presence of wedges, wanes and knots, an investigation was done to see if

samples which received the same grading had a similar structural response in matter of the obtained maximum vertical load per specimen. In case of a positive correlation it would have been possible to individuate the feature able to influence directly the mechanical characteristic of the retrofitting technique. All the samples were grouped following the grading values of the considered feature (Table 9) and in a second moment the mean value of the vertical load recorded during the tests was calculated for both glued and unglued elements (Table 10).

The possible influence of the cracks was not considered in this analysis because all the samples got a grade equal to III.

Table 9 – Grouping of the samples ruled by the visual grading.

a)   b)   c)

Table 10 – Mean values of vertical load per each feature of the visual grading.

	F_{mean} (kN)					
	GLUED SAMPLES			UNGLUED SAMPLES		
	Wedges	Wanes	Knots	Wedges	Wanes	Knots
I	92.59	82.30	95.15	82.26	83.16	81.69
II	92.37	99.27	83.37	85.37	78.65	81.27
III	87.37	94.93	94.90	76.67	80.25	81.17

The values collected were plotted and analysed. Regarding the glued samples (Figure 38a) it is possible to notice a light influence when the wedges are considered, as the higher the grading the higher the mean vertical load recorded. Nevertheless, this correlation is not strong enough to be considered univocally predominant in the structural response of the samples. On the other hand no substantial difference is noticeable in the case of unglued specimens which display an almost constant response (Figure 38b).

These elements lead to the consideration that apparently none of the aspect considered by the visual gradin nor the cross-section irregularity itself were significant for the mechanical characteristics of the studied retrofitting technique. To further prove this conclusion, an analysis of variance (ANOVA)was made to the different clusters of the samples. In this case, ANOVA was used to test whether visual grading contributes significantly to the variation of vertical load. In this case, a single-factor ANOVA and a confidence level of 95% revealed a non-significant variance in maximum load. Therefore, it is demonstrated that the partition of the results with consideration to the visual strength classes did not allow to obtain samples with significant statistic variation values between them, thus evidencing non different clusters of measurements. Accounting this premise, visual inspection grading was not able to be an indicator to distinguish specimens with different load values.

In conclusion one may say that a lower value of Cov and thus a lower variation in the output was found for the unglued sample which presented a than the glued sample.
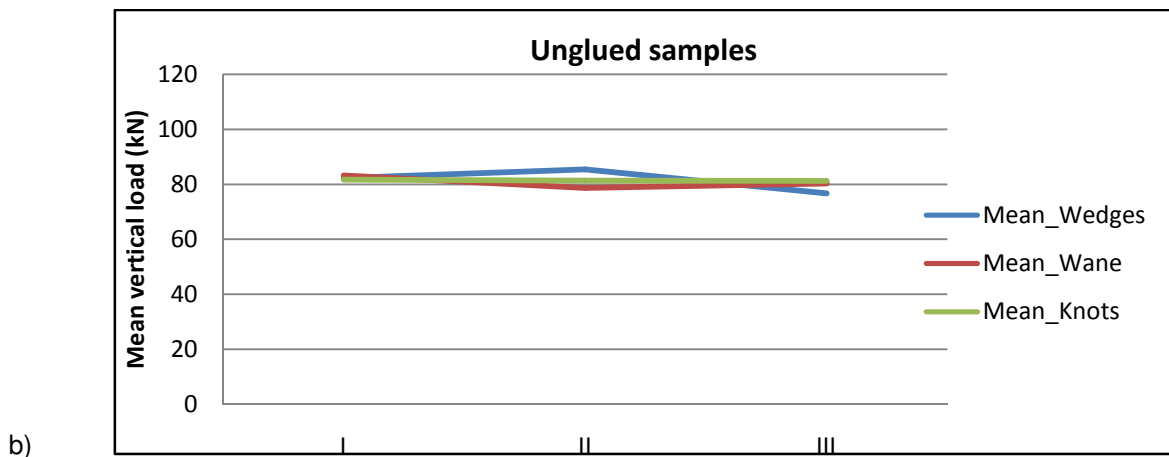

a)

b)
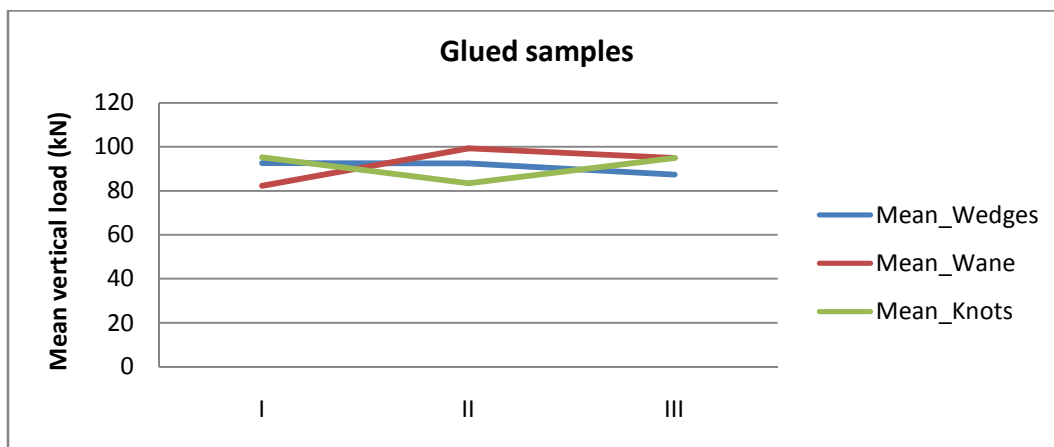
Figure 38 – Plot of mean values of vertical load considering the visual grading for glued (a) and unglued (b) specimens.

5.1.5 PEGS

Two glued and two unglued specimens were then chosen to be opened longitudinally in order to observe the failure modes of the pegs. The aim was to observe the wide range of failure modes occurred. Two different scenarios were recorded: the first which leads to the formation of one hinge and the resulting division of the fastener in two separate segments, the second failure mode is characterised by the formation of two hinges whose presence can bring to the division of the timber dowel in three separated elements (Figure 39).

In general, a higher amount of brittle failure of the connection was recorded in the unglued samples. An example of more ductile behaviour was performed by the glues specimens. Figure 40 compares a glued sample (I-P-G-6 on the left) with an unglued example (I-P-NG-2 on the right): 3 out of 6 pegs connecting the unglued sample failed in a brittle way, while in the glued example 5 fasteners out of 6 maintained a ductile behaviour.

Is important to underline that if along the peg's length a void was present between the pine plank and the chestnut beam, the peg evidenced a higher tendency to break with a fragile behaviour.
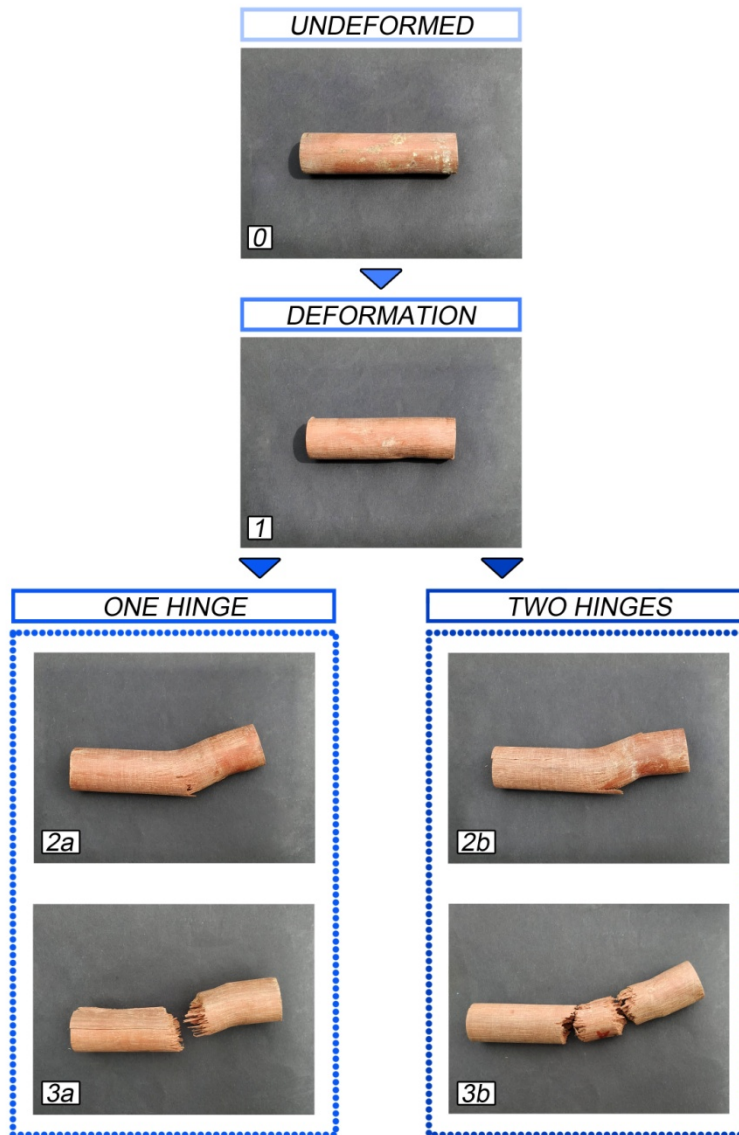
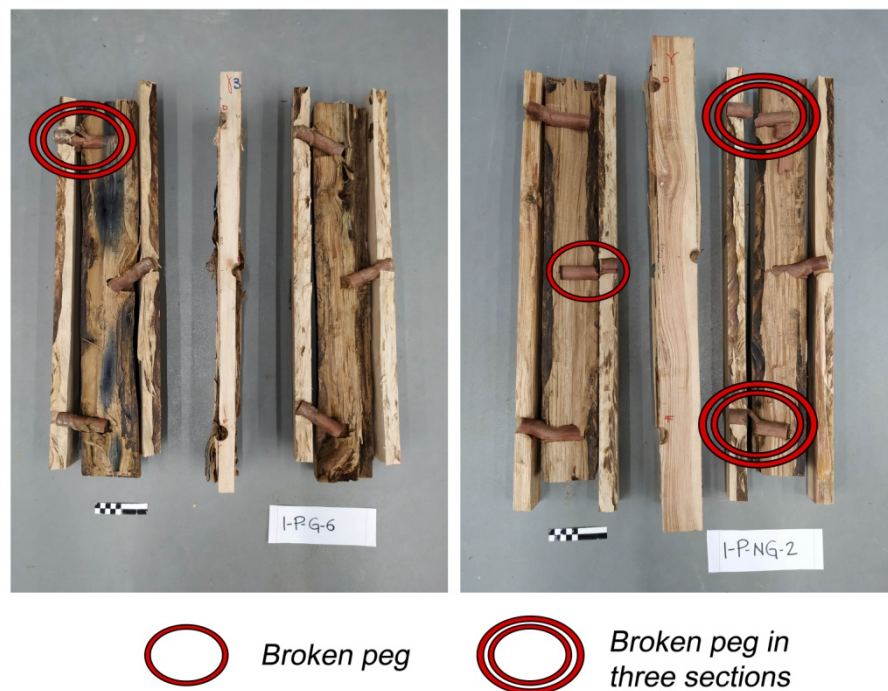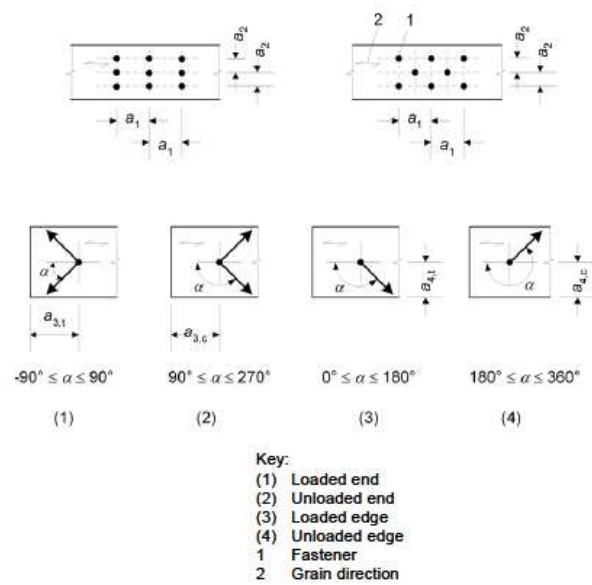**Figure 39 – Failure modes of Massaranduba pegs.**

Figure 40 – Samples I-P-G-6 (left) and I-P-NG-2 (right) after the cut.

The results so far clearly showed that even a weak type of adhesive is able to influence heavily the structural response of the element, as a difference of 12% in matter of vertical load recorded was found between the glued and unglued specimens. At the same time glued samples were characterized by a stiffness twice the unglued one and displayed a more ductile performance, as showed by the failure modes of the pegs.

The last feature considered in the analysis was the spacing between the pegs. As already said the geometry of the specimens is characterized by a randomness in the placement of the pegs that is ruled by the geometry of the existing structure, the judgement proper of the technician that applies the retrofitting technique and the presence on existing defects such as cracks and knots. For these reasons was impossible to define a regular and constant spacing between the Massaranduba fasteners. Nevertheless, an accurate geometrical survey was carried out and the found results were compared with the minimum spacing reported in the Eurocode5 [5]. Because of the lack of code ruling the design of connection with timber pegs, the values for metal dowel were taken as reference (Table 11).

Table 11 – Minimum spacings and edge and end distances for dowels [5]**.**

Spacing and edge/end distances (see Figure 8.7)	Angle	Minimum spacing or edge/end distance
a_1 (parallel to grain)	$0° \leq \alpha \leq 360°$	$(3 + 2\left| \cos \alpha \right|) \, d$
a_2 (perpendicular to grain)	$0° \leq \alpha \leq 360°$	$3 \, d$
$a_{3,t}$ (loaded end)	$-90° \leq \alpha \leq 90°$	$\max(7 \, d; \, 80 \text{ mm})$
$a_{3,c}$ (unloaded end)	$90° \leq \alpha < 150°$	$\max(a_{3,t}\left| \sin \alpha \right|) \, d; \, 3d)$
	$150° \leq \alpha < 210°$	$3 \, d$
	$210° \leq \alpha \leq 270°$	$\max(a_{3,t}\left| \sin \alpha \right|) \, d; \, 3d)$
$a_{4,t}$ (loaded edge)	$0° \leq \alpha \leq 180°$	$\max([2 + 2\sin \alpha) \, d; \, 3d)$
$a_{4,c}$ (unloaded edge)	$180° \leq \alpha \leq 360°$	$3 \, d$

Key:
(1) Loaded end
(2) Unloaded end
(3) Loaded edge
(4) Unloaded edge
1   Fastener
2   Grain direction

Following the formula of the codes the minimum spacing needed for a timber peg of a diameter of 25 mm were computed (Table 12) and then compared with the values collected during the geometrical survey previously carried out (Table 13).

Table 12 – Minimum spacing considering EC5 formula.

MINIMUM SPACING (mm)	
a_1	97.4
a_2	75
$a_{3,t}$	175
$a_{3,c}$	75
$a_{4,c}$	75

Table 13 – Geometrical survey of the pegs' spacing in the double shear tests.

PEGS' SPACING (mm)					PEGS' SPACING (mm)			
	Mean value		Min value			Mean value		Min value	
Samples	a_1	a_2	$a_{3,c}$	$a_{4,c}$	Samples	a_1	a_2	$a_{3,c}$	$a_{4,c}$
R-S-G-1	261	92	75	40	I-P-NG-4	267	72	80	45
R-S-G-2	265	85	55	40	I-P-NG-5	262	61	75	47
R-S-G-3	275	87	32	45	I-SC-G-1	261	100	65	40
R-S-NG-1	262	90	80	50	I-SC-G-2	257	107	75	45
R-S-NG-2	267	107	80	50	I-SC-G-3	256	92	75	45
I-P-G-1	259	80	50	45	I-SC-G-4	257	97	90	45
I-P-G-2	255	80	80	39	I-SC-G-5	257	112	70	45
I-P-G-3	265	117	75	40	I-SC-NG-1	270	90	80	42
I-P-G-4	262	94	75	50	I-SC-NG-2	270	100	75	52
I-P-G-5	261	32	85	40	I-SC-NG-3	264	53	77	35
I-P-G-6	256	30	80	40	I-SC-NG-4	268	40	80	37
I-P-G-7	260	32	70	40	I-SC-NG-5	253	32	80	40
I-P-NG-1	264	87	80	50	I-C-G-1	256	51	70	45
I-P-NG-2	270	60	80	50	I-C-G-2	259	69	76	40
I-P-NG-3	257	60	83	47	I-C-G-3	260	72	72	42

The elements highlighted in red are the values which were recognised lower than what demanded by the code. It is visible how the minimum spacing for a_1 was widely satisfied, while the values for a_2 and $a_{3,c}$ presents some underestimated spacing. On the other hand, not a single specimen satisfied the minimum value requested for $a_{4,c}$.

Of all these the values, marked in green are the one which did not suffer failure dependent on that spacing value, in yellow the values which suffered minor damages such as the formation of cracks which did not reach collapse and the elements which suffered a failure are highlighted in orange. It is important to underline that, out of all the undersized minimum spacing, only one sample faced the formation of a crack (Figure 41) and only one reached the collapse of the edge (Figure 42), both of them were placed in the unloaded end.

Figure 41 – Failure of sample I-SC-G-1.

Figure 42 – Failure of sample R-S-G-3.

Looking at the general behaviour of the sample one can say that a safe threshold was found for $a_{3,c} \geq 2.8d$ and for $a_{4,c} \geq 1.4d$.Nonetheless, the results made with this analysis lead to the conclusions that what ruled by the codes regarding the minimum spacing required, is valid and applicable to the retrofitting technique here studied.

5.2   4-POINT BENDING TEST

With the scope of verifying the global performance of the retrofitting technique and its influence on the mechanical properties of a timber element, the last step of the experimental campaign focused on full size structural elements. Two4-point bending test were carried out on two real scale beams, one specimen with glued connection and one other with unglued connection, similarly to what was done on the local scale for the double shear tests. Named with the same criterion adopted for the double shear tests, the two beams were defined as B-I-G-1 for the glued element and B-I-NG-1 for the unglued sample.

Built as described in chapter 3, both the specimens were composed by a central existing timber beam in chestnut of the same origin and age of the timber used for the local scale tests to which were applied two pine planks connected by means of massaranduba pegs of 25 mm of diameter.

Equal in length, the two elements displayed some irregularities regarding the geometry of the cross-section. Figure 48 shows the design followed for the construction of the two reinforced beams which were assembled in the carpentry and brought ready to be tested.
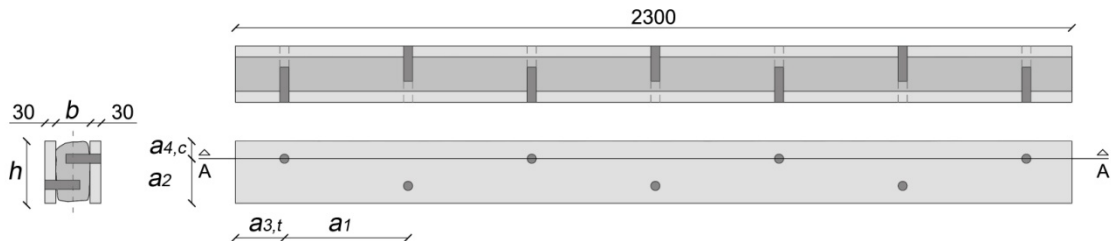

Figure 43 – Design for the 4-point bending tests.

5.2.1 PREPARATION OF THE SAMPLES

Following the same methodology as for the 30 sample tested in double shear, an accurate and detailed geometrical survey was required by the peculiar irregularity of the specimens. In order to provide a satisfying accuracy in the process, values for area, inertia and visual grading were evaluated as the mean value among the two main faces A and B of the beam and 5 internal cross-sections. These were named in roman numbers from I to V and located at 50 cm of distance starting from the centre of the span. Figure 44 and Figure 45 show the location of the internal cross-section respectively for B-I-G-1 and B-I-NG-1 used in the survey. The geometrical survey performed on the beams was done manually: after an initial location of all the 5 cross-section, measurements of the planks and the central element were progressively taken. The irregularity of the timber beam was measured on the two visible faces aiming to illustrate a simplified but precise representation of the cross-section. The two sides of the chestnut element which were not visible because covered by the pine planks, were estimated with a conservative approach through a straight connection between the two visible and measurable faces. Figure 46 shows and example of the performed survey. Once concluded the manual measurement, all the drawings were converted in two dimensional drawings and the values of area and inertia were calculated considering both the central element alone and the composite beam. Table 14 and Table 15 present the values of area and inertia found for the different cross-sections.
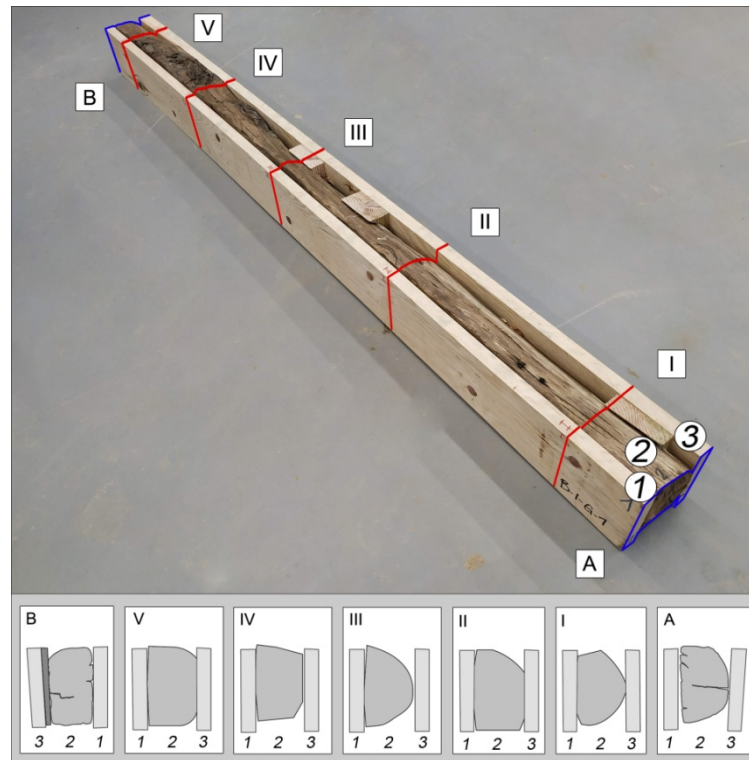
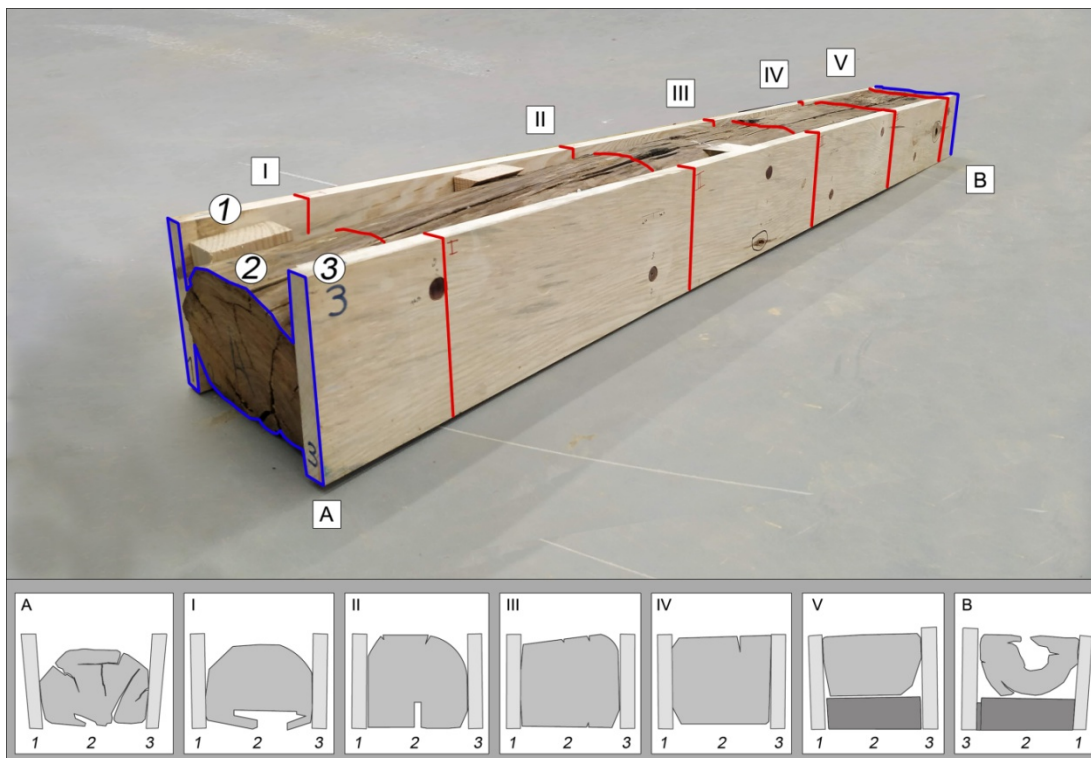**Figure 44 – B-I-G-1 location of the five cross-sections.**

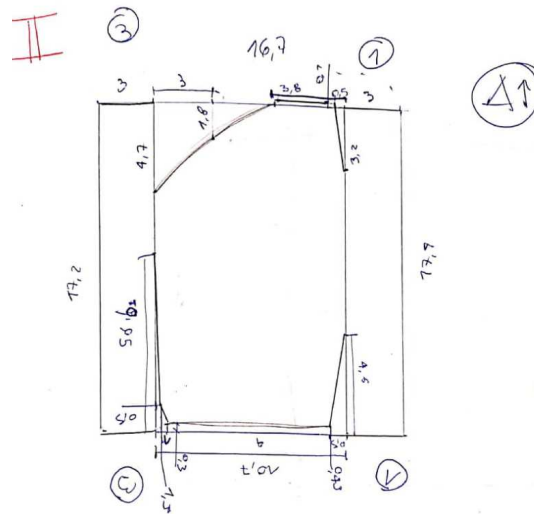**Figure 45 – B-I-NG-1 location of the five cross-sections.**

Figure 46 – B-I-G-1: example of geometrical survey of the cross-section II.

Table 14 – Geometrical survey of beams: area.

		Area (cm²)						
		A	I	II	III	IV	V	B
B-I-G-1	Central element	137.5	128.2	162.4	133.2	142.8	165.5	144.2
	Composite beam	240.8	231.5	265.7	236.5	246.2	268.9	261.9
B-I-NG-1	Central element	315.58	325.1	387.9	391.1	388.7	256.1	322.3
	Composite beam	434.7	444.1	506.9	510.1	507.8	510.8	446.7

Table 15 – Geometrical survey of beams: inertia.

		Inertia (cm⁴)						
		A	I	II	III	IV	V	B
B-I-G-1	Central element	2443.9	2009.8	3453.3	2298.5	2572.1	3565.3	2870.4
	Composite beam	4999.8	4565.8	6009.3	4854.5	5128.1	6121.3	5831.5
B-I-NG-1	Central element	6046.6	6602.5	11617.1	11434.7	11181.8	3498.8	7545.0
	Composite beam	10167.4	5358.6	15737.9	15555.5	15302.6	8138.6	7072.8

According to the codes (UNI 11119_2004)[26], a visual grading was carried out and the presence of wedges, wanes, knots and cracks was evaluated. It is important to underline that the studied specimens were characterized by a considerable and spread decay. The example of B-I-NG-1 is

reported as the most extreme between the two. In this case an evident decay due to insect attack was located in the intrados of the beam from the face A to the cross-section II (Figure 47)
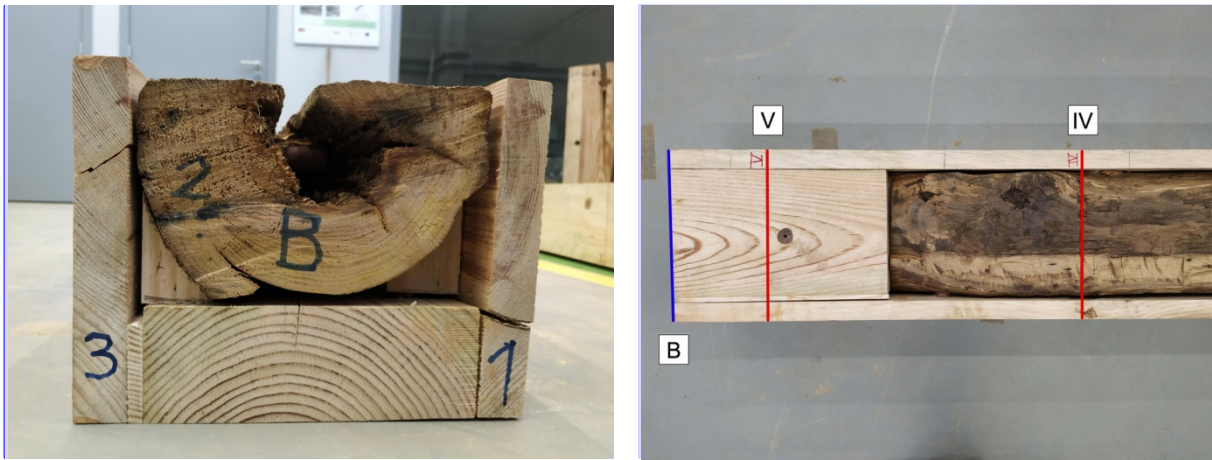

Figure 47 – B-I-NG-1: decay due to insect attack on the face B (left) and along the intrados of the opposite end (right).

Because of the consistent irregularity of the cross-section along with the heavy presence of wanes and voids, both the samples were supposed to be graded with less than the lowest value. As the mechanical characteristic were needed as reference, it was decided to give the third class, to both the specimens, as a upper limit. Table 16 reports the summary of both geometrical survey and visual grading.

Table 16 – Mean values of the geometrical survey of the 4-point bending test samples.

		Mean values			Visual grading			
		Area (cm^2)	Length (cm)	Inertia (cm^4)	Wedges	Wanes	Knots	Cracks
B-I-G-1	Central element	144.2	231.5	2744.8	III	III	III	III
	Composite beam	250.2	231.5	5358.6				
B-I-NG-1	Central element	322.3	230.5	7544.91	III	III	III	III
	Composite beam	480.2	230.5	11047.6				

Considering the visual grading evaluation, it was possible to have a reference value estimation of the modulus of elasticity of the specimens from the codes (Table 17) equal or inferior of 8000 N/mm^2. This was the value to compare with the final results of the test in order to verify if and which percentage the retrofitting technique applied was able to influence the structural behaviour of the timber beams.

Table 17 – Mechanic characteristics considering the visual grading[26]**.**

Species	On site grade	Maximum Stresses (N/mm²)					
		compression		static bending	tension parallel to the grain[1]	shear parallel to the grain	bending MOE
		parallel to the grain	perpendicular to the grain				
	III	7,5	2,0	8,5	7	0,9	13500
Pine	I	11	2,0	12	11	1,0	13000
	II	9	2,0	10	9	0,9	12000
	III	7	2,0	8	6	0,8	11000
Sweet Chestnut	I	11	2,0	12	11	0,8	10000
	II	9	2,0	10	9	0,7	9000
	III	7	2,0	8	6	0,6	8000

5.2.2 SET UP

The tests were carried out using an actuator of 200 kN of maximum vertical load and the protocol adopted was ruled by the codes (EN 408)[29].

Both the beams were simply supported and loaded symmetrically along their length in two points located at 65 cm from the lateral supports (Figure 48).
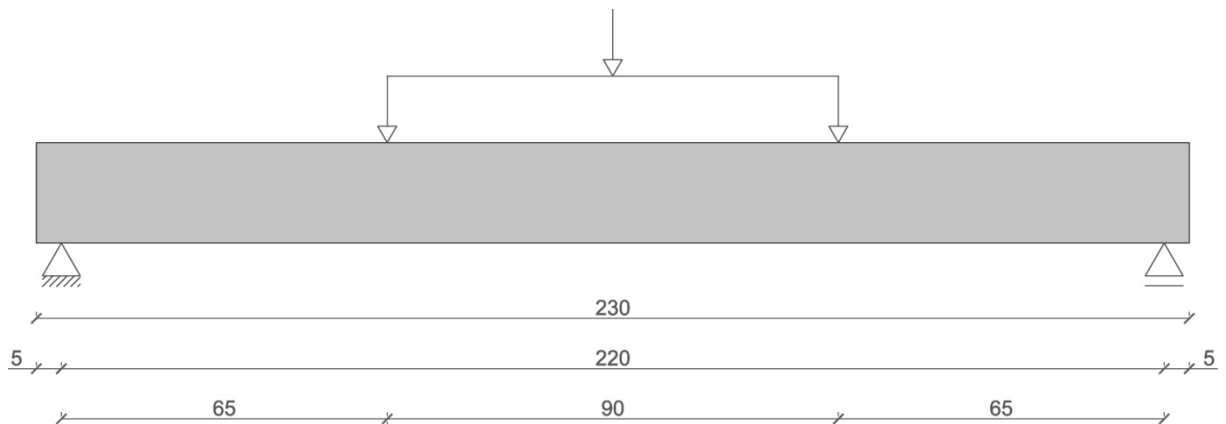
Figure 48 – Set up of the 4-poin bending test [29], measurements in cm.

5.2.3 TESTS

The load was then applied with displacement control at a velocity equal to 0.16 mm/s, until a displacement of 20 mm (0.4 of the maximum displacement estimated) was reached. Always with a displacement control the load was then decreased to zero at the same constant velocity. This procedure was repeated three times in total and eventually the load was applied at a constant velocity of 0.16 mm/sec until the failure occurred. The first cycles were considered to accommodate the

loading points with the beam and to avoid the influence of possible gaps between elements before the final cycle.

The predicted maximum displacement was evaluated with the equation of the global modulus of elasticity for the 4-point bending test:

$$E_{m,g} = \frac{3al^2 - 4a^3}{2bh^3 \left(2\frac{w_2 - w_1}{F_2 - F_1} - \frac{6a}{5Gbh} \right)} \tag{7}$$

where:

- a is the distance between the two point of application of the load in mm;
- l is the spacing between the two supports in mm;
- $F_2 - F_1$ is the range of vertical load considered in kN;
- $w_2 - w_1$ is the range of vertical displacement considered in mm;
- G is the shear modulus;
- b is the base of the sample in mm;
- h is the height of the sample in mm.

From the values found with the destructive tests carried out on the chestnut samples, was possible to evaluate the estimated maximum displacement for the beams. More precisely, substituting the modulus of elasticity and range of vertical load in equation (7), a value of w_{max} equal to 50 mm was found, thus $0.4w_{max}$ is equal to 20 mm.

In order to monitor the vertical displacement of the central element in chestnut with respect the pine planks, a total amount of 4 LVDTs were placed: 2 in the middle of the span and aligned with cross-section III, the other two were located on the right end and aligned with the peg present between the internal cross-sections I and II (Figure 49). More precisely, the LVDTs A and C were connected to the chestnut element, while the B and D to the external planks.

The extrados of the sample was also smoothed in order to provide a plain surface so that the vertical load could be uniformly applied on the specimen (Figure 50).
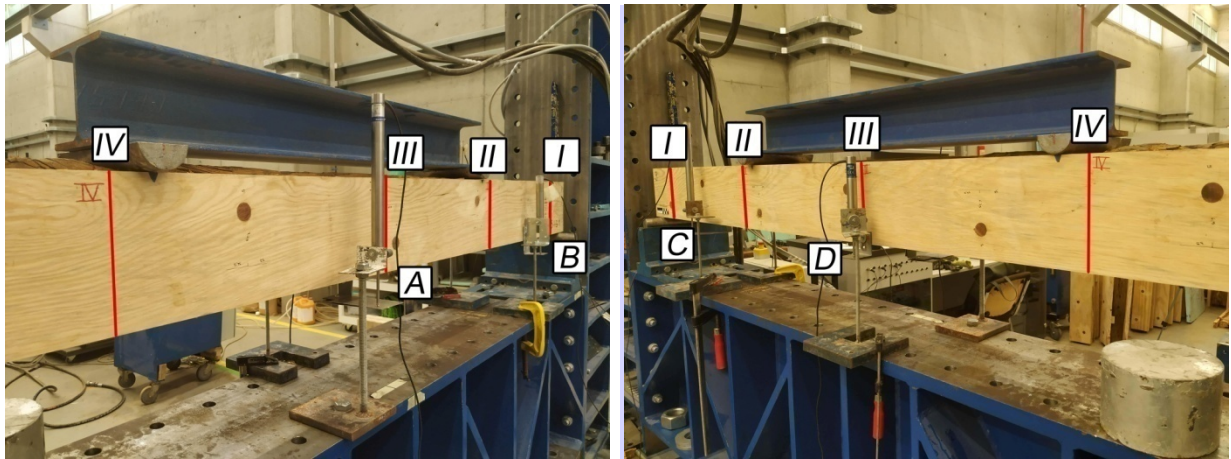
Figure 49 – B-I-G-1: location of the LVDTs on the front (left) and back (right).

Figure 50 – B-I-G-1: extrados smoothed in order to provide a plain surface for the loading point.

A photographic campaign was also performed with a camera Panasonic Model No. DMC-FZ300 with a resolution of 4000x2672 pixels and a sensor of 12.8 Megapixels (effective pixels of the sensor equal to 12.1). One picture every 5 seconds was taken since the beginning of the last phase of the protocol until collapse occurred. Regardless of the kind and location of the decay and defects present, the beams were tested as they were placed in situ, first the glued sample and then element B-I-NG-1.

Values of maximum vertical load and displacements relative to the placed LVDTs were recorded during the test. Eventually the time lapse done with the pictures of the photographic campaign was analysed with the use of the software Python in order to identify the estimated displacement of the pegs and the actuator through a measurement of the displacement by pixel recorded on the video. To this value was applied a coefficient of correction of the scale due to the natural perspective which the pictures with the camera were subjected.

To be recognised and monitored by the software, the pegs were numbered progressively from left to right from P0 to P6, the actuator was identified as P7. The estimated displacement of each single peg

was provided and compared with the data collected from the 4-point bending test to verify the presence of a correlation.

5.2.4 B-I-G-1

The first tested was the beam with the pegs inserted with the help of white glue. Figure 51 shows the sample before the test being carried out and highlights the pegs numbered progressively as previously described.

With the data collected at the end of the test was possible to plot the graphs of the displacement dependent on the vertical load for each of the 4 LVDTs present (Figure 52). The presence of a mean initial deflection equal to 3.71 mm on the vertical axis was recorded by the LVDTs as a consequence of the initial three cycles of the test.

The modulus of elasticity was evaluated with equation (7) while the value of the bending strength was calculated with equation (8) [29] and was found equal to 25.5 N/mm^2:

$$f_m = \frac{3Fa}{bh^2} \qquad\qquad (8)$$

Where:

- F is the maximum vertical load recorded in N;
- a is the distance between the two point of application of the load in mm;
- b is the base of the sample in mm (all the 3 elements are considered);
- h is the height of the sample in mm (all the 3 elements are considered).
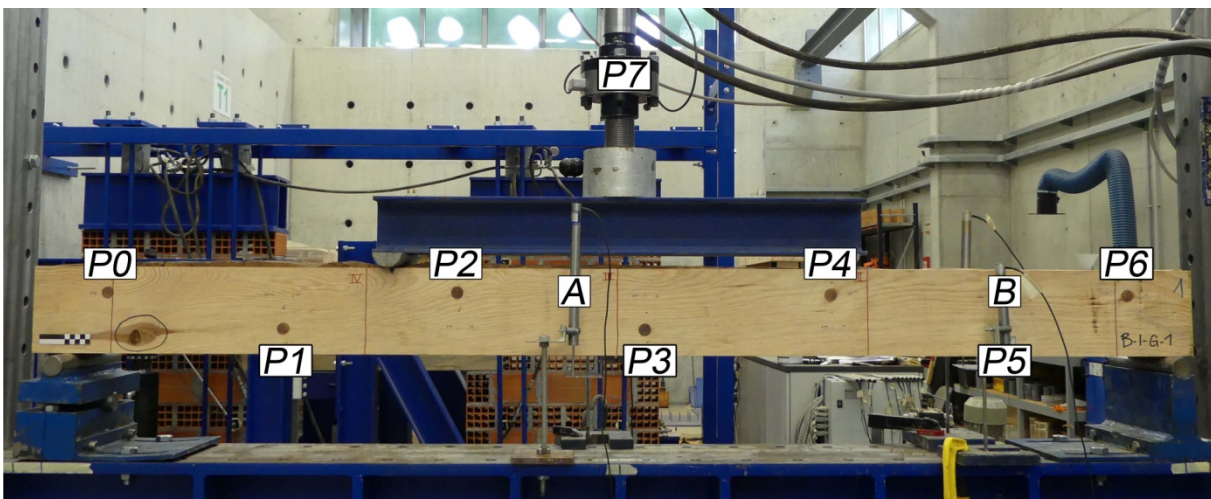
Figure 51 – B-I-G-1:test setup and location of pegs.
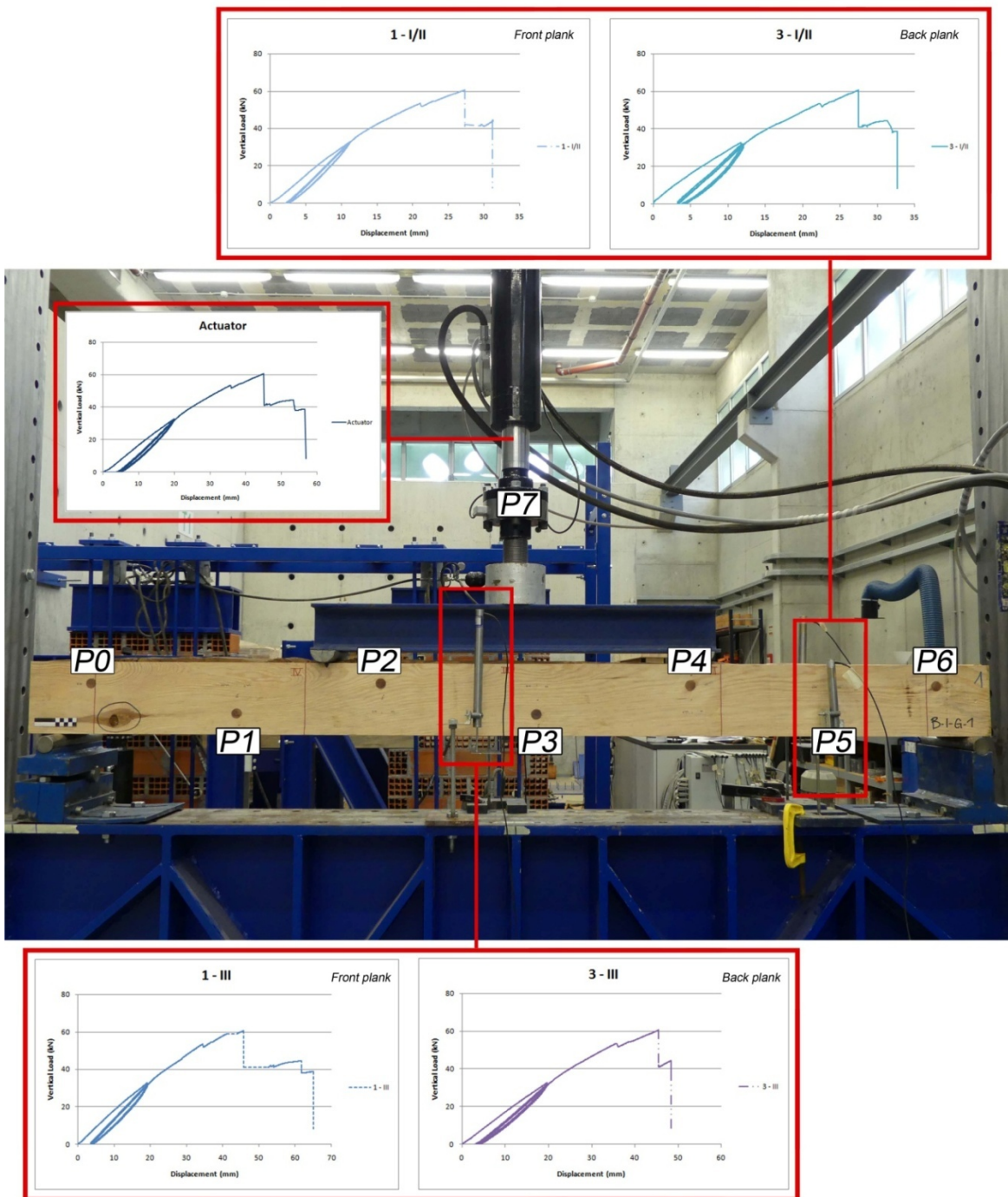
Figure 52 – B-I-G-1: graphs of the LDVTs and the actuator.

Table 18 summarize the values obtained from the processing of the data collected from the 4-point bending test of B-I-G-1:

Table 18 – B-I-G-1: data elaborated from the 4-point bending test.

Vertical load (kN)	60.5
Vertical load per each peg (kN)	4.3
Displacement from the actuator (mm)	56.8
Displ. from LVDT 1 – III (mm)	65
Displ. from LVDT 1 – I/II (mm)	31.2
Displ. from LVDT 3 – III (mm)	48.4
Displ. from LVDT 3 – I/II (mm)	32.7
Modulus of elasticity (N/mm^2)	5288.6
Bending strength (N/mm^2)	25.5

The failure occurred at a maximum load of 60.5 kN on the front plank (plank number 1)between the pegs P4 and P3 near the right support of the vertical load (Figure 53a). The failure initiated by the presence of a group of knots in the intrados of the beam (Figure 53d), caused the formation of an oblique crack that connected the two fasteners and partially the fibre in tension. This phenomenon is mirrored in the plank number 3 on the back of the beam (Figure 53b). When the failure occurred the sudden loss of energy caused an abrupt horizontal displacement visible in Figure 54b. On the back of the sample, located in P4a was noticed the consequently failure of the corresponding peg on the other side of the element due to the presence of a knot in the chestnut beam (Figure 54e). None of the pegs experimented failure nor ductile deformation.

a)
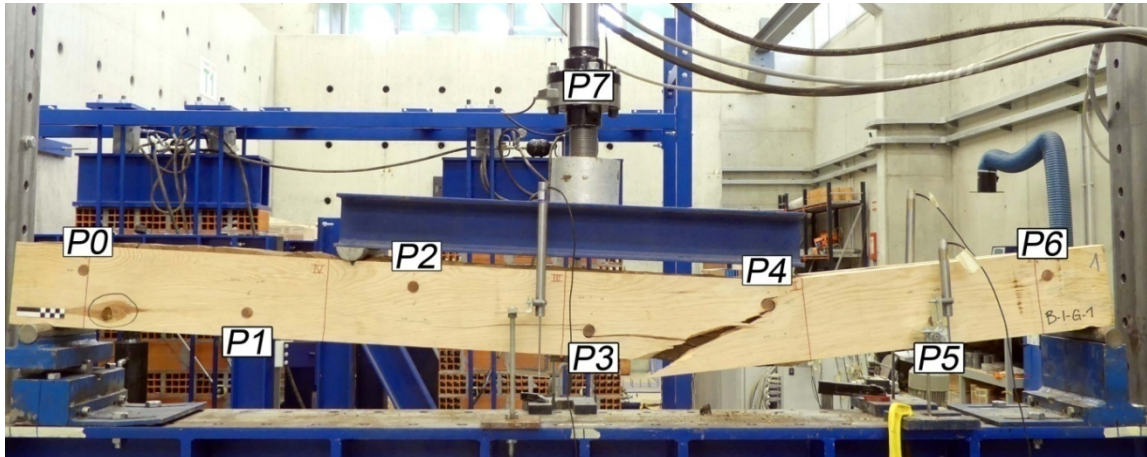
b)
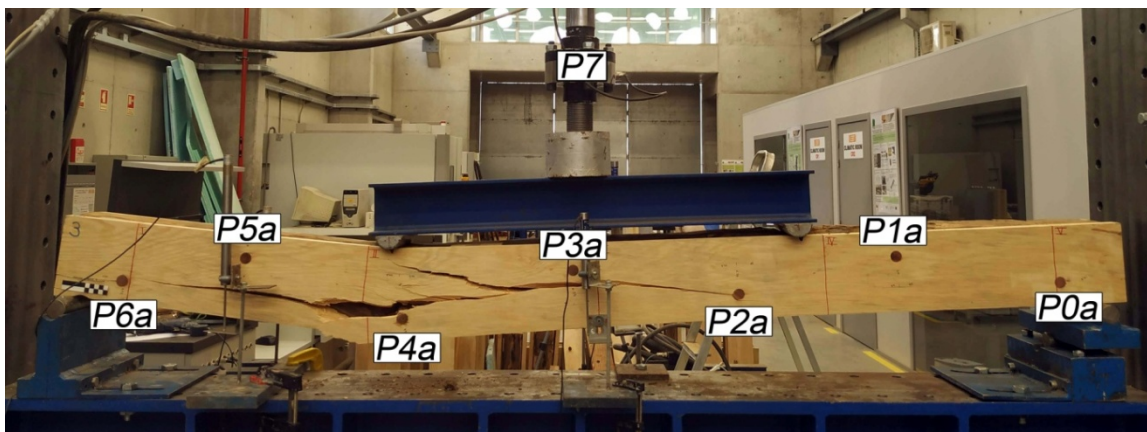
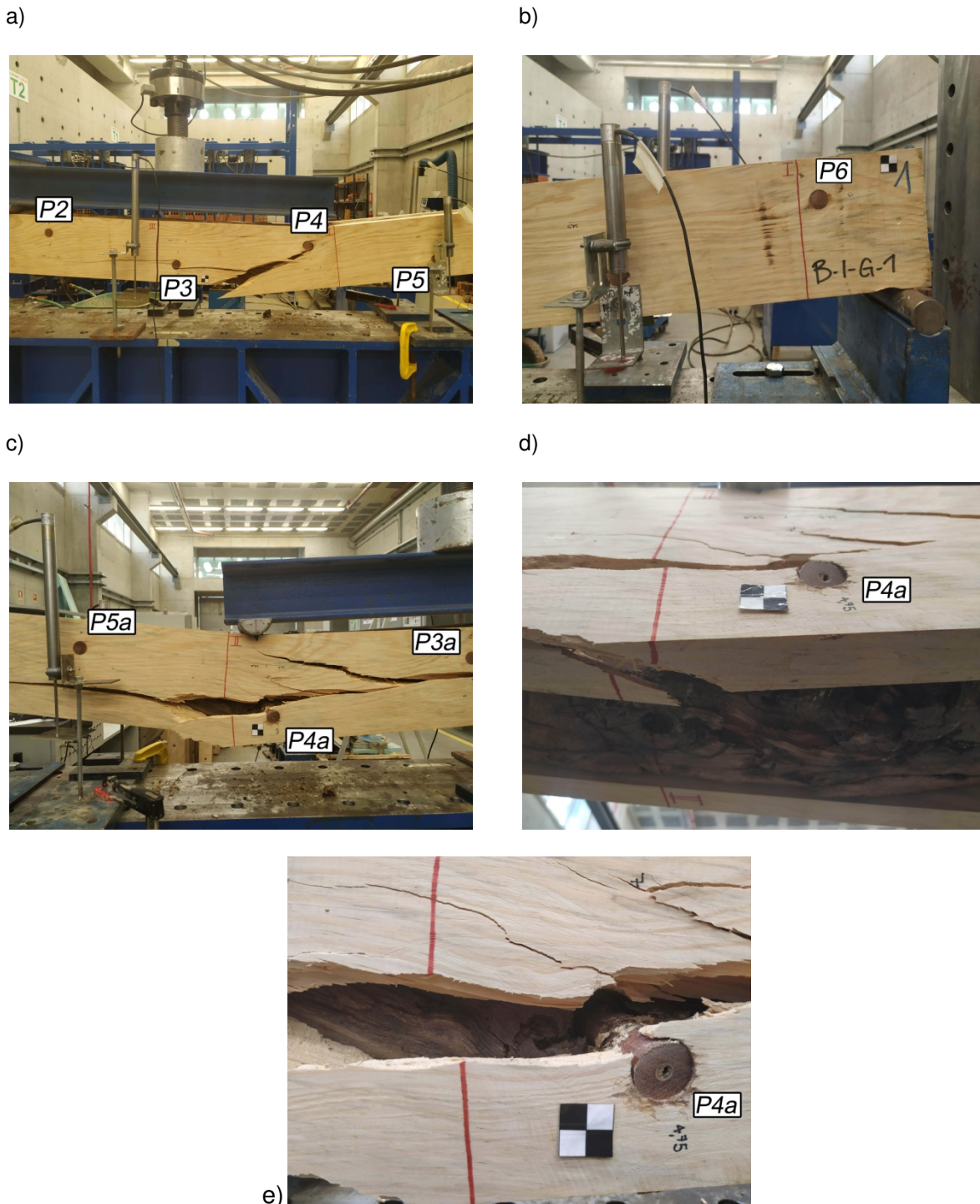**Figure 53 – B-I-G-1: failure on the front plank (a) and the back plank (b).**

a) b)

c) d)

e)

Figure 54 – B-I-G-1: zoom in on the failure on the front (a and b) and the back (c and d).

Through the analysis of the time lapse recorded during the test was possible to estimate the displacement of each peg present on plank number 1 by a correlation time-displacement, both vertical and horizontal displacement were considered (Figure 55 a and b). It is possible to notice how for the

vertical displacement a mirrored behaviour was monitored for the couple of pegs P0-P6, P1-P5 and P2-P4. Same performance occurred regarding the horizontal displacement for the couple of pegs P0-P6 and P1-P5. The fasteners P2, P3 and P4 were not considered for the horizontal displacement (Figure 55b) because they lied inside the area of application of the vertical load (Figure 56), therefore not subjected to shear actions and having a very small value of displacement.

a)

b)
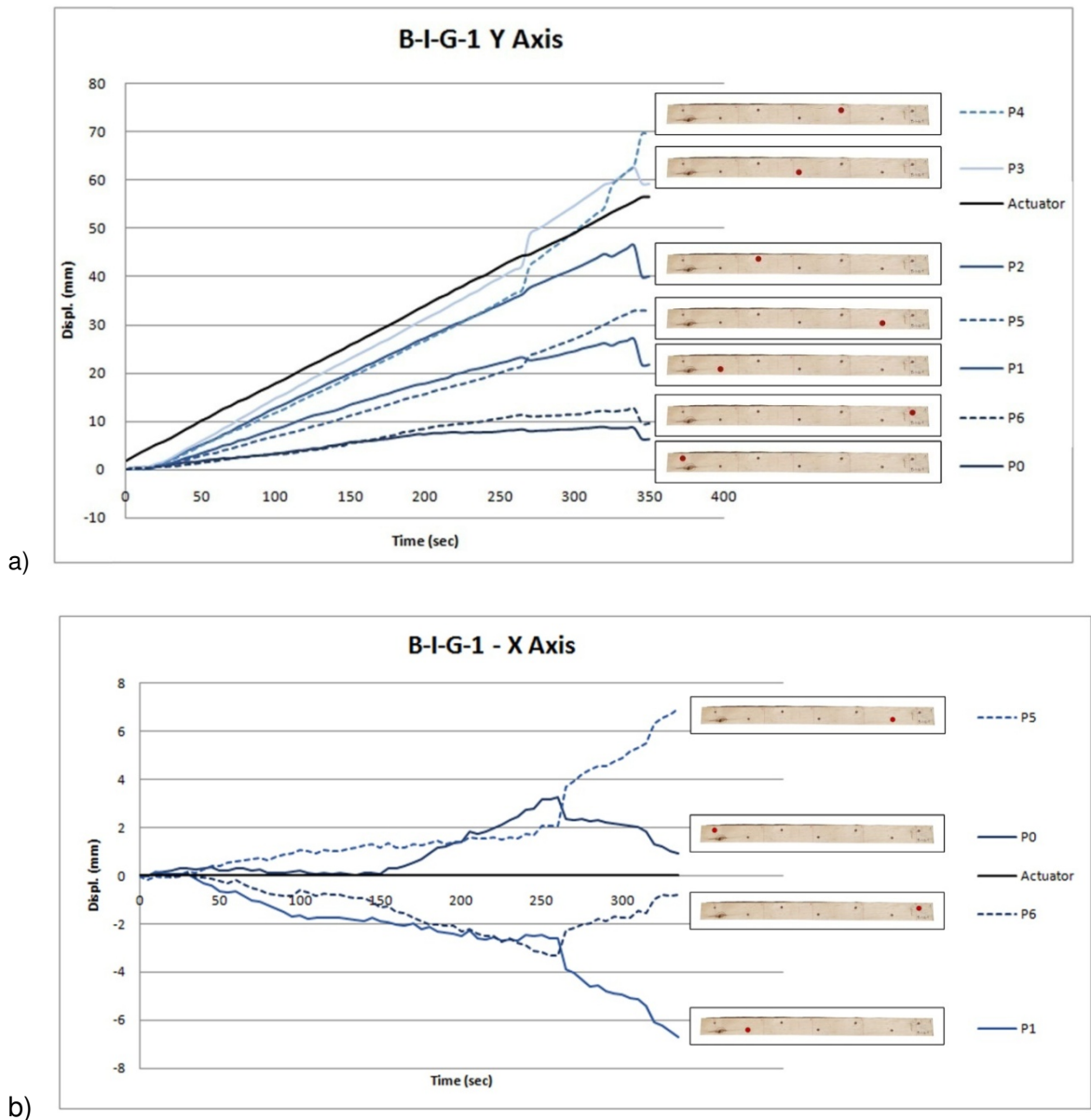
Figure 55 – B-I-G-1: displacement of the pegs on the y axis (a) and x axis (b).
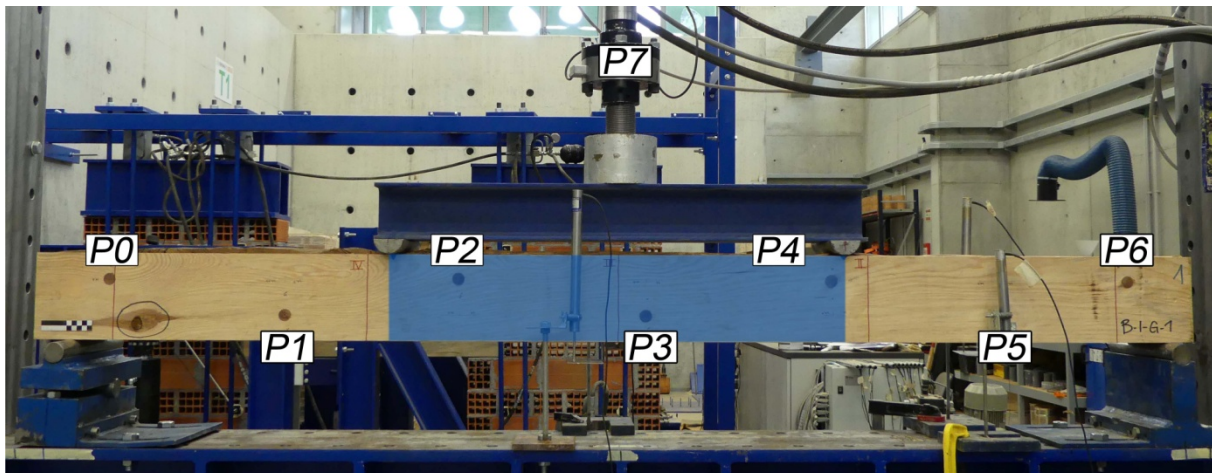
Figure 56 – B-I-G-1: pegs within the point of load application.

A correlation between the time-displacement relation extrapolated from the video analysis and the force-displacement documented during the test was found. This allowed to plot a graph force-displacement of the 6 fasteners of B-I-G-1 and a consequential comparison between the values provided by the LVDTs. Figure 57 shows the plotting of all the fasteners (a), followed by a comparison between the displacement of the actuator accordingly with the performed test and the video analysis (b), the same comparison for the LVDT located in the middle of the span and the peg P3 (c) and the LVDT located between the cross-section I and II compared with the displacement of P5.

Although some inaccuracies were present, one can say that the overall result was satisfying as was possible to estimate the displacement that the peg which brought to failure the structure can be estimated. In this particular case the peg which firstly collapsed was P4 which experienced a vertical displacement equal to 61 mm due to the presence of a knot in the intrados of the beam.
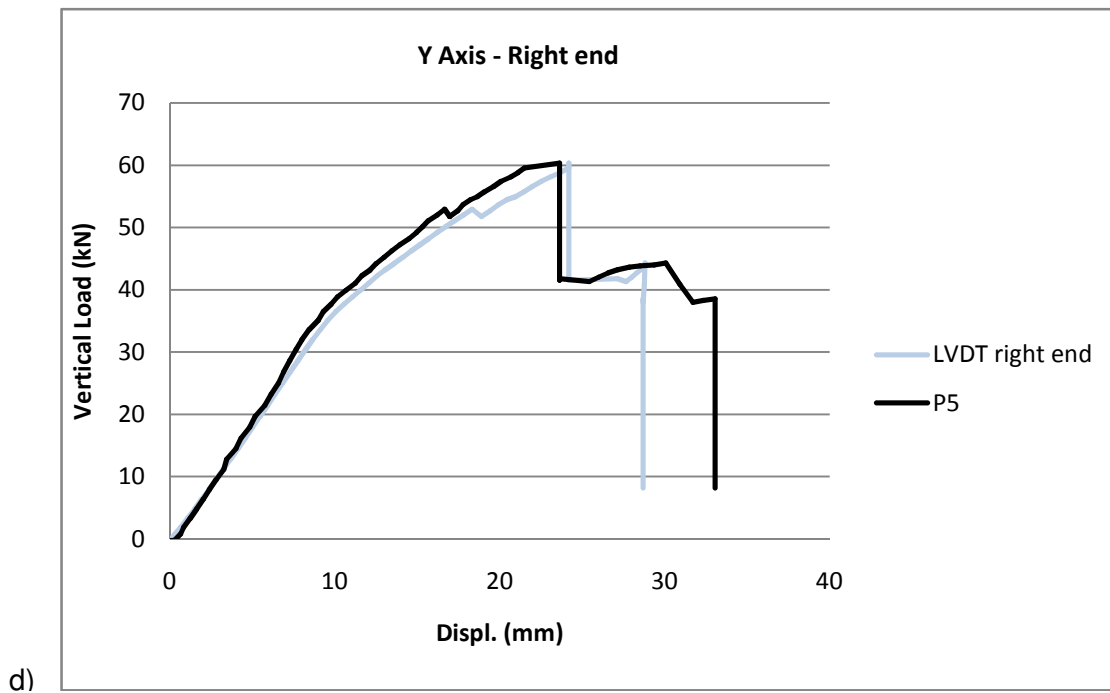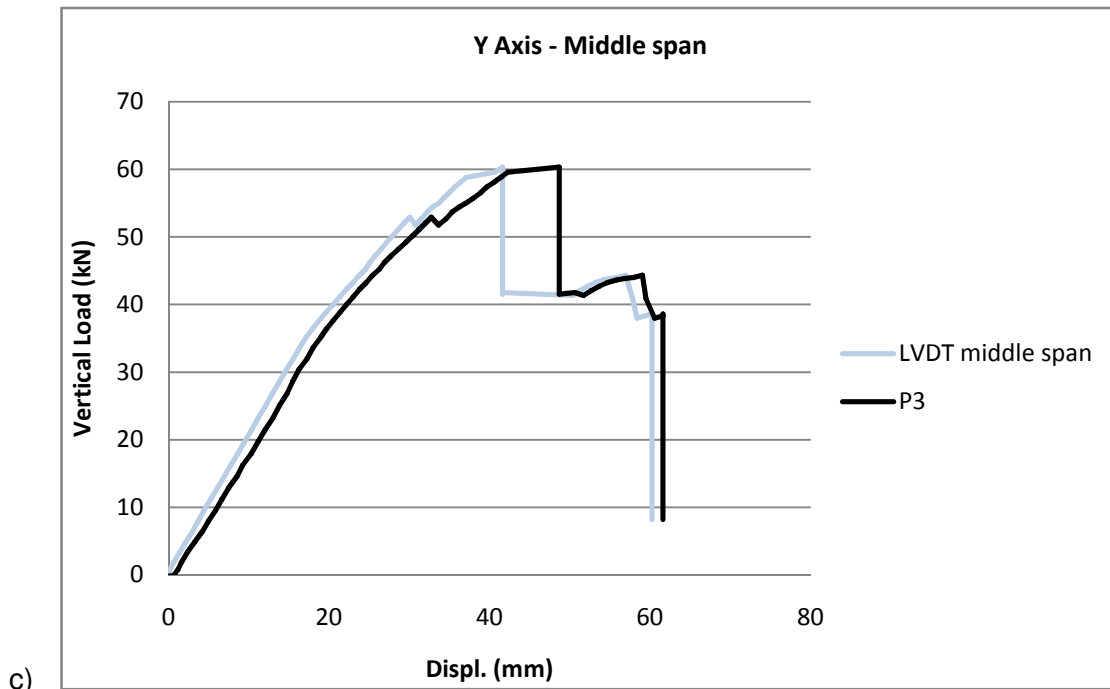
a)

b)

c)

d)
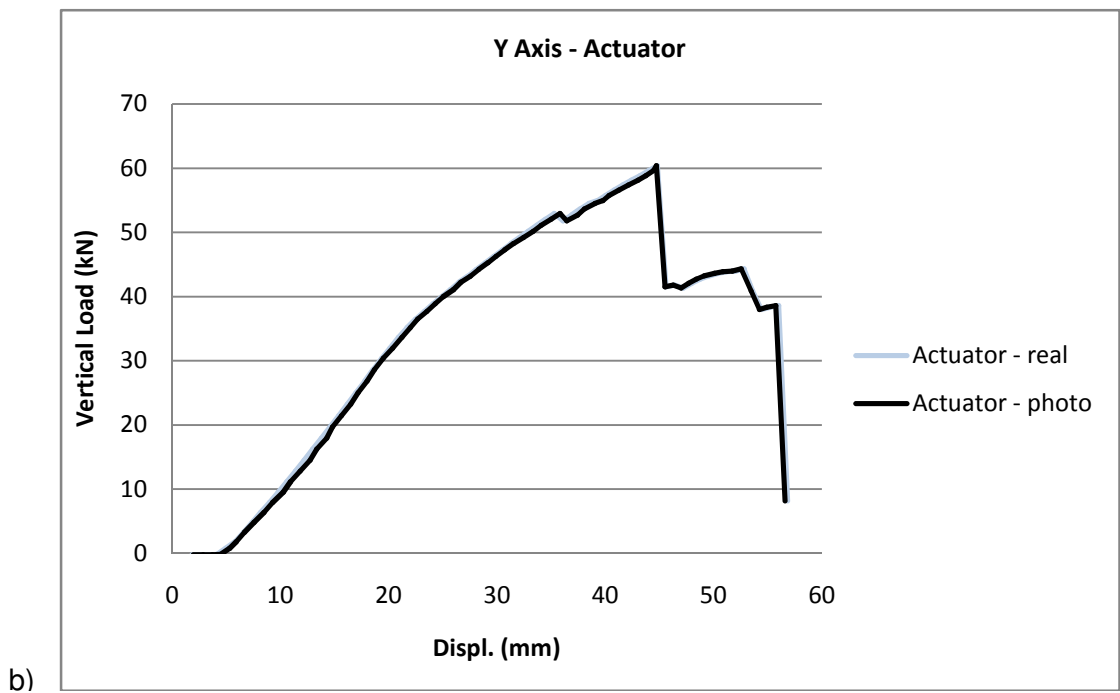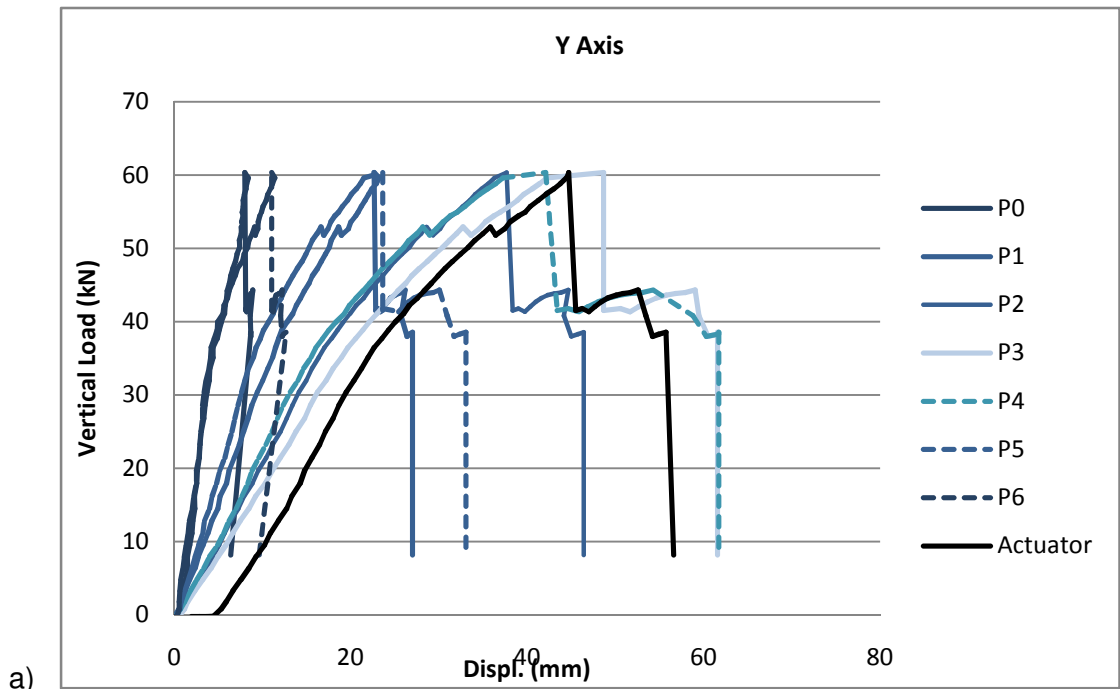
Figure 57 – B-I-G-1: comparison between LVDTs and displacement of the pegs.

5.2.5 B-I-NG-1

The same procedure adopted for B-I-G-1 was replicated for the test of the beam with the retrofitting planks connected by means of a dry timber connection (not glued). It is important to underline that, considering the difference of mechanical properties between glued and unglued specimens noted during the experiments on the local scale, lower results were expected in matter of vertical load and modulus of elasticity. Nevertheless, the unglued beam presented considerable higher dimensions in the cross-section then the glued one, and even though a remarkable presence of decay was highlighted by the survey and visual grading carried out previously, the possibility to monitor higher mechanical properties was taken into account.

Another peculiarity of the specimen is the presence of a plank located as wedge in the intrados of the beam, as the cross-section in that end was insufficient respect the height of the planks (Figure 58).

Figure 58 – B-I-NG-1: plank located in the intrados of the beam.

As done previously for B-I-G-1, the pegs were numbered progressively from P0 to P6 and the actuator was named P7 in order to allow a visual analysis of the time lapse with the software Python (Figure 59).
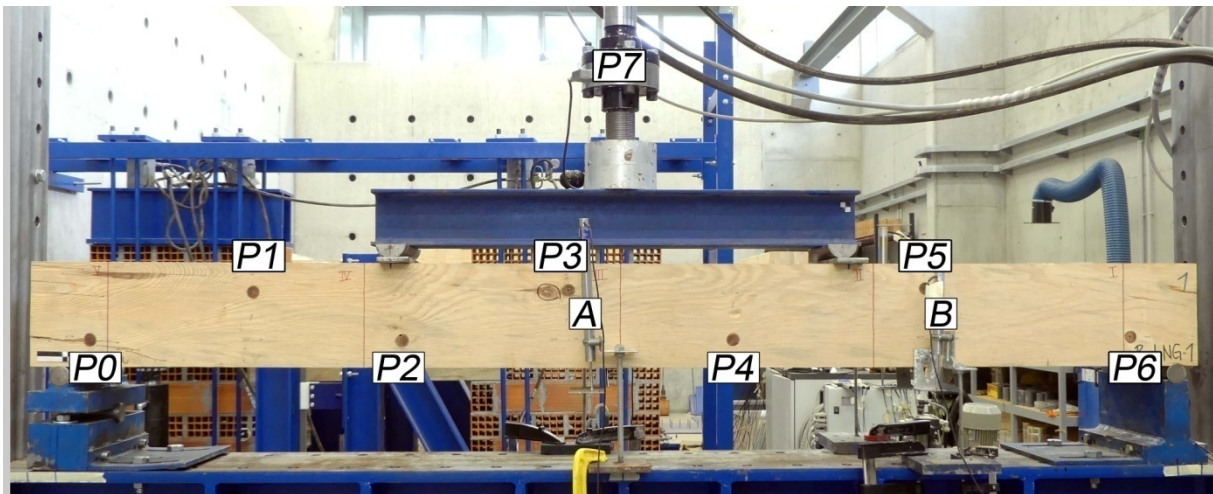
Figure 59 – B-I-NG-1: location of pegs.

Graphs of force-displacement of the 4 LVDTs and the actuator were then plotted (Figure 60) and, as happened for the glued sample, a mean deformation equal to 4.1 mm took place and was recorded by the LVDTs at the end of the first three cycles of the test.
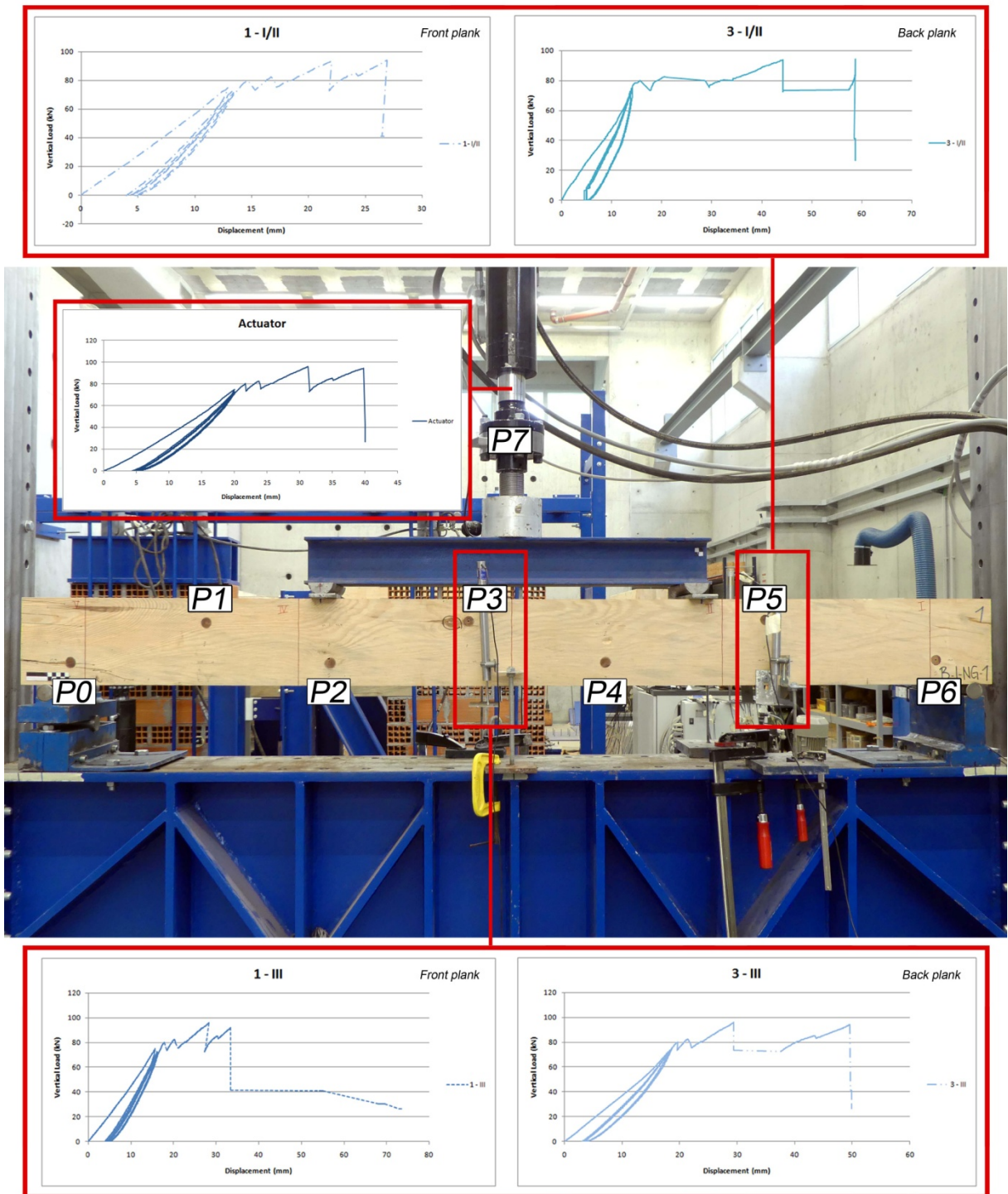
Figure 60 – B-I-NG-1: graphs of the LDVTs and the actuator.

From the collection of data was possible to evaluate the vertical displacement occurred at the failure for the LVDTs applied to the specimen, along with the maximum vertical load and the global modulus of elasticity calculated with equation (7) and the bending strength with equation (8) (Table 19).

Table 19 – B-I-NG-1: data elaborated from the 4-point bending test.

Vertical load (kN)	95.8
Vertical load per each peg (kN)	6.8
Displacement from the actuator (mm)	40.1
Displ. from LVDT 1 – III (mm)	73.6
Displ. from LVDT 1 – I/II (mm)	26.9
Displ. from LVDT 3 – III (mm)	49.96
Displ. from LVDT 3 – I/II (mm)	58.7
Modulus of elasticity (N/mm^2)	6119.7
Bending strength (N/mm^2)	21.5

As postulated previously, a higher vertical load than the glued sample was recorded, in fact the beam collapsed with a load equal to 95.8 kN due to failure of the chestnut member. Figure 61 (a and b) shows a detachment of part of the timber beam in the intrados between cross-sections I and III. This event caused the sudden failure of the back plank (plank number 3) through the formation of a similar crack located on the opposite side of the beam which expands from P4a to the intrados under P2a (Figure 61 b). This caused a twist along the cross-section which eventually lead also the plank number 1 to collapse and the formation of a crack parallel to the fracture occurred in the chestnut element, which from P4 almost reached P1 (Figure 61a).

Figure 62 shows a zoom in on the failure. More detail is given in Figure 62a and 58b regarding the behaviour of the pegP4, where it is interesting to notice how both the plank and the beam display the same pattern of fracture caused by the vertical displacement of the peg. This is a demonstration of the fact that the used timber peg allows the composite beam to behave as a single cross-section. Figure 62c and 58d show a zoom in on the intrados of the beam where the main detachment was registered, here it is possible to see part of the peg number 6 through the formed crack. In the same way, Figure 62e and 58f show an identical behaviour for peg P5a. This explains the reason of the failure of the

main beam: the decay present on the existing structure weakened the cross-section to the point that was impossible to distribute the internal stresses and a sudden brittle failure occurred.

It is important to underline that in both the bending tests carried on the beams, none of the pegs experimented failure nor ductile deformation. This means that, even though able to connect the planks to the main beam and provide a composite cross-section capable of an uniform behaviour, the thickness of the pegs was not fully optimized.

a)
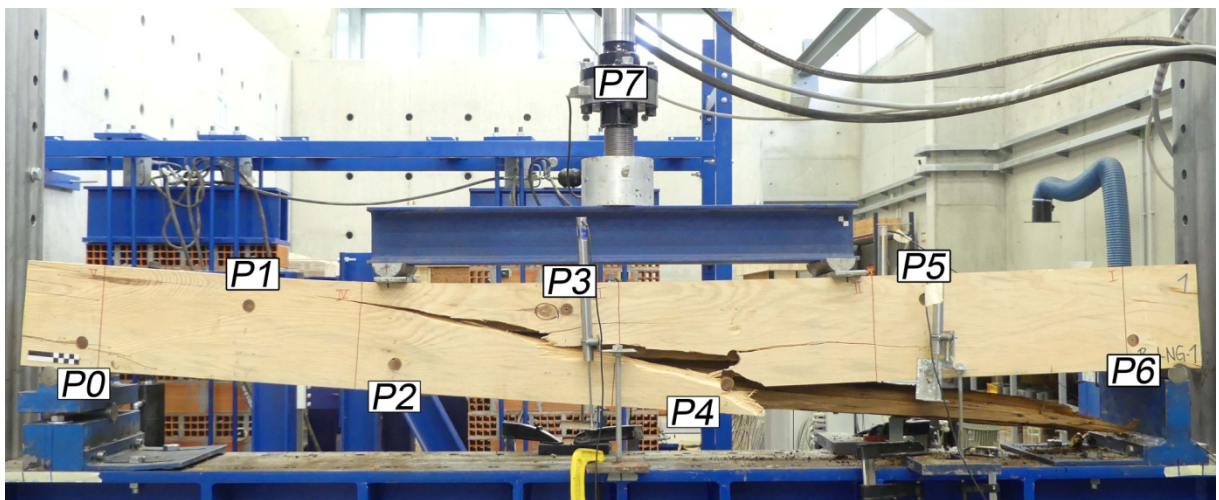
b)
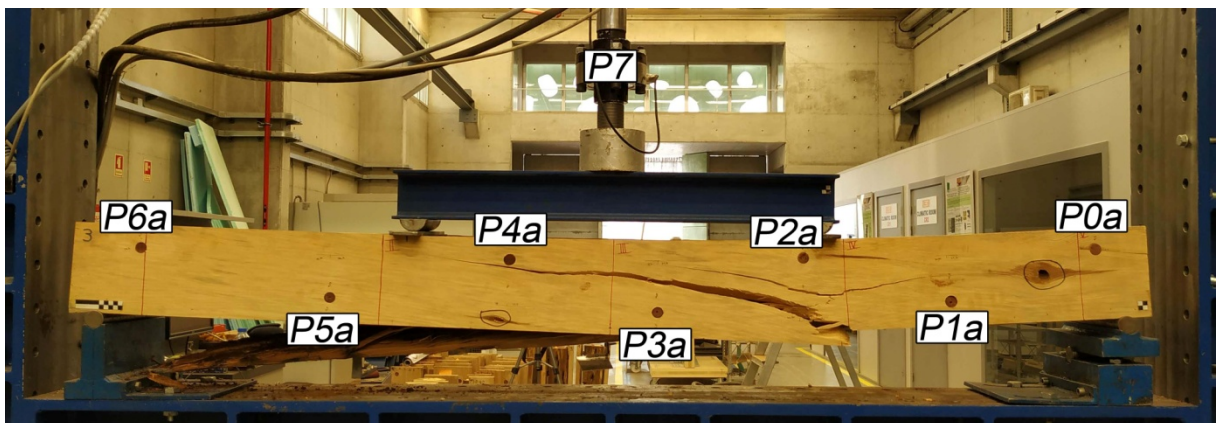
Figure 61 – B-I-NG-1: failure on the front plank (a) and the back plank (b).

a)

b)

c)

d)

e)

f)
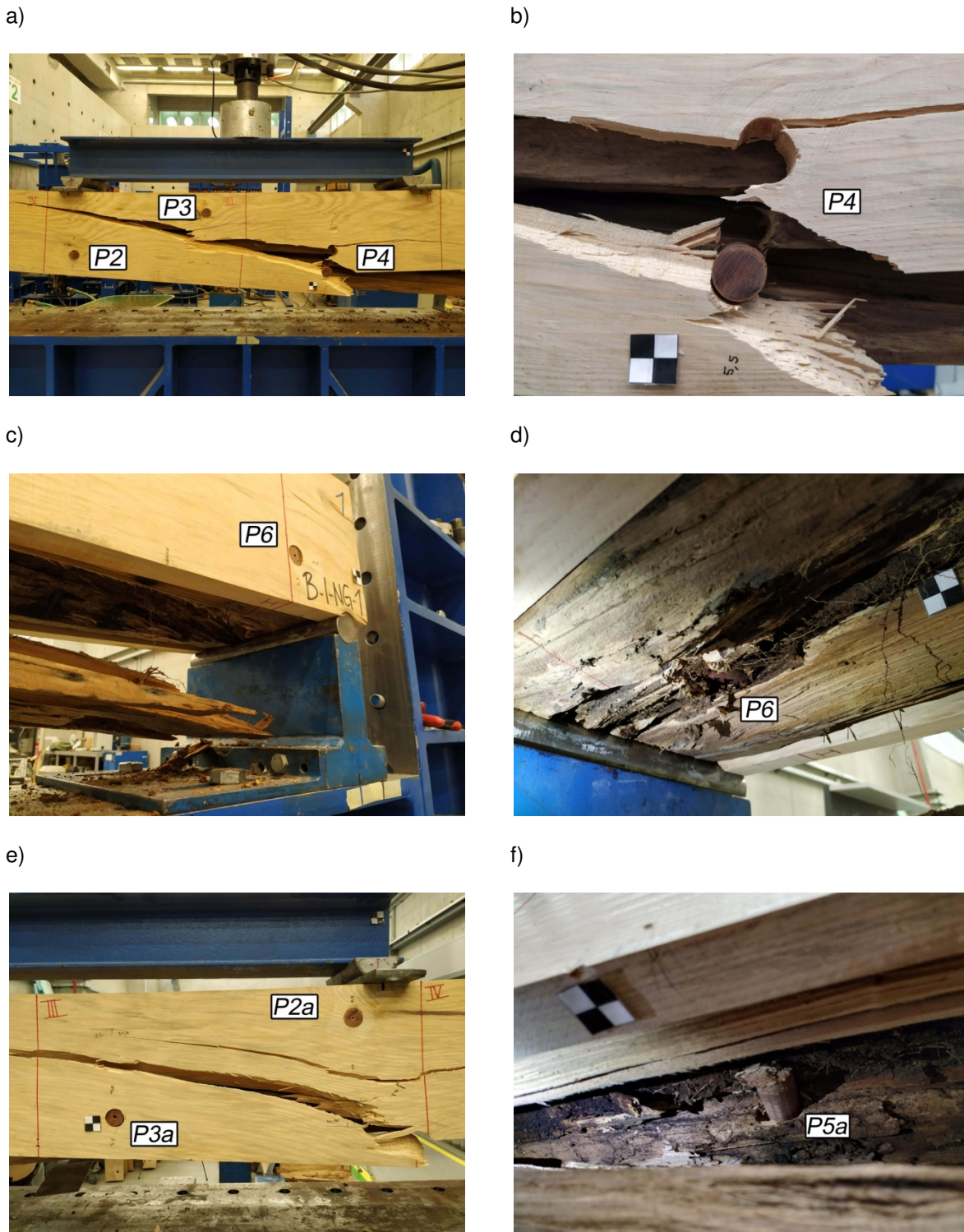
Figure 62 – B-I-NG-1: failure zoom-in on the front (from a to do) and the back (e and f).

As done for the first bending test, the displacement on the y and x axis was plotted on the relation time-displacement through the video analysis of the time lapse (Figure 63a and b). The same

symmetric behaviour noticed previously for the couples of pegs P0-P6, P1-P5 and P2-P4 is visible in the graph reporting the displacement along the y axis. While P3, as the closest peg in the middle of the span, registered a slightly higher vertical displacement (Figure 63a). On the other hand, Figure 63b shows the displacement on the horizontal axis, here the fastener P3 and P4 were neglected because lying between the two application points of the vertical load. Unlike B-I-G-1, P2 was not neglected because located exactly under the left point of application of the vertical load and therefore still subjected to shear (Figure 64).

a)

b)
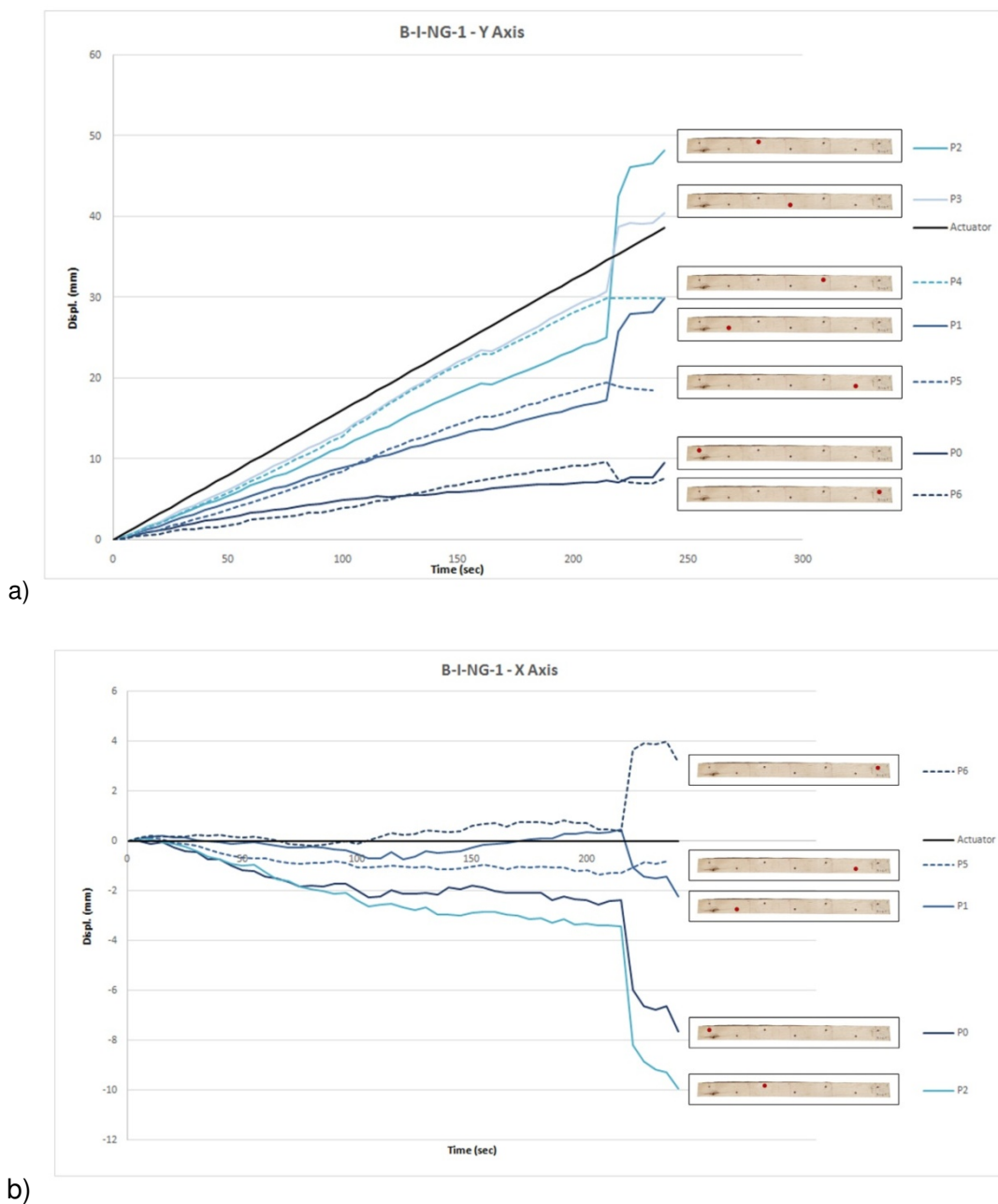
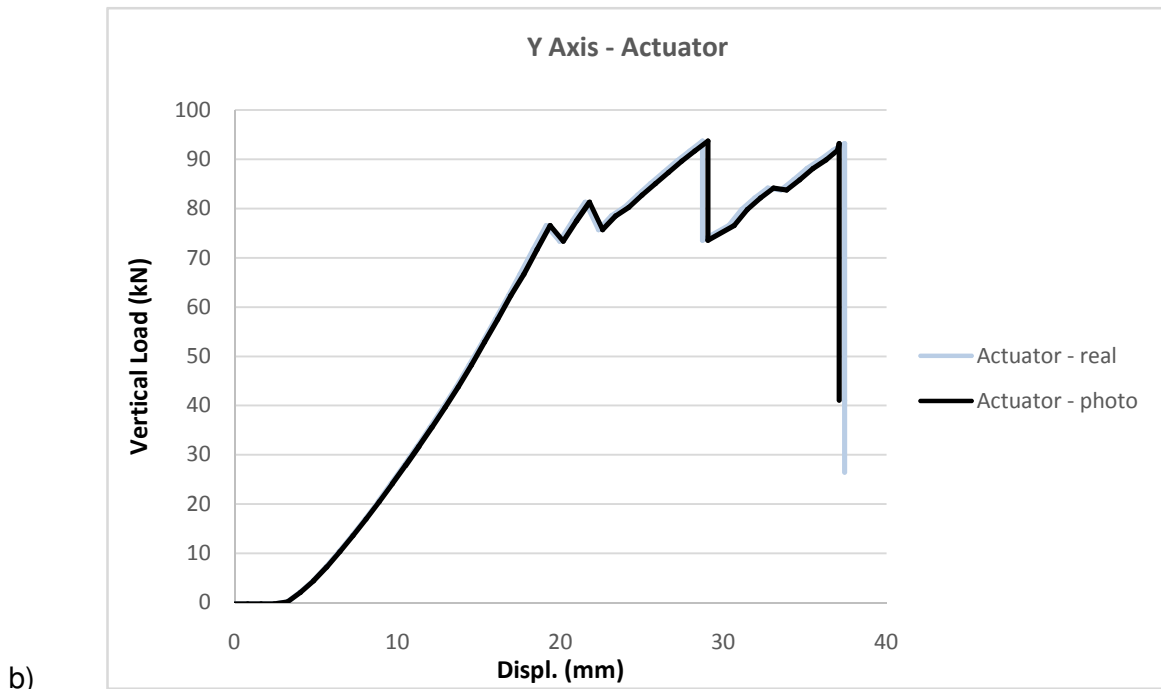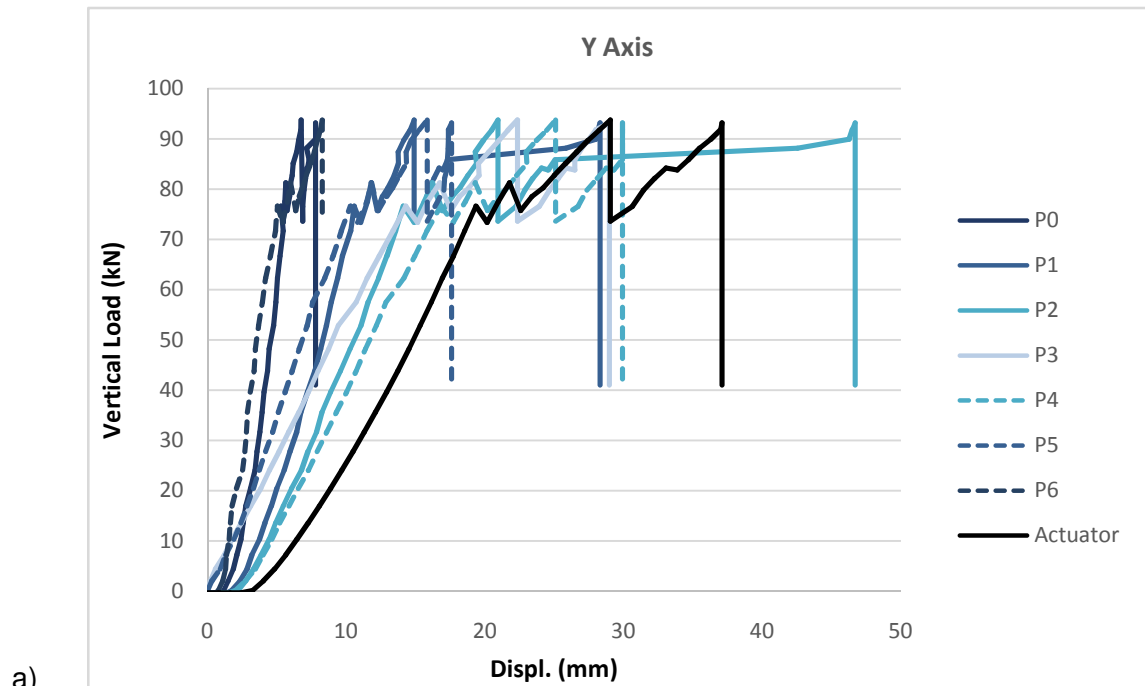**Figure 63 – B-I-NG-1: displacement of the pegs on the y axis (a) and x axis (b).**
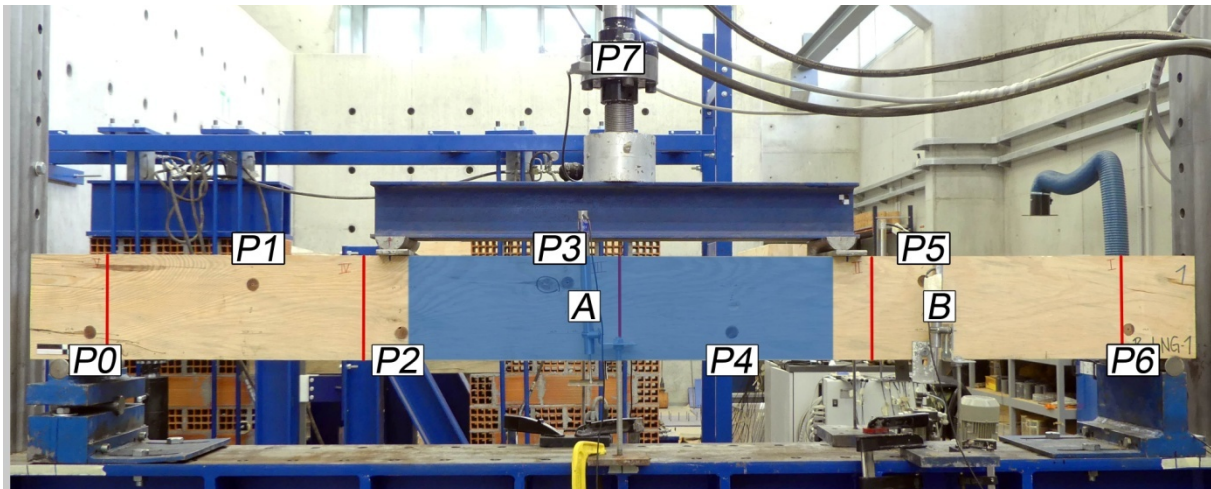
Figure 64 – B-I-NG-1: pegs within the point of load application.

Eventually the vertical displacement of the pegs based on time-displacement extrapolated from the video analysis was converted in force-displacement. A comparison between the values provided by the LVDTs during the tests was thus possible. Figure 65a shows the behaviour of all the pegs, while Figure 65b compares the vertical displacement of the actuator with the displacement of P7. Figure 65c shows the relation between the LVDT along the cross-section III related with P3, while Figure 65d displays the comparison between the LVDT B and the peg number 5. Except for Figure 65c, the presented comparison provides a satisfying correlation. The difference of result in the plot regarding the end of the beam, is related with the twisting effect that occurred at the failure and the location of the two elements, as P5 was close the extrados and the location of the LVDT was in the intrados. Moreover, due to the fact that the collapse occurred on the back of the sample, is not possible to provide an estimated vertical displacement of the peg.
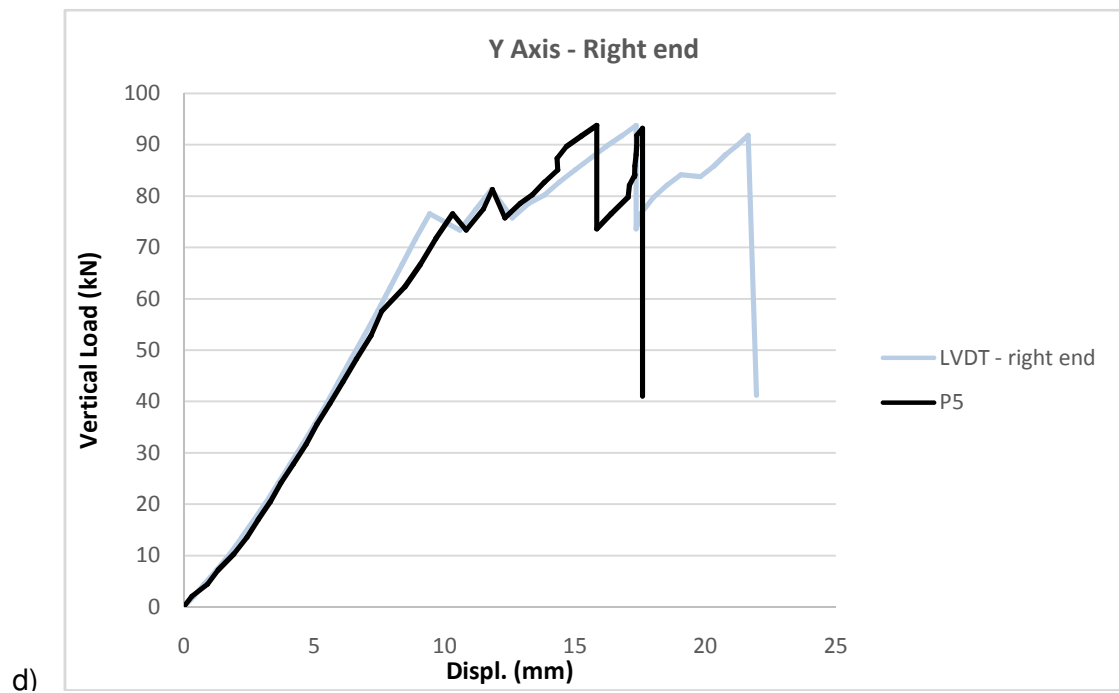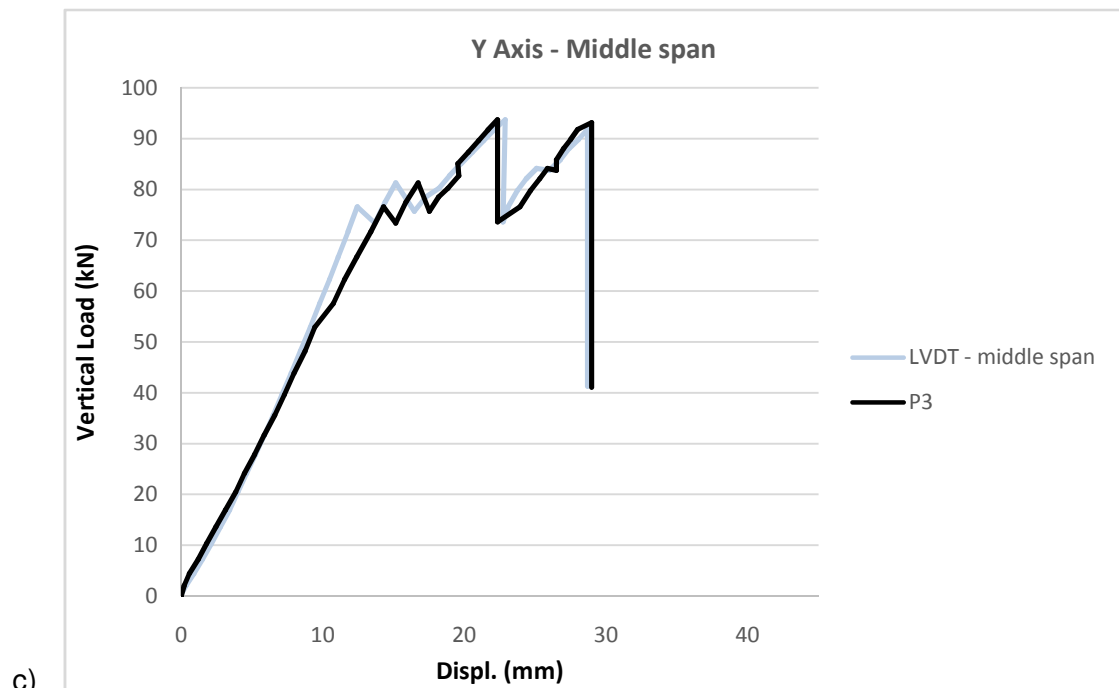
a)

b)

c)

d)

Figure 65 – B-I-NG-1: comparison between LVDTs and displacement of the pegs.

5.3   COMPARISON BETWEEN GLUED AND UNGLUED SPECIMENS

After testing, a comparison was made of the data recorded and extrapolated by the two 4-point bending tests (Table 20), where unlike what was expected is noted an apparent better result of the unglued sample respect the glued one. This is actually due to the fact that the cross-section of B-I-NG-1, even if affected by defects and decay, was consistently bigger the cross-section of B-I-G-1 and thus more inclined to reach higher results. The calculation of the bending strength however highlighted a different result: once the influence of the geometrical dimension is neglected the glued beam display a strength 18 % higher than the unglued element. In this way the tendency observed on a local scale with the double shear test that pointed out as able to reach higher results the glued specimens is confirmed. Even thought the modulus of elasticity found for the two beams cannot be used as objective element of comparison due to the difference of cross-section, its value results lower than the one provided by the visual grading [26] (8000 N/mm^2), which prove and raise in the stiffness of the reinforced specimens.

Table 20 – Comparison between B-I-G-1 and B-I-NG-1 results.

	B-I-G-1	B-I-NG-1
Vertical load (kN)	60.5	95.8
Vertical load per each peg (kN)	4.3	6.8
Displacement from the actuator (mm)	56.8	40.1
Displ. from LVDT 1 – III (mm)	65	73.6
Displ. from LVDT 1 – I/II (mm)	31.2	26.9
Displ. from LVDT 3 – III (mm)	48.4	49.96
Displ. from LVDT 3 – I/II (mm)	32.7	58.7
Modulus of elasticity (N/mm^2)	5288.6	6994.9
Bending strength (N/mm^2)	25.5	21.5

5.4   NUMERICAL MODEL

In order to verify the retrofit solution in terms of structural performance, a simple two-dimensional linear numerical model was built considering the modelling of the inner beams (chestnut beams) using two assumptions for the mechanical properties: i) the information obtained from the small clear specimens which were after affected by a reduction factor (see chapter 4); and ii) the reference values obtained through UNI 11119:2004 (see Table 5) for chestnut elements graded as class III.

The geometry of each beam, without planks, was taken by segments considering the mean value of area and inertia of the nearest measured cross-section. A representation of the model is given in Figure 66, with indication of the length of each considered segment. For these models a linear elastic material model was considered with brittle failure when the ultimate bending strength was reached. The load was applied by consideration of two point loads with equal value along the simulation and the beam was considered to be simply supported, aiming at simulating the experimental setup configuration.
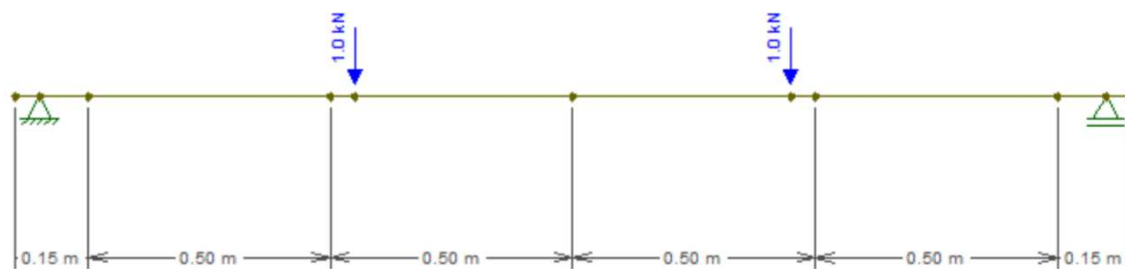

Figure 66 – Representation of the numerical model.

The results are presented in Figure 67 and Figure 68 respectively for the beams B-I-G and B-I-NG. In the case of the beam B-I-G, comparing to the numerical model assuming the results taken from the small clear specimens, it is clearly visible that the implementation of the retrofit solution allowed to obtain a higher load (11.3% higher), even if a lower displacement (9.2% lower) is seen for the failure moment. The increase of inertia and area were sufficient to guarantee a better performance and to obtain a stiffer element that the individual chestnut beam. In this case, it is also important to notice that failure itself was not governed by the any significant existing defect on the chestnut element. On the other hand, for beam B-I-NG the retrofitted solution did not reach the same level of load predicted by the model. This is mainly due to the reason that the chestnut beam itself governed the failure with a large detachment of part of the beam due to the existence of a significant crack and inner decay. Therefore, the numerical model could not efficiently reflect the existing beam due to the existence of these very significant defects. Nevertheless, it must be noted that the retrofitting solution allowed to avoid a complete brittle failure of the beam has the planks were able to sustain load even after the local failure of the inner beam. In any case, it is important to note that the efficiency of the planks was more visible on the B-I-G beams since their height and width with relation to the cross-section were significantly higher. This is especially important due to the increase of inertia to the beam.

In both cases, it was found that the consideration of the values given by the reference codes were very conservative in terms of bending strength even if suitable for indication of the bending modulus of elasticity.
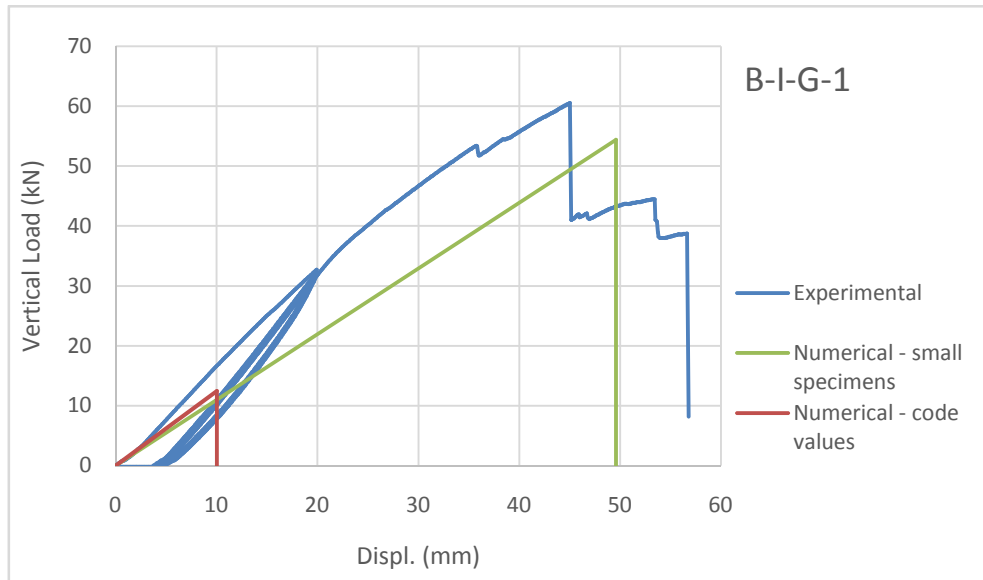

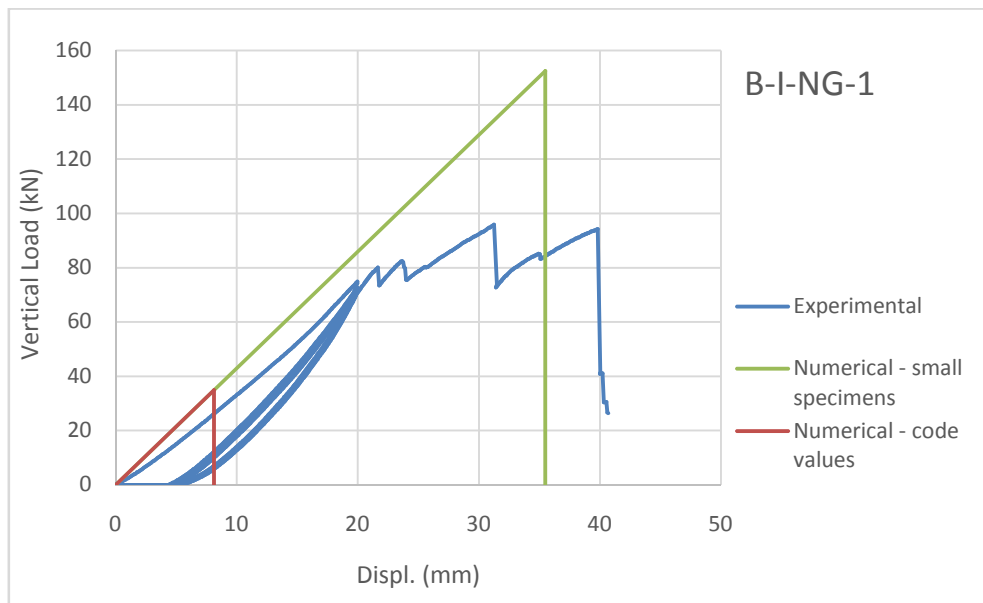**Figure 67 – B-I-G-1: Comparison between experimental and numerical results.**

Figure 68 – B-I-G-1: Comparison between experimental and numerical results.

6.   CONCLUSIONS

The work carried out and presented in this dissertation was done with the purpose of experiment a new retrofitting technique (derivation of a traditional strengthening method) based on dry timber connections suitable for historic timber structures. The aim was to elaborate, study and evaluate through an experimental campaign, a technique that can be applicable on single elements such as roof or floor beams with irregular cross-section, characterised by a fast and easy application able to conserve as much as possible the existing structure and to save on the new material applied by using a compatible material. The design of the technique was elaborated thanks to the collaboration with AOF regarding the availability of material but also by the share of knowledge and onsite expertise. Guidelines were also provided to illustrate the steps necessary to the installation of the technique.

Chestnut for the beam and Pine as retrofitting elements were chosen because they are widely present in the panorama of the historic construction in Portugal. Massaranduba was used as timber pegs due to its mechanical properties. Even if considered a reinforcement based on dry connections, part of the tests considered the use of a weak white glue, adhesive which is often used in carpentry work in order to maintain in place the timber elements for the time necessary to finish the installation. The use of white glue was taken into account in order to replicate in laboratory a series of circumstances as much as possible close to what could happen in reality, where the positive contribution of a retrofitting technique as the one studied is mainly based on a subjective judgement of the technician who performs the work.

The experimental campaign performed as a first approach to this technique, focused initially on a local scale in order to evaluate the shear behaviour of retrofitting solution and the performance of the connection made with wooden pegs. Because the aim of this solution is to bemeant to be used on historic structures, the samples tested involved a wide range of geometry regarding the cross-section of the chestnut beams, as the purpose of the work was also to evaluate if and how much the technique could have been influenced by this factor. Other elements such the presence of defects and decay were analysed with the same purpose.

The second step of the experimental campaign studied the strengthening method on a real scale aiming to a global evaluation of the reinforcement response. As for the local scale, one sample considered the use of glue in the connection, while the second specimen was subjected to the use of dry connections. The results recorded during the experimental campaign were then compared and a numerical model was made taking into account the prior information obtained by small size sample testing and visual inspection grading.

6.1 RECOMMENDATIONS

While performing the analysis, a series of considerations were done starting from what was observed from the collected data. Elaborated directly from the results of the tests performed and based on how the samples performed, these observations were mainly focused on how to perform the work in situ in the best possible way. Through the implementation of these recommendations, a better result could be reached and errors which could jeopardize the final result can be avoided. Table 21 collects what was considered recommended and what was considered not recommended.

Table 21 – Recommendation.

RECOMMENDED	NOT RECOMMENDED
- Consider the use of thinner fasteners then the one sudied in this work (d = 25 mm) in order to promore a ductile behaviour; - Always carry out visual inspection in order to assess the internal decay before installing the reinforcement; - If possible the same technician should carry out the entire work (same judgement approach); - If a considerable crack parallel to the grain is present, the penetration length has to include the crack itself regardless the dimension of the cross-section; - Provide a suitable spacing between the edge and the peg in order to avoid localized failure, the use of the minimum spacing provided by the EC 5 is strongly suggested; - Maintain as much as possible a symmetric distribution of the pegs both in cross section and length of the beam; - Mantain propping system and clamps for the entire duration of the work;	- No need of planks in the intrados was recorded; - Do not use planks previously cracked especially if in correspondence of the pegs; - Do not locate pegs near or over knots; - Avoid empty gaps between planks and beam in correspondence of a peg with wedges.

6.2 FUTURE WORKS

As already said the preformed work presented in this dissertation represents a first approach to the. Although a consistent range of cross-section and a significant number of specimens were tested, the overall considered sample was not enough to comprehend and consider all the possible geometries of cross-section. In the case of the double shear tests, for example, it was not possible to test unglued

specimens with a circular cross-section. Regarding the global scale, on the other hand, a total amount of two specimens was not enough to reach an univocally clear result. In other words, the overall number of studied element was not enough to reach strong results in matter of statistical analysis.

In order to overcome these problems and provide more results, it is strongly recommended to perform a deeper and wider analysis focused on the study of several scenarios considering thinner pegs able to reach a ductile behaviour on the global scale and in general a higher number of samples on both the considered scales. It also is advised to contemplate a study with different timber species. This will lead to a statistical analysis able to define with more precision values regarding the structural response of the technique and its possible dependence by other elements such as minimum spacing between pegs and the presence of defects in the existing structure.

Another aspect that has to be studied is the influence of the glue when used on the fasteners. Proof of its influence was found in the presence of a higher shear strength of the pegs which showed also a more ductile behaviour when the adhesive was used. A stiffness twice the value for the sample with completely dry connections was also recorded. Nevertheless, it is not known the period of influence of the adhesive itself. Considering that different types of glue present different grade of influence regarding both mechanical properties and period of time, an analysis focused on several types of adhesive characterised by different levels of strength is firmly advised.

6.3   CONCLUDING REMARKS

Considering all the analysis carried out, the observation done and the results presented, it is possible to assert that the reinforcing technique studied in this work gave satisfying results and was able to provide a higher performance to the historic timber beams to which may applied.

Considerable differences were observed between the samples with completely dry connections and where glue was used. In the first case a more uniform response was recorded when subjected to double shear test, while glued specimens reached higher vertical load and performed in a more ductile way. More in detail, for the double shear test the ultimate load recorded for the specimens with glued fasteners was equal to 111.5 kN, 15% higher than the unglued elements which performed with a maximum load of 97 kN. Values of stiffness are almost double in case of glued connection when compared with the dry fasteners (respectively 16 N/mm^2 against 9 N/mm^2). Other than outline a generally higher response of the glued sample, was possible to evaluate more precisely the structural behaviour of the specimens studied on a local scale through the evaluation of the Coefficient of Variation (Table 22) which shows a more constant output for the unglued specimens, characterized by a more regular cross-section.

Table 22 – Double shear tests: Coefficient of Variation.

	CoV	
	Glued	Unlgued
Ultimate load	15.7	8.9
Stiffness	42.2	28.1

Both of the beams tested behaved well under bending stresses showing higher performance for B-I-G-1 (glued) than B-I-NG-1 (unglued) with respectively a bending strength of 25.5 N/mm^2 against 21.5 N/mm^2. These values confirm the general behaviour monitored on the local scale and the influence that the use of an adhesive has on the structural response.

Even if strictly related with the dimensions of the cross-section, a decreased modulus of elasticity compared with the one estimated through the destructive tests carried out on clear samples was found. The glued beam displayed a MOE= 5288.6 N/mm^2 while the unglued element provided a value equal to 6119.7 N/mm^2. The decreased value extrapolated from the DTs was found equal to 7092.5 N/mm^2, in line with the visual grading performed on the tests subjected to bending (class III for chestnut and thus MOE=8000 N/mm^2.

Nevertheless, because of the distinctive ability of this method to adapt to the existing structure, it is not possible nor is the objective of this work to stabilise if is better to consider the use of adhesive or not.

On a general level, none of the defects proper of a timber element such as wane, crack or knots seems to affect the final results of both local and global tests for this technique. On the other hand, wedges showed an apparent influence on the mechanical properties of the element subjected to retrofit. Most probably this tendency is related with location of the peg itself: when fasteners were installed in correspondence of a void between the plank and the beam, a brittle failure was more likely to occur.

As the minimum spacing between the pegs in strictly related with the geometry of the beam itself, it was impossible to provide a clear and constant value especially of the pegs located along the cross-sections.

According to the obtained results, the proposed retrofit solution posed as a viable solution for use in existing timber elements even with irregular cross-sections.
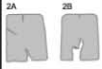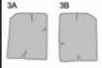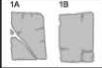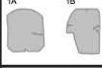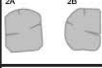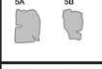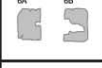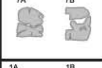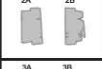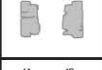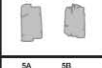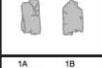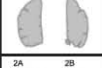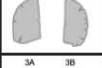
REFERENCES

[1]   J. M. Branco and T. Descamps, "Analysis and strengthening of carpentry joints," *Constr. Build. Mater.*, vol. 97, pp. 34–47, 2015.

[2]   M. R. Valluzzi, E. Garbin, and C. Modena, "Flexural strengthening of timber beams by traditional and innovative techniques," vol. 3, no. 2, pp. 125–143, 2007.

[3]   A. Gubana, "State-of-the-Art Report on high reversible timber to timber strengthening interventions on wooden floors," *Constr. Build. Mater.*, vol. 97, pp. 25–33, 2015.

[4]   S. Franke, B. Franke, and A. M. Harte, "Failure modes and reinforcement techniques for timber beams – State of the art," *Constr. Build. Mater.*, vol. 97, pp. 2–13, 2015.

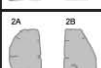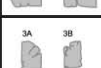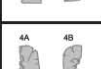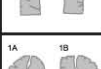[5]   E. Standard, *Eurocode 5 : Design of timber structures - Part 1-1 : General - Common rules and rules for buildings.* 2004.

[6]   "Experimental evaluation of timber- -to-timber connections using wood dowels," no. November, 2016.

[7]   A. Gubana and M. Melotto, "Experimental tests on wood-based in-plane strengthening solutions for the seismic retrofit of traditional timber floors," *Constr. Build. Mater.*, vol. 191, pp. 290–299, 2018.

[8]   M. R. Valluzzi, E. Garbin, and M. D. Benetta, "In-plane strengthening of timber floors for the seismic improvement of masonry buildings."

[9]   I. I. Congress and H. Monuments, "International charter for the conservation and restoration of monuments and sites (the Venice charter 1964)," 1965.

[10]   N. Gattesco, "High reversibility technique for in-plane stiffening of wooden floors," pp. 1035–1042, 2008.

[11]   M. Piazza, C. Baldessari, and R. Tomasi, "The role of in-plane floor stiffness in the seismic behaviour of traditional buildings," no. c, 2008.

[12]   P. Franchetti and D. Oliveira, "SAHC Programme - SA3_09_Damage and collapsing mechanisms in existing buildings." p. 27, 2019.

[13]   J. M. Branco, H. S. Sousa, and E. Tsakanika, "Non-destructive assessment , full-scale load-carrying tests and local interventions on two historic timber collar roof trusses," vol. 140, pp. 209–211, 2017.

[14]   E. Poletti and J. Branco, "SAHC Programme - SA5.7 - Strengthening of Timber Structures." p. 9, 2019.

[15]   C. C. C. D. Ambra and M. L. A. Prota, "Restoring of timber structures : connections with timber pegs," *Eur. J. Wood Wood Prod.*, vol. 75, no. 6, pp. 957–971, 2017.

[16]   C. O. Loinsigh *et al.*, "Experimental study of timber-to-timber composite beam using welded-through wood dowels," *Constr. Build. Mater.*, vol. 36, pp. 245–250, 2012.

[17]   C. Modena, M. R. Valluzzi, E. Garbin, and F. Porto, "A strengthening technique for timber floors using traditional materials," no. 1956, pp. 911–922, 2005.

[18]   M. Riggio, R. Tomasi, and M. Piazza, "Refurbishment of a Traditional Timber Floor with a Reversible Technique : Importance of the Investigation Campaign for Design and Control of the Intervention," vol. 3058, 2014.

[19]   J. M. Branco, I. Teodorescu, and B. Pereira, "Ligações com cavilhas de madeira : Aplicações e quantificação da sua resistência Wood dowel-type connections : Applications and assessment of their load-carrying capacity."

[20]   E. Standard, *EN 338 - Structural timber - Strength classes*. 2010.

[21]   W. Conshohocken, "ASTM D 143 - Standard Methods of Testing Small Clear Specimens of Timber."

[22]   International Standard, "ISO_3130 Wood - Determination of moisture content for physical and mechanical tests," vol. 1975, pp. 0–3, 1975.

[23]   International Standard, "ISO_3131," 1975.

[24]   H. M. Sousa, "Methodology for safety evaluation of existing timber elements - Universidade do Minho," 2013.

[25]   S. Behaviour, "Artur Jorge de Oliveira Feio Inspection and Diagnosis of Historical Timber Structures : NDT Correlations and Structural Behaviour Inspecção e Diagnóstico de Estruturas Históricas de Madeira : Correlações com Métodos Não Destrutivos e Comportamento Estrutural," 2005.

[26]   T. Della Norma, "UNI 11119_2004 Manufatti lignei Strutture portanti degli edifici - Ispezione in situ per la diagnosi Load-bearing structures - On site inspections for the diagnosis of timber members," 2004.

[27]   T. Della Norma, "UNI EN 26891 : 1991," 1991.

[28]   W. Muñoz and A. Salenikovich, "Determination of yield point and ductility of timber assemblies: in search for a hormonised approach."

[29]   E. Standard, "EN 408 : 2010 + A1 - Determination of some physical and mechanical properties," 2012.

[30]   G. Qiao, T. Li, and Y. F. Chen, "Assessment and retrofitting solutions for an historical wooden pavilion in China," *Constr. Build. Mater.*, vol. 105, pp. 435–447, 2016.

ANNEXES

DOUBLE SHEAR – geometrical survey

	Cross sections	Area (cm²)	Length (cm)	Inertia (cm⁴)	Wedges	Wane	Knots	Groups of knots	Cracks
R-S-G-1		320.8	69.5	10843.5	I	I	-	I	III
R-S-G-2		325.2	66.8	9758.9	I	I	-	II	III
R-S-G-3		316.8	66.1	10360.2	I	I	III	-	III
R-S-NG-1		278.2	72.3	8110.2	I	I	-	I	III
R-S-NG-2		282.4	73.2	9229.8	I	I	-	I	III
I-P-G-1		254.8	65.5	7103.9	III	II	III	-	III
I-P-G-2		264.0	68.4	6768.8	I	II	I	-	III
I-P-G-3		213.6	68.7	7231.6	II	III	III	-	III
I-P-G-4		218.7	68.2	7221.1	I	I	II	-	III
I-P-G-5		114.7	69.9	1654.3	II	I	I	-	III
I-P-G-6		117.6	68.6	2126.1	I	I	II	-	III
I-P-G-7		101.0	68.6	477.1	III	I	II	-	III
I-P-NG-1		254.6	73.6	7218.4	II	III	II	-	III
I-P-NG-2		123.5	73.8	2308.5	I	I	II	-	III
I-P-NG-3		114.5	75.1	2118.8	II	I	I	-	III
I-P-NG-4		122.3	73.4	2100.9	I	I	III	-	III
I-P-NG-5		107.1	73.3	1700.6	II	I	-	-	III
I-SC-G-1		159.3	67.1	4455.5	III	III	I	-	III
I-SC-G-2		176.3	67.7	4712.8	II	III	III	-	III
I-SC-G-3		142.4	68.3	4170.3	III	III	I	-	III

	Cross sections	Area (cm^2)	Length (cm)	Inertia (cm^4)	Wedges	Wane	Knots	Groups of knots	Cracks
I-SC-G-4		272.5	69.8	8212.3	II	III	-	II	III
I-SC-G-5		185.0	69.1	6152.4	II	III	III	-	III
I-SC-NG-1		196.9	73.9	4972.4	III	III	-	I	III
I-SC-NG-2		219.3	73.9	5711.5	III	II	II	-	III
I-SC-NG-3		81.1	73.1	847.1	III	III	II	-	III
I-SC-NG-4		72.3	73.9	556.6	II	III	-	I	III
I-SC-NG-5		86.8	71.0	915.1	III	II	II	-	III
I-C-G-1		219.1	67.3	4423.1	III	III	-	I	III
I-C-G-2		248.5	68.7	6011.5	III	III	-	II	III
I-C-G-3		222.1	68.4	4670.7	III	III	II	-	III

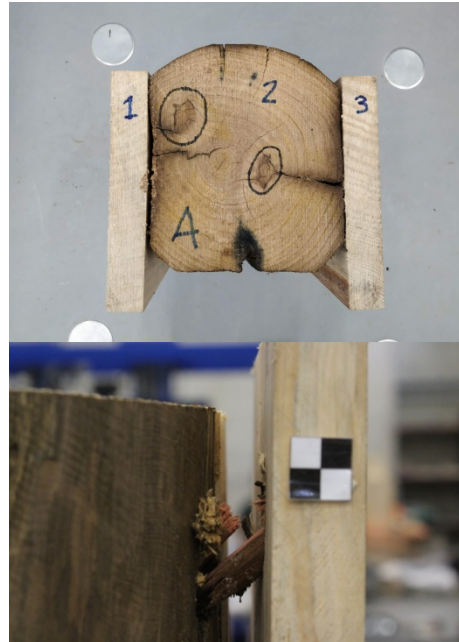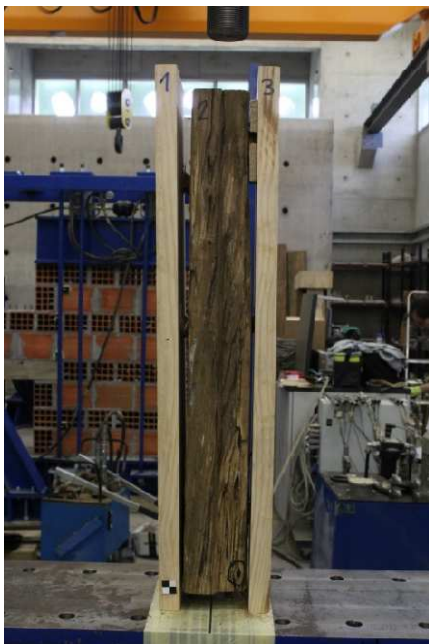*DOUBLE SHEAR – Extract of the photographic campaign of the tests.*

I-C-G-1

I-C-G-2

I-C-G-3

I-P-G-1

I-P-NG-2

I-P-NG-3

I-SC-NG-1

R-S-NG-2